

**GIS-BASED STRUCTURAL PERFORMANCE ASSESSMENT OF  
SAKARYA CITY AFTER 1999 KOCAELI-TURKEY EARTHQUAKE  
FROM GEOTECHNICAL AND EARTHQUAKE ENGINEERING POINT  
OF VIEW**

**A THESIS SUBMITTED TO  
THE GRADUATE SCHOOL OF NATURAL AND APPLIED SCIENCES  
OF  
MIDDLE EAST TECHNICAL UNIVERSITY**

**BY**

**ZEYNEP YILMAZ**

**IN PARTIAL FULFILLMENT OF THE REQUIREMENTS**

**FOR**

**THE DEGREE OF MASTER OF SCIENCE**

**IN**

**CIVIL ENGINEERING**

**JULY 2004**

**Approval of the Graduate School of Natural and Applied Sciences**

---

**Prof. Dr. Canan ÖZGEN**

**Director**

**I certify that this thesis satisfies all the requirements as a thesis for the degree of Master of Science.**

---

**Prof. Dr. Erdal ÇOKÇA**

**Head of Department**

**This is to certify that we have read this thesis and that in our opinion it is fully adequate, in scope and quality, as a thesis for the degree of Master of Science.**

---

**Assoc. Prof. Dr. Kemal Önder ÇETİN**

**Supervisor**

**Examining Committee Members**

**Prof. Dr. Orhan EROL (METU - CE) \_\_\_\_\_**

**Assoc. Prof. Dr. Kemal Önder ÇETİN (METU - CE) \_\_\_\_\_**

**Prof. Dr. Erdal ÇOKÇA (METU - CE) \_\_\_\_\_**

**Assist. Prof. Dr. Ahmet YAKUT (METU - CE) \_\_\_\_\_**

**Dr. Mutlu AKDOĞAN (Geoteknik Çözüm&Proje Ltd) \_\_\_\_\_**

**I hereby declare that all information in this document has been obtained and presented in accordance with academic rules and ethical conduct. I also declare that, as required by these rules and conduct, I have fully cited and referenced all material and results that are not original to this work.**

**Name, Last Name: ZEYNEP YILMAZ**

**Signature:**

## **ABSTRACT**

# **GIS-BASED STRUCTURAL PERFORMANCE ASSESSMENT OF SAKARYA CITY AFTER 1999 KOCAELI-TURKEY EARTHQUAKE FROM GEOTECHNICAL AND EARTHQUAKE ENGINEERING POINT OF VIEW**

Yılmaz, Zeynep

M.S., Department of Civil Engineering

Supervisor: Assoc. Prof. Dr. Kemal Önder Çetin

July 2004, 100 pages

The August 17, 1999 Kocaeli-Turkey Earthquake ( $M_w=7.4$ ) caused severe damage to the structures and lifelines in the Marmara region. Soil liquefaction was identified as one of the major causes of this damage. The aim of this study is to determine geotechnical and earthquake engineering factors that contribute to the structural damage observed in Sakarya city after 1999 Kocaeli Earthquake.

For this purpose, the results of an extensive field investigation program compiled by General Directorate of Disaster Affairs including subsurface soil characterization and documenting structural performance data were used. The database was carefully screened for poor quality data and was transferred to

geographic information system (GIS) framework. Maximum likelihood methodology for the probabilistic assessment of seismically induced structural performance was chosen as the statistical tool. After series of sensitivity analyses, important geotechnical and earthquake engineering parameters of the problem were selected as i) liquefaction severity index, ii) post liquefaction volumetric settlement, iii) peak ground acceleration and, iv) spectral acceleration defined at the period range of conventional buildings. In addition to these parameters, structural performance defined as a) no damage and light, b) moderate damage, c) heavy damage and collapse, as well as the number of storeys of each structure were used as to correlate structural damage with geotechnical earthquake engineering factors.

As a conclusion series of vulnerability functions specific to Adapazari shaken by Kocaeli Earthquake were developed. Performance predictions of these vulnerability functions were shown to be consistent with as high as 65 percent of the observed structural performance.

**Keywords:** Liquefaction, structural performance, local soil conditions, geographic information systems (GIS), vulnerability functions.

## ÖZ

# 1999 KOCAELİ DEPREMİNDE SAKARYA İLİNİN YAPISAL PERFORMANSININ GEOTEKNİK VE DEPREM MÜHENDİSLİĞİ YÖNÜNDEN CBS TABANLI İNCELENMESİ

Yılmaz, Zeynep

Yüksek Lisans, İnşaat Mühendisliği Bölümü

Tez Yöneticisi: Doç. Dr. Kemal Önder Çetin

Temmuz 2004, 100 sayfa

17 Ağustos 1999 Kocaeli Depremi ( $M_w=7.4$ ) Marmara Bölgesindeki alt ve üst yapıda ciddi boyutta hasara sebep olmuştur. Zemin sıvılaşması bu hasardaki en önemli etkenlerden biri olarak kabul edilmiştir. Bu çalışmanın amacı 1999 Kocaeli Depreminden sonra Sakarya İlinde gözlemlenen yapı hasarlarını etkileyen geoteknik ve deprem mühendisliği faktörlerinin belirlenmesidir.

Bu amaçla, Afet İşleri Genel Müdürlüğü tarafından, zemin karakteristiklerini ve yapıların sismik performanslarını içeren bir saha etüd programı düzenlenmiştir. Oluşturulan veri tabanı kalitesiz verilerden dikkatle arındırılarak coğrafi bilgi sistemleri formatına aktarılmıştır. Yapıların sismik performanslarının istatistiksel değerlendirilmesi için maksimum olasılık yöntemi seçilmiştir. Yapılan hassasiyet analizleri sonucunda yapı hasarını

etkileyen faktörler şu şekilde belirlenmiştir; i) sivilaşma indeksi, ii) sivilaşmaya bağlı zemin oturması, iii) maksimum yer ivmesi ve iv) bina periodlarına denk gelen yer ivme değerleri. Yapı performansı, a) hasarsız-az hasarlı, b) orta hasarlı, ve c) ağır hasarlı-yıkık olarak olarak sınıflandırılmıştır. Geoteknik parametrelere ek olarak her binanın kat sayısı ve yapı performansı da kullanılarak hasar bağıntıları elde edilmiştir.

Yapılan çalışmaların sonucunda 1999 Kocaeli depremiyle sarsılan Adapazarı İli için bir seri hasar görebilirlik fonksiyonu elde edilmiştir. Bu hasar görebilirlik fonksiyonlarının hepsinin gözlenen yapısal performanslarla yüzde 65 mertebelerinde tutarlı tahminler yapabildiği görülmüştür.

**Anahtar Kelimeler:** Sivilaşma, yapı performansı, yerel zemin etkileri , coğrafi bilgi sistemleri, hasar görebilirlik fonksiyonları.

To my family

## **ACKNOWLEDGMENTS**

I would like to express my thanks to my advisor, Dr. K. Önder Çetin, for helpful guidance, training, and support throughout the entire process of researching and writing this work. His great motivation, tolerance and support teach me that everything is possible, and help me in development of my academic vision. I thank to Professor Muvaffak Üzümeri for his guidance, encouragement, and tolerance through my graduate studies and assistantship period. Thanks are extended to Dr. Erhan Karaesmen for his academic and non-academic guidance, and helping me in constructing my future life.

Thanks and acknowledgements are given to all my friends for their friendship, fellowship and encouraging support. I am grateful to Emrah Erduran, Günes Goler, Fatma Özkahriman, Berna Unutmaz and Volkan Yargıcı for their brilliant ideas and technical support during researching and writing this work. I also want to thank the best friends that a person can have in this world, Seda Selçuk and Duygu Yüksel, for their motivation, patience, trust and support in nearby or kilometers away.

For once again in my life, but I believe not for the last time, I want to thank my parents and my sister. I cannot possibly begin to describe how much their love meant to me.

## TABLE OF CONTENTS

ABSTRACT.....	iv
ÖZ.....	vi
DEDICATION.....	viii
ACKNOWLEDGMENTS .....	ix
TABLE OF CONTENTS.....	x
LIST OF FIGURES .....	xiv
LIST OF TABLES .....	xix
LIST OF SYMBOLS.....	xxi

### CHAPTER

1. INTRODUCTION.....	1
1.1 Research Statement .....	2
1.2 Problem Significance and Limitations of Previous Studies	3
1.3 Scope.....	4
2. AN OVERVIEW OF AVAILABLE METHODS FOR THE ASSESSMENT OF LIQUEFACTION AND IDENTIFYING THE LIQUEFACTION POTENTIAL.....	5
2.1 Introduction and Definitions .....	5

2.2	Selection of Soils Vulnerable to Liquefaction .....	10
2.2.1	Cohesionless Soils.....	10
2.2.2	Cohesive Soils .....	11
2.3	Assessment of Liquefaction Potential .....	14
3.	SITE - SPECIFIC RESPONSE ANALYSES AND RESULTS OF THE ANALYSES .....	28
3.1	Introduction .....	28
3.2	Compilation of Necessary Parameters For Site Specific Response Analysis.....	29
3.2.1	Determination of Shear Wave Velocities.....	31
3.2.2	Determination of Unit Weight of the Soil Samples .....	32
3.2.3	Effects of Plasticity of Clay Layers on Soil Response .....	33
3.3	Preparation of Input Files.....	37
3.3.1	Determination of Soil Profiles.....	37
3.3.2	Input Strong Ground Motion.....	43
3.4	Site Specific Response Analysis.....	44
3.5	Results .....	46

4.	SEISMIC SOIL LIQUEFACTION ASSESSMENT AND RESULTS OF THE ANALYSES .....	52
4.1	Introduction .....	52
4.2	Liquefaction Assessment of Local Soils in Adapazarı .....	53
4.3	Selection of Liquefaction Related Parameters That Correlates the Building Damage .....	54
4.3.1	Liquefaction Severity Index.....	54
4.3.2	Thickness of the Liquefiable Layer .....	58
4.3.3	Representative Depth to the Liquefiable Layer....	61
4.3.4	Post Liquefaction Volumetric Settlements .....	62
4.4	Summary and Conclusions .....	67
5.	DEVELOPMENT OF PROBABILISTIC MODELS FOR THE ESTIMATION OF DAMAGE INDEX .....	68
5.1	Introduction .....	68
5.2	Sensitivity Studies.....	69
5.3	Construction of Limit State Function .....	74
5.4	Formulation of the Likelihood Function .....	77
6.	SUMMARY AND CONCLUSION .....	82
7.	REFERENCES.....	83

**APPENDICES**

A ..... 93

B ..... CD at the back cover

## LIST OF FIGURES

### FIGURES

2.1	Key Elements of Soil Liquefaction Engineering (After Seed et al., 2001).....	9
2.2	Modified Chinese Criteria (After Finn et al., 1994).....	12
2.3	Liquefaction Susceptibility of Silty and Clayey Sands (after Andrews and Martin, 2000).....	13
2.4	Criteria for the Evaluation of the Liquefaction Susceptibility of Fine-grained Soils at Low Confining Stresses (After Bray et al., 2003) ....	14
2.5	Illustration of Simplified Procedure (After Seed and Idriss, 1971) ....	16
2.6	$R_d$ versus Depth Curves Developed by Seed and Idriss (1971) with Added Mean-Value Lines Plotted (After Youd et al., 2001) .....	17
2.7	$R_d$ Results from Response Analyses Superimposed with Heavier Lines Showing (a) the Earlier Recommendations of Seed and Idriss (1971), and (b) the Mean and + 1 Standard Deviation Values (After Seed et al., 2001) .....	19
2.8	SPT Clean-Sand Base Curve for Magnitude 7.5 Earthquakes with Data from Liquefaction Case Histories (Modified from Seed et al. 1985).....	21
2.9	(a) Recommended Probabilistic SPT-Based Liquefaction Triggering Correlation (for $M_w=7.5$ ) (After Seed et al., 2001).....	22

2.9	Recommended “Deterministic” SPT-Based Liquefaction Triggering Correlation (for Mw=7.5), with Adjustments for Fines Content (After Seed et al., 2001) .....	23
2.10	Recommended CR Values (Rod Length from Point of Hammer Impact to Tip of Sampler) (After Seed et al., 2001) .....	26
3.1	Location of Boreholes throughout Sakarya City.....	30
3.2	The Correlations Used in Converting SPT-N Values to Shear Wave Velocities.....	32
3.3	The Scatter of the Unit Weight of Soil Samples Tested in the Laboratory.....	33
3.4	Modulus Reduction Curves for Fine-Grained Soils of Different Plasticity (After Vucetic And Dobry, 1991).....	34
3.5	Modulus Reduction Curves for Sands (After Seed And Idriss, 1970).....	35
3.6	Damping Curves for Fine-Grained Soils of Different Plasticity (After Vucetic And Dobry, 1991).....	36
3.7	Damping Curves for Sands (After Seed And Idriss, 1970) .....	36
3.8	Plasticity Index Values for Tested Soil Samples.....	37
3.9	Variation of Bedrock Depth throughout Adapazarı (Sakarya University, 1998).....	39
3.10	Borehole Data Corresponding To Grid No: Q10.....	40
3.11	Representative Soil Profile for Grid No: Q10 .....	40
3.12	Second Set Of Borehole Logs (Deep) .....	42
3.13	Modeled Deep Borehole Logs .....	42

3.14	The Acceleration vs. Time (East – West) Plot Recorded At Sakarya Strong Ground Motion Station .....	43
3.15	(a) Distribution of Peak Ground Acceleration throughout Adapazarı (b) Peak Ground Acceleration Map Overlaid on Damaged Buildings throughout Adapazarı. ....	47
3.16	Distribution of Spectral Acceleration for T=0.1 second throughout Adapazarı. ....	48
3.17	Distribution of Spectral Acceleration for T=0.2 second throughout Adapazarı. ....	49
3.18	Distribution of Spectral Acceleration for T=0.3 second throughout Adapazarı. ....	49
3.19	Distribution of Spectral Acceleration for T=0.4 second throughout Adapazarı. ....	50
3.20	Distribution of Spectral Acceleration for T=0.5 second throughout Adapazarı. ....	50
3.21	Distribution of Spectral Acceleration for T=0.6 second throughout Adapazarı. ....	51
4.1	(a) Liquefaction Severity Index Map, (b) Damaged Buildings (Black Dots) Overlaid on the Map of Liquefaction Severity Index. ....	57
4.2	Proposed Boundary Curves for Site Identification of Liquefaction-Induced (Surface) Damage (After Ishihara, 1985).....	59
4.3	(a) Thickness of the Potentially Liquefiable Layer Map (b) Damaged Buildings (Black Dots) Overlaid on the Map of Thickness of the Potentially Liquefiable Layer .....	60

4.4	(a) Representative Depth to the Potentially Liquefiable Layer Map (b) Damaged Buildings (Black Dots) Overlaid on the Map of Representative Depth to the Potentially Liquefiable Layer .....	62
4.5	Chart for Determination of Post-Liquefaction Volumetric Strain of Clean Sands (After Tokimatsu and Seed, 1984) .....	63
4.6	Chart for Determination of Post-Liquefaction Volumetric Strain of Clean Sands as a Function of Factor of Safety (After Ishihara, 1996) .....	64
4.7	(a) Post Liquefaction Volumetric Settlement Map (b) Damaged Buildings (Black Dots) Overlaid on the Map of Post Liquefaction Volumetric Settlement.....	67
5.1	Distribution of the Percent Number of Damaged Buildings with Number of Stories.....	70
5.2	(a) Distribution of the Percentage of Damaged Buildings with PGA for 4-Storey Buildings, (b) Distribution of the Percentage of Damaged Buildings with PGA for 5-Storey Buildings.....	71
5.3	(a) Distribution of the Percentage of Damaged Buildings with Spectral Acceleration Corresponds to $T = 0.4$ Sec for 4-Storey Buildings, (b) Distribution of the Percentage of Damaged Buildings with Spectral Acceleration Corresponds to $T = 0.5$ Sec for 5-Storey Buildings.....	73
5.4	Distribution of the Cumulative Number of Damaged Buildings with Liquefaction Severity Index.....	73
5.5	Distribution of the Percent Number of Damaged Buildings with Liquefaction Induced Ground Settlements.....	74
5.6	Percentage on True Predictions for Damaged and Non-damaged	

	Cases in Model 1 and Model 2 .....	80
5.7	Percentage on True Predictions for Damaged and Non-damaged Cases in Model 3 and Model 4 .....	80
5.8	Percentage on True Predictions for Damaged and Non-damaged Cases in Model 5 and Model 6 .....	81

## LIST OF TABLES

### TABLES

2.1	Recommended Corrections for SPT Equipment, Energy and Procedures .....	27
3.1	A Summary of Available Data in the Database .....	29
3.2	The Correlations Used in Converting SPT-N Values to Shear Wave Velocities.....	31
3.3	The Unit Weight Values Used in Response Analyses .....	33
5.1	Statistics of Buildings in Adapazarı.....	68
5.2	Maximum Likelihood Estimates of Model Parameters .....	79

## LIST OF SYMBOLS

amax	:	Maximum ground acceleration
CPT	:	Cone penetration test
CSR	:	Cyclic stress ratio
CRR	:	Cyclic resistance ratio
DPLL	:	Depth to the potentially liquefiable layer
FC	:	Fines content
g	:	Gravitational acceleration
GDDA	:	General Directorate of Disaster Affairs
GIS	:	Geographic Information Systems
IL	:	Liquefaction potential index
LL	:	Liquid limit
LSI	:	Liquefaction severity index
Mw	:	Moment magnitude of the earthquake
N	:	Number of storeys
N <sub>1,60</sub>	:	SPT blow counts corrected for energy and overburden
PGA	:	Peak ground acceleration
PI	:	Plasticity index
PL	:	Probability of liquefaction
rd	:	Nonlinear shear mass participation factor
S	:	Liquefaction induced ground settlements

SA	:	Spectral acceleration
SPT	:	Standard penetration test
SPT-N	:	Standard penetration test blow counts
TH	:	Thickness of the potentially liquefiable layer
Vs	:	Shear wave velocity
W <sub>c</sub>	:	Water content
$\sigma_v$		Total vertical stress
$\sigma_v'$		Vertical effective stress
$\varepsilon$	:	Model correction term
$\varphi$	:	Normal probability density function
$\sigma$	:	Standard deviation
$\theta$	:	Model parameters

# CHAPTER 1

## INTRODUCTION

In August 17, 1999 a magnitude  $M_w=7.4$  earthquake struck Kocaeli and Sakarya provinces, which are densely populated regions in the industrial heartland of Turkey. The region affected by the earthquake is both geographically extensive and economically dynamic. The August 17, 1999 Earthquake is considered to be one of the largest events that has devastated a modern, industrialized area since the 1923 Tokyo Earthquake. This earthquake caused severe damage to the structures and lifelines in the Marmara Region. The majority of building collapses were observed in the towns located on southern shorelines of Marmara Sea and in the city of Sakarya. Within the confines of this thesis the effects of local soil conditions on the observed damage will be investigated.

The influence of local soil conditions on the nature of earthquake damage has been recognized for many years. Since the early observations, the effects of local site conditions on ground motions have been illustrated after various earthquakes all around the world. Additionally, soil liquefaction was identified as one of the major causes of damage after 1999 Kocaeli Earthquake. In Sakarya, located over young riverbed sediments with soft and liquefiable silts and sands, hundreds of buildings sank as much as 1.5 m or tilted due to shear failure of the foundation media and liquefaction. Surface manifestations of liquefaction in Adapazari and Sapanca included sand boils and lateral spreading.

It is of substantial importance, to back calculate areas vulnerable to liquefaction as well as to rank them from the most vulnerable to the least for

the calibration of available liquefaction initiation models and cross correlate structural performance with soil liquefaction initiation potential. Predicting the influence of local soil conditions on strong ground motion is also very important, since differences can be observed in characteristics of the ground motion due to various local soil conditions, which effects the overall distribution of building damage in the city. Therefore, an empirically based vulnerability function for cross correlating structural damage and geotechnical earthquake engineering parameters estimating the risk of building failure will be the most valuable result of this study.

## **1.1 Research Statement**

The aim of this study is to determine geotechnical engineering factors that contribute to the structural damage observed after 1999 Kocaeli Earthquake. For this purpose an extensive field investigation program was implemented including subsurface soil characterization, and documenting structural performance data. The database, after carefully screened for poor quality data, was transferred to geographic information system (GIS) framework. After series of sensitivity analyses, important engineering parameters of the problem were selected as i) peak ground acceleration, ii) spectral acceleration values corresponding to the period range of conventional buildings, iii) liquefaction severity index, iv) thickness of the possibly liquefied layer, v) representative depth to possibly liquefied layer, vi) post liquefaction volumetric settlement. In addition to these geotechnical engineering parameters, structural performance defined as a) no damage, b) moderate damage, c) heavy damage and collapse, as well as the number of storeys of each structure were used as to correlate structural damage with these engineering factors.

## **1.2 Problem Significance and Limitations of Previous Studies**

Existence of local site effects on the strong ground motion has been recognized for many years. On the other hand, the influence of local soil conditions on earthquake damage was a matter of some debate in past years. Since the 1920's seismologist and, more recently, geotechnical earthquake engineers have worked toward the development of quantitative methods for predicting the influence of local soil conditions on strong ground motion and distribution of earthquake damage. Soil liquefaction is found to be one of the most important contributors for the account of local site conditions. Many researchers around the world have studied this phenomenon extensively and significant progress has occurred.

Currently, there are various methods, including the one implemented in these studies, for the estimation of the effects of local soils on strong ground motion and liquefaction initiation of a soil layer. Unfortunately, it is of more importance to estimate the potential of ground failure or building damage at a given site rather than estimating the effects of local soil conditions on strong ground motion. It must also be noticed that the damage to structures due to liquefaction is considerably affected by the severity of the liquefaction potential. However, the researchers did not focus on the effects of local soil conditions, especially soil liquefaction, on the earthquake damage until last 20 years. Since that time, several researchers tried to correlate the observed damage with various parameters related to local soils like; peak ground acceleration (PGA), or liquefaction related parameters such as; factor of safety due to liquefaction or post-liquefaction settlement. Building dimensions like number of storeys is also used in correlations evaluating the structural damage level. But in neither of these studies, both the effects of local soils to ground motion and soil liquefaction, in addition to building related parameters, are correlated with each other and building damage level. The empirically based vulnerability function evaluated in this study, correlating structural damage to geotechnical earthquake engineering parameters and estimating the risk of building failure, is an important contribution to the previous studies on earthquake damage estimation.

### 1.3 Scope

The scope of this thesis is defined as follows:

In the first chapter the research statement and introductory comments are presented. Chapter 2 contains a discussion of available methods for the assessment of seismic soil liquefaction potential and methodologies regarding liquefaction triggering assessment used in this study.

Chapter 3 presents the efforts on database compilation and the methodology used in site-specific response analyses. Geotechnical characteristics of the local soils in Adapazarı were evaluated using the deep and shallow borehole logs and measured parameters from field and laboratory. This data is employed for developing representative one-dimensional site response models, and these models are used in site-specific response analysis.

In Chapter 4, parameters related to soil liquefaction affecting the earthquake damage distribution will be highlighted, and GIS-based applications of liquefaction triggering methodologies summarized in Chapter 2 will be demonstrated for the cities of Sakarya and Gölcük after August 17, 1999 Kocaeli Earthquake of  $M_w=7.4$ .

In Chapter 5, the probabilistic models for seismic performance of buildings under different local soil conditions, using evaluated geotechnical engineering parameters, are developed.

In the final chapter, research findings of this work are summarized, and the conclusions of the research are presented.

Finally in the Appendix, the database of the collected and resultant data of this research is given.

## CHAPTER 2

### AN OVERVIEW OF AVAILABLE METHODS FOR THE ASSESSMENT OF SEISMIC SOIL LIQUEFACTION

#### 2.1 Introduction and Definitions

Liquefaction is one of the most important damage causes and thus is an important topic of geotechnical earthquake engineering. Its devastating effects sprang to the attention of geotechnical engineers in a three-month period in 1964, when the Good Friday Earthquake ( $M_w=9.2$ ) in Alaska was followed by the Niigata Earthquake ( $M_w=7.5$ ) in Japan. “Modern” engineering treatment of liquefaction-related issues evolved initially in these two earthquakes in which seismically induced liquefaction produced spectacular and devastating effects including slope failures, bridge and building foundation failures, and flotation of buried structures. Over the past 40 years following these earthquakes, liquefaction has been studied extensively by many researchers around the world and significant progress has occurred. Different terminologies, procedures, and methods of analysis have been proposed, and a prevailing approach has been slow to emerge.

The term liquefaction has been used to describe a number of different, though related phenomena. Before describing the methods to evaluate the liquefaction potential, it is important first to define the terms used to explain soil liquefaction. Terzaghi and Peck (1948) referred to “spontaneous liquefaction” to describe the sudden loss of strength of very loose sands that caused flow slides due to a slight disturbance. But the term “liquefaction”, originally coined by Mogami and Kubo (1953) and used in conjunction with a variety of phenomena that involve soil deformations caused by monotonic,

transient, or repeated disturbance of saturated cohesionless soils under undrained conditions. The progress of work on soil liquefaction has been described in detail in a series of state of art papers, such as Yoshimi et al. (1977), Seed (1979), Finn (1981), Ishihara (1993), Robertson and Fear (1995). The definition of liquefaction suggested by NCEER working group at 1997 is as follows:

**Liquefaction:** The term liquefaction refers to a change of state from a solid granular material to a dense viscous liquid without consideration of possible deformation or instability of the liquefied material. Thus evaluation of liquefaction resistance refers to the determination of the capacity of a soil to resist this change of state or in other words triggering of the liquefied condition.

Liquefaction phenomena can be divided into two main groups: flow liquefaction and cyclic softening.

**Flow liquefaction** produces the most dramatic effects of all the liquefaction related phenomena, tremendous instabilities known as flow failures. Flow liquefaction can occur when the shear stress required for the static equilibrium of soil mass (the static shear stress) is greater than the shear strength of the soil in its liquefied state. Once triggered, the large deformations produced by flow liquefaction are actually driven by static shear stresses. The cyclic stress may simply bring the soil to an unstable state at which strength drops sufficiently to allow the static stresses to produce the flow failure. Flow liquefaction:

- i. Applies to strain softening soils only
- ii. Requires a strain softening response in undrained loading resulting in constant shear stress and effective stress
- iii. Requires in-situ shear stresses greater than the ultimate or minimum undrained shear strength
- iv. Either monotonic or cyclic loading can trigger flow liquefaction
- v. For failure of a soil structure to occur, such as a slope, a sufficient volume of material must strain soften. The resulting failure can be a slide or a flow depending on the material

characteristics and ground geometry. The resulting movements are due to internal causes and can occur after the triggering mechanism occurs.

- vi. Can occur in any metastable saturated soil, such as very loose granular deposits, very sensitive clays and loess deposits.

**Cyclic softening** is another phenomenon that can also produce unacceptably large permanent deformations during earthquake shaking. In contrast to flow liquefaction, cyclic softening occurs when static shear stress is less than the shear strength of the soil. The deformations produced by cyclic softening are driven by both cyclic and static shear stresses. Cyclic softening:

- i. Applies to both strain softening and strain hardening soils.
- ii. Two terms can be used: cyclic liquefaction and cyclic mobility.

**Cyclic liquefaction:**

- i. Requires undrained cyclic loading during which shear stress reversal occurs or zero shear stress can develop.
- ii. Requires sufficient undrained cyclic loading to allow effective stresses to reach essentially zero.
- iii. At the point of zero effective stress no shear stress exists. When shear stress is applied, pore pressure drops as the material tends to dilate, but a very soft initial stress-strain response can develop resulting in large deformations.
- iv. Deformations during cyclic loading can accumulate to large values, but generally stabilize when cyclic loading stops. The resulting movements are due to external causes and can occur only during cyclic loading.
- v. Can occur in almost all saturated sands provided that the cyclic loading is sufficiently large in magnitude and duration.
- vi. Clayey soils can experience cyclic liquefaction but deformations are generally small due to the cohesive strength at zero effective stress. Rate effects (creep) often control deformations in cohesive soils.

**Cyclic mobility:**

- i. Requires undrained cyclic loading during which shear stresses are always greater than zero; i.e. no shear stress reversal develops.
- ii. Zero effective stress will not develop.
- iii. Deformations during cyclic loading will stabilize, unless the soil is very loose and flow liquefaction is triggered. The resulting movements are due to external causes and occur only during the cyclic loading.
- iv. Can occur in almost any saturated sand provided that the cyclic loading is sufficiently large in magnitude and duration, but no shear stress reversal occurs.
- v. Cohesive soils can experience cyclic mobility, but rate effects (creep) usually control deformations

Both flow liquefaction and cyclic liquefaction can cause very large deformations. Hence, it can be very difficult to clearly identify the correct phenomenon based on the observed deformations following earthquake loading. Both the flow liquefaction and cyclic mobility can produce damage at a particular site and a complete evaluation of liquefaction hazards requires that the potential for each be addressed. The most common form of soil liquefaction observed in the field has been cyclic softening due to earthquake loading. Much of the existing research work on soil liquefaction has been related to cyclic softening, primarily cyclic liquefaction (NCEER, 1997).

Today, the area of “soil liquefaction engineering” is emerging as a semi-mature field of practice in its own right. This area now involves a number of discernable sub-issues or sub-topics, as illustrated schematically in Figure 2.1.

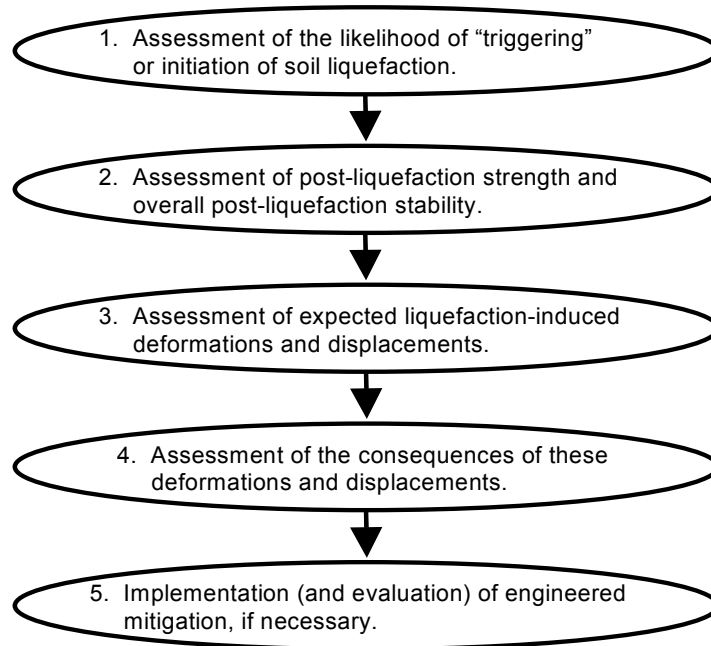


**Fig. 2.1: Key Elements of Soil Liquefaction Engineering (After Seed et al., 2001)**

As shown in Figure 2.1, the first step in most engineering treatments of soil liquefaction continues to be (1) assessment of "liquefaction potential", or risk of "triggering" (initiation) of liquefaction. It is not possible, within the confines of this chapter, to fully address all of these issues summarized in Figure 2.1 (a textbook would be required!). Instead, methodologies regarding liquefaction triggering assessment will be highlighted in this chapter, and GIS-based applications of these liquefaction triggering methodologies will be demonstrated for the city of Sakarya after August 17, 1999 Kocaeli Earthquake of  $M_w=7.4$  in Chapter 4.

## **2.2 Selection of Soils Vulnerable To Liquefaction**

The first step in engineering assessment of the potential for “triggering” or initiation of soil liquefaction is the determination of whether or not soils of “potentially liquefiable nature” are present at a site. This, in turn, raises the important question regarding which types of soils are potentially vulnerable to soil liquefaction. Additionally two other conditions necessary for vulnerability to liquefaction are: (1) saturation (or at least near-saturation), and (2) “rapid” (largely “undrained”) loading. It should be remembered that phreatic conditions are variable both with seasonal fluctuations and irrigation, and that the rapid cyclic loading induced by seismic excitation represents an ideal loading type (Seed et al., 2001).

### **2.2.1 Cohesionless Soils**

It has long been recognized that relatively “clean” sandy soils, with few fines, are potentially vulnerable to seismically induced liquefaction. There has, however, been significant controversy and confusion regarding the liquefaction potential of coarser, gravelly soils and rock fills. The cyclic behavior of coarse, gravelly soils differs little from that of “sandy” soils, as Nature has little or no respect for the arbitrary criteria established by the standard #4 sieve. Coarse, gravelly soils are potentially vulnerable to cyclic pore pressure generation and liquefaction. These soils do, however, often differ in behavior from their finer, sandy brethren in two ways: (1) they can be much more pervious, and so can often rapidly dissipate cyclically generated pore pressures, and (2) due to the mass of their larger particles, the coarse gravelly soils are seldom deposited gently and so do not often occur in the very loose states more often encountered with finer sandy soils. Sandy soils can be very loose to very dense, while the very loose state is uncommon in gravelly deposits and coarser soils.

The apparent drainage advantages of coarse, gravelly soils can be defeated if their drainage potential is circumvented by either; (1) their being surrounded and encapsulated by finer, less pervious materials, (2) if drainage is internally impeded by the presence of finer soils in the void spaces between

the coarser particles (it should be noted that the  $D_{10}$  particle size, not the mean or  $D_{50}$  size, most closely correlates with the permeability of a broadly graded soil mix), or (3) if the layer or stratum of coarse soil is of large dimension, so that the distance over which drainage must occur (rapidly) during an earthquake is large. In these cases, the coarse soils should be considered to be of potentially liquefiable type, and should be evaluated accordingly. For the sake of completeness, all cohesionless soils from silty sand to coarse gravel under the groundwater table level are assumed to be potentially liquefiable in this paper.

### **2.2.2 Cohesive Soils**

Questions regarding the potential liquefiability of finer, “cohesive” soils (especially “silts”) are increasingly common at meetings and professional short courses and seminars. Over the past ten years, a group of approximately two dozens leading experts has been attempting to achieve consensus regarding a number of issues involved in the assessment of liquefaction potential. This group, referred to hereafter as the NCEER Working Group, has published many of their consensus findings (or at least near-consensus findings) in the NSF-sponsored workshop summary paper (NCEER, 1997), and additional views are coming in a second paper published at 2001 in the ASCE Journal of Geotechnical and Geoenvironmental Engineering (Youd et al., 2001). A brief summary of discussions on liquefaction susceptibility of fine-grained soils is given below.

Using the data from sites where liquefaction was and was not observed after earthquakes in China, Wang established that any clayey soil containing less than 15% to 20% particles by weight smaller than  $5\ \mu\text{m}$  and having water content ( $w_c$ ) to liquid limit (LL) ratio greater than 0.9 is susceptible to liquefaction. Based on these data, Seed and Idriss stated that “clayey soils” could be susceptible to liquefaction only if all three of the following conditions are met: (1) Percent less than  $5\ \mu\text{m}$  < 15%, (2)  $LL < 35$ , and (3)  $w_c / LL > 0.9$ . Due to its origin, this standard is known as the “Chinese criteria.” Koester noted that the determination of LL by means of the fall cone used in China

produced values that are about 4 points higher than those values determined by means of the Casagrande percussion device. Hence, Koester recommended a slight “modification” of the LL condition of the Chinese criteria before using it as a screening tool when the Casagrande method has been used (known as Modified Chinese Criteria). Figure 2.2 illustrates the “Modified Chinese Criteria” for defining potentially liquefiable soils.

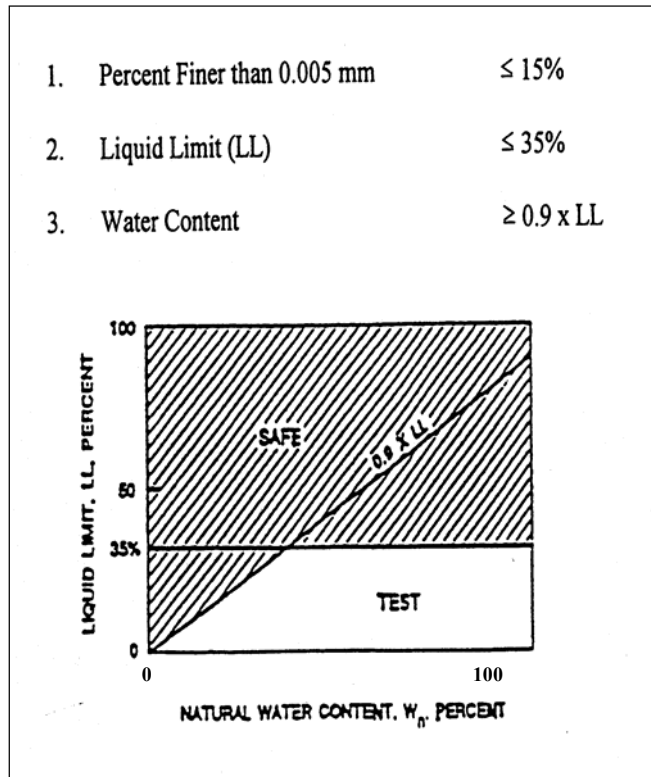


**Fig. 2.2: Modified Chinese Criteria (After Finn et al., 1994)**

Andrews and Martin (2000) have re-evaluated the liquefaction field case histories from the database of Seed et al. (1984, 1985), and have transposed the “Modified Chinese Criteria” to standard conventions (with clay sizes defined as those less than about 0.002 mm). Their findings are largely summarized in Figure 2.3. Andrews and Martin recommend that soils with less than about 10% clay fines (< 0.002 mm) and a Liquid Limit (LL) in the minus #40 sieve fraction of less than 32% be considered potentially liquefiable, that

soils with more than about 10% clay fines and  $LL \geq 32\%$  are unlikely to be susceptible to classic cyclically-induced liquefaction, and that soils intermediate between these criteria should be sampled and tested to assess whether or not they are potentially liquefiable.

	Liquid Limit <sup>1</sup> < 32	Liquid Limit $\geq 32$
Clay Content <sup>2</sup> < 10%	Susceptible	Further Studies Required <i>(Considering plastic non-clay sized grains – such as Mica)</i>
Clay Content <sup>2</sup> $\geq 10\%$	Further Studies Required <i>(Considering non-plastic clay sized grains – such as mine and quarry tailings)</i>	Not Susceptible

1. Liquid limit determined by Casagrande-type percussion apparatus.
2. Clay defined as grains finer than 0.002 mm.

**Fig. 2.3: Liquefaction Susceptibility of Silty and Clayey Sands (After Andrews and Martin, 2000)**

Currently a study on liquefaction susceptibility of fine-grained soils was performed using the soil samples taken from Adapazarı by Bray et al. Based on the results of this study (Fig. 2.4), a soil deposit is considered to be susceptible to liquefaction or cyclic mobility if the ratio of the water content to liquid limit is equal to or greater than 0.85 ( $w_c/LL = 0.85$ ), and the soil plasticity index is equal to or less than twelve ( $PI = 12$ ). Soils that do not meet these conditions but have plasticity index greater than twelve and less than or equal to twenty ( $12 < PI = 20$ ) and water content to liquid limit ratio greater to or equal than eight tenths ( $w_c/LL = 0.8$ ) may be moderately susceptible to liquefaction or cyclic mobility, and they should be tested in the laboratory to assess the strain potential and liquefaction susceptibility under the loading

conditions existing in the field. Soils with  $PI > 20$  are considered too clayey to liquefy. However, structures founded on these soils, and for that matter, under any soil, may undergo significant deformations if the cyclic loads approach or exceed the dynamic strength of the soil (Bray et al., 2003). This criterion is used for evaluating the liquefiability of cohesive soils in this study, since it is developed depending on the tests applied on the soils of Adapazarı.

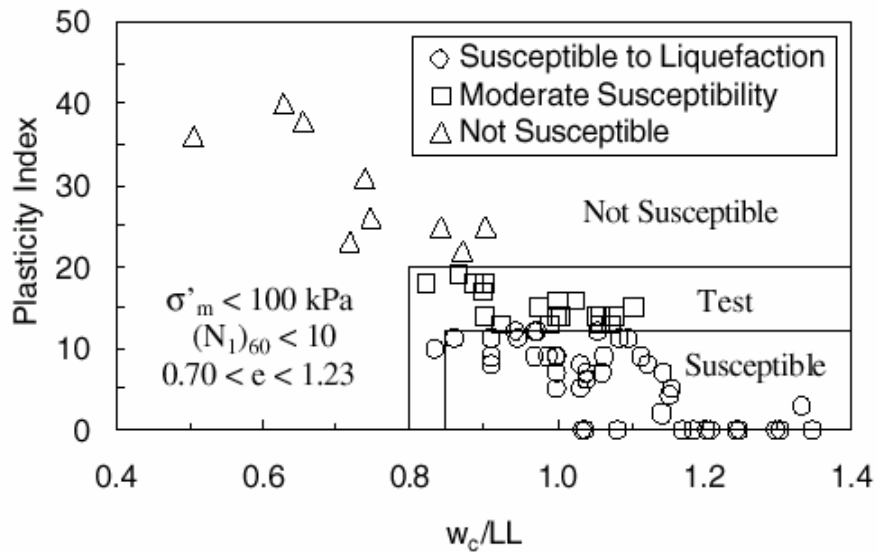


**Fig. 2.4: Criteria for the Evaluation of the Liquefaction Susceptibility of Fine-grained Soils at Low Confining Stresses. (After Bray et al., 2003)**

### 2.3 Assessment of Liquefaction Potential

Quantitative assessment of the likelihood of “triggering” or initiation of liquefaction is the necessary first step for most projects involving potential seismically induced liquefaction. Calculation, or estimation, of two variables is required for evaluation of liquefaction resistance of soils: (1) the seismic demand on a soil layer, expressed in terms of CSR; and (2) the capacity of the soil to resist liquefaction, expressed in terms of CRR. The latter variable has been termed the cyclic stress ratio or the cyclic stress ratio required to generate liquefaction. Definitions of CSR and CRR are given below:

**Cyclic stress ratio (CSR):** As used in the original development of simplified procedure the term cyclic stress ratio refers to both the cyclic stress ratio generated by the earthquake and the cyclic stress ratio required to generate a change of state in the soil to a liquefied condition. To avoid confusion between these two uses cyclic stress ratio refers only to the cyclic stress ratios generated by the earthquake in this text.

**Cyclic resistance ratio (CRR):** The stress ratio required to cause a change of state of the soil to a liquefied condition is referred to throughout this text as the cyclic resistance ratio. This change of terminology is recommended for standard use in engineering practice in NCEER, 1997.

The late Professor H.B. Seed and his co-workers developed a comprehensive approach to estimate the potential for cyclic softening due to earthquake loading. The approach requires an estimate of cyclic stress ratio profile caused by design earthquake. A site-specific seismicity analysis can be carried out to determine the design CSR profile with depth. A simplified method to estimate CSR was also developed by Seed and Idriss in 1971 based on maximum ground surface acceleration ( $a_{max}$ ) at the site. Seed and Idriss also introduced the stress reduction coefficient  $r_d$  as a parameter describing the ratio of cyclic stresses for a flexible soil column to the cyclic stresses for a rigid soil column, as illustrated in Figure 2.5. They obtained values of  $r_d$  for a range of earthquake ground motions and soil profiles having sand in the upper 15± m (50 ft) and suggested an average curve for use as a function of depth. The average curve, which was extended only to a depth of about 12 m (40 ft), was intended for all earthquake magnitudes and for all profiles. This simplified approach can be summarized as follows:

$$CSR_{peak} = \left( \frac{a_{max}}{g} \right) \cdot \left( \frac{\sigma_v}{\sigma'_v} \right) \cdot (r_d) \quad (\text{Eq. 2.1})$$

Where;

- $a_{max}$  = the peak horizontal ground surface acceleration,
- $g$  = the acceleration of gravity,
- $\sigma_v$  = total vertical stress,
- $\sigma'_v$  = effective vertical stress, and
- $r_d$  = the nonlinear shear mass participation factor.

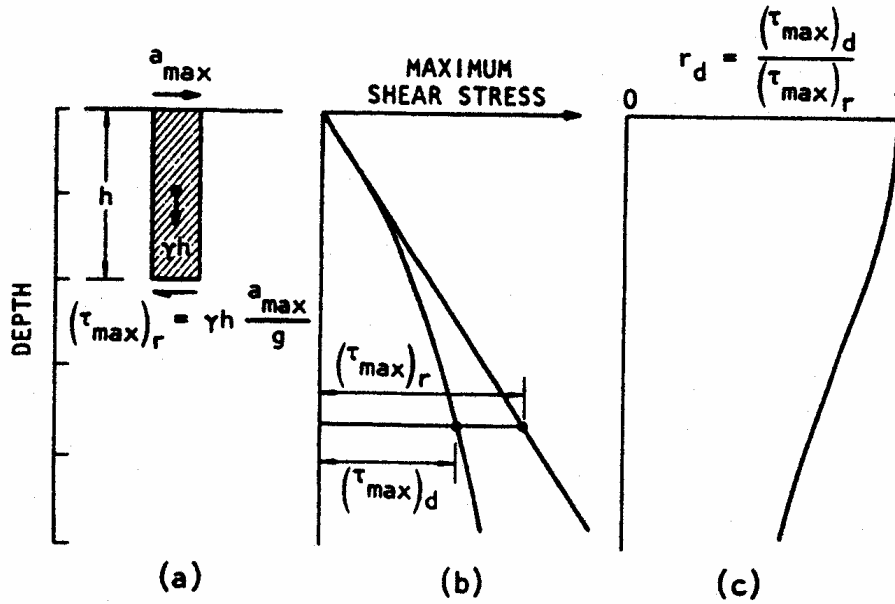
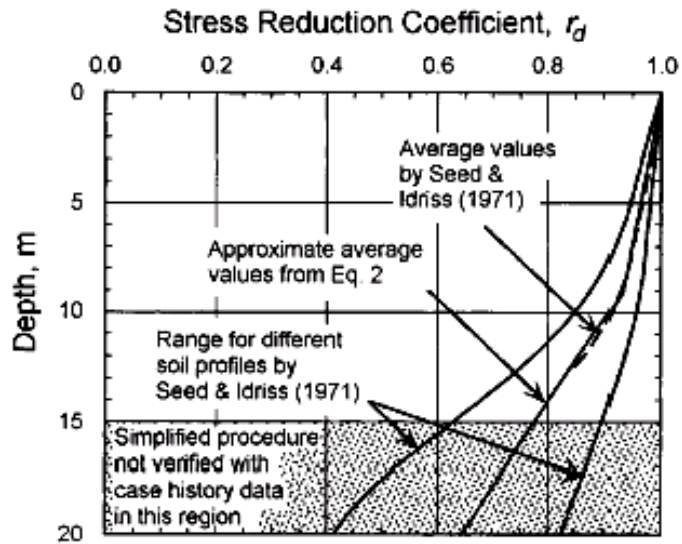


Fig. 2.5: Illustration of Simplified Procedure (After Seed and Idriss, 1971)

The factor  $r_d$  can be estimated using the following tri-linear function, which provides a good fit to the average of suggested range in  $r_d$  originally proposed by Seed and Idriss in 1971.

$$\begin{aligned}
 r_d &= 1.0 - 0.00765 \times z && \text{if } z < 9.15 \text{ m} \\
 r_d &= 1.174 - 0.0267 \times z && \text{if } z = 9.15 \text{ to } 23 \text{ m} \\
 r_d &= 0.744 - 0.008 \times z && \text{if } z = 23 \text{ to } 30 \text{ m} \\
 r_d &= 0.5 && \text{if } z > 30 \text{ m}
 \end{aligned}
 \tag{Eq. 2.2.}$$

The first two formulae in Equation 2.2 were recommended by Liao and Whitman in 1986. The third formula has been added by Robertson and Wride in 1998, to provide a better match with the average of the range in suggested by Seed and Idriss at depths between 23 m and 30 m where  $z$  is depth below ground surface in meters. But some investigators have suggested that evaluation of liquefaction at these greater depths is beyond the depths where the simplified procedure is verified and where routine applications should be applied. Mean values of  $r_d$  calculated from Eq. 2.2 are plotted in Fig. 2.6, along with the mean and range of values proposed by Seed and Idriss.



**Fig. 2.6:  $r_d$  versus Depth Curves Developed by Seed and Idriss (1971) with Added Mean-Value Lines Plotted (After Youd et al., 2001)**

Over the past 25 years “simplified procedure” has evolved as a standard of practice for evaluating the liquefaction resistance of soils. That procedure has been modified and improved periodically since that time, primarily through landmark papers by Seed (1979), Seed and Idriss (1982), and Seed et al. (1985). In 1985, Professor Robert V. Whitman convened workshop on behalf of the National Research Council (NRC) in which 36 experts and observers thoroughly reviewed the state-of-knowledge and the state-of-the-art for assessing liquefaction hazard. That workshop produced a report (NRC 1985) that has become a widely used standard and reference for liquefaction hazard assessment. In January 1996, T. L. Youd and I. M. Idriss convened a workshop of 20 experts to update the simplified procedure and incorporate research findings from the previous decade.

Seed et al. (2001) proposed the use of  $r_d$  values that are not only a function of depth and earthquake magnitude, but also of the level of shaking and the average shear wave velocity over the top 40 ft (12 m) of the site. Cetin and Seed (2000, 2001) propose a new, empirical basis for estimation of  $r_d$  as a function of; (1) depth, (2) earthquake magnitude, (3) intensity of shaking, and (4) site stiffness (as expressed in Equation 2.3).

**d < 19.8 m:**

$$r_d = \left[ \frac{1 + \frac{-23.013 - 2.949 \cdot a_{\max} + 0.999 \cdot M_w + 0.016 \cdot V_{s,40}^*}{16.258 + 0.201 \cdot e^{0.104 \cdot (-d + 0.0785 \cdot V_{s,40}^* + 24.888)}}}{1 + \frac{-23.013 - 2.949 \cdot a_{\max} + 0.999 \cdot M_w + 0.016 \cdot V_{s,40}^*}{16.258 + 0.201 \cdot e^{0.104 \cdot (0.0785 \cdot V_{s,40}^* + 24.888)}}} \right] \pm \sigma_{\varepsilon r_d}$$

**d ≥ 19.8 m:**

$$r_d = \left[ \frac{1 + \frac{-23.013 - 2.949 \cdot a_{\max} + 0.999 \cdot M_w + 0.016 \cdot V_{s,40}^*}{16.258 + 0.201 \cdot e^{0.104 \cdot (-65 + 0.0785 \cdot V_{s,40}^* + 24.888)}}}{1 + \frac{-23.013 - 2.949 \cdot a_{\max} + 0.999 \cdot M_w + 0.016 \cdot V_{s,40}^*}{16.258 + 0.201 \cdot e^{0.104 \cdot (0.0785 \cdot V_{s,40}^* + 24.888)}}} \right] - 0.0014 \cdot (d - 65) \pm \sigma_{\varepsilon r_d}$$

**where**

$$\sigma_{\varepsilon r_d}(d) = d^{0.850} \cdot 0.0072 \quad [\text{for } d < 12.192 \text{ m}], \text{ and}$$

$$\sigma_{\varepsilon r_d}(d) = 40^{0.850} \cdot 0.0072 \quad [\text{for } d \geq 12.192 \text{ m}] \quad (\text{Eq.2.3})$$

The original  $r_d$  values proposed by Seed and Idriss (1971) are shown by the heavy lines in Figure 2.7(a). The numerous light gray lines in Figures 2.7(a) and (b) show the results of 2,153 seismic site response analyses performed by Cetin, 2001 to assess the variation of  $r_d$  over ranges of (1) site conditions, and (2) ground motion excitation characteristics. The mean and  $\pm 1$  standard deviation values for these 2,153 analyses are shown by the heavy lines in Figure 2.7(b). As shown in Figures 2.7(a) and (b), the earlier  $r_d$  proposal of Seed and Idriss (1971) understates the variance, and provides biased (generally high) estimates of  $r_d$  at depths of between 10 and 50 feet (3 to 15 m.) Unfortunately, it is in this depth range that the critical soil strata for most of the important liquefaction (and non-liquefaction) earthquake field case histories occur. This, in turn, creates some degree of corresponding bias in relationships developed on this basis (Seed et al., 2001). In these new correlations, in-situ cyclic stress ratio (CSR) is taken as the “equivalent uniform CSR” equal to 65% of the single (one-time) peak CSR as:

$$CSR_{eq} = (0.65) \cdot CSR_{peak} \quad (\text{Eq. 2.4})$$

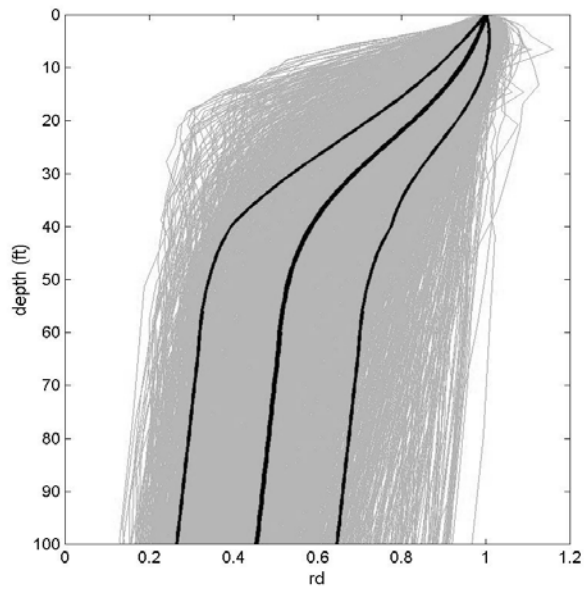
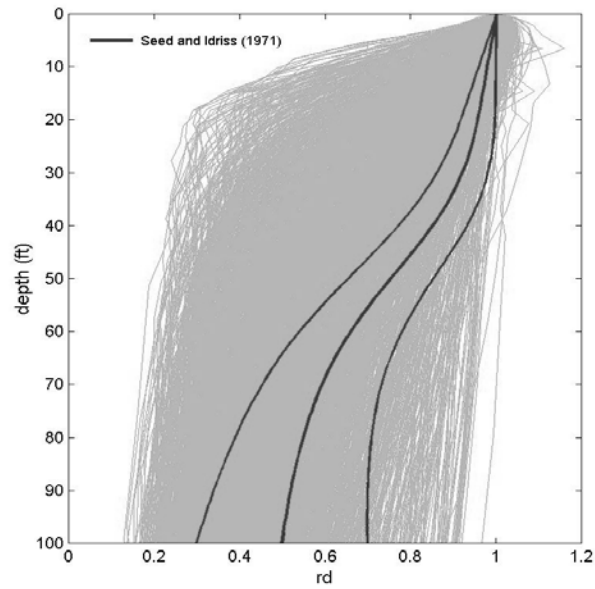


**Fig. 2.7: Rd Results from Response Analyses Superimposed with Heavier Lines Showing (a) the Earlier Recommendations of Seed and Idriss (1971), and (b) the Mean and + 1 Standard Deviation Values (After Seed et al., 2001)**

On the other hand, capacity of the soil to resist liquefaction should also be determined for a complete liquefaction assessment. The CSR profile from the earthquake can be compared to the estimated CRR profile for the soil deposit, adjusted to the same magnitude. There are two general types of approaches available for this: (1) use of laboratory testing of “undisturbed” samples, and (2) use of empirical relationships based on correlation of observed field behavior with various in-situ “index” tests. The use of laboratory testing is complicated by difficulties associated with sample disturbance during both sampling and reconsolidation. It is also difficult and expensive to perform high-quality cyclic simple shear testing, and cyclic triaxial testing poorly represents the loading conditions of principal interest for most seismic problems. Both sets of problems can be ameliorated, to some extent, by use of appropriate “frozen” sampling techniques, and subsequent testing in a high quality cyclic simple shear or torsional shear apparatus. The difficulty and cost of these delicate techniques, however, places their use beyond the budget and scope of most engineering studies. Accordingly, the use of in-situ “index” testing is the dominant approach in common engineering practice.

Criteria for evaluation of liquefaction resistance based on the SPT have been rather robust over the years. Those criteria are largely embodied in the CSR versus  $N_{1,60}$  plot reproduced in Fig. 2.8.  $N_{1,60}$  is the SPT blow count normalized to an overburden pressure of approximately 100 kPa and a hammer energy ratio or hammer efficiency of 60%. The normalization factors for these corrections will be discussed later. Fig. 2.8 is a graph of calculated CSR and corresponding  $N_{1,60}$  data from sites where liquefaction effects were or were not observed following past earthquakes with magnitudes of approximately  $M_w=7.5$ . CRR curves on this graph were conservatively positioned to separate regions with data indicative of liquefaction from regions with data indicative of non-liquefaction. Curves were developed for granular soils with the fines contents of 5% or less, 15%, and 35% as shown on the plot. The CRR curve for fines contents < 5% is the basic penetration criterion for the simplified procedure and is referred to hereafter as the “SPT clean sand base curve.” The CRR curves in Fig. 2.8 are valid only for magnitude 7.5 earthquakes (Youd et al., 2001)

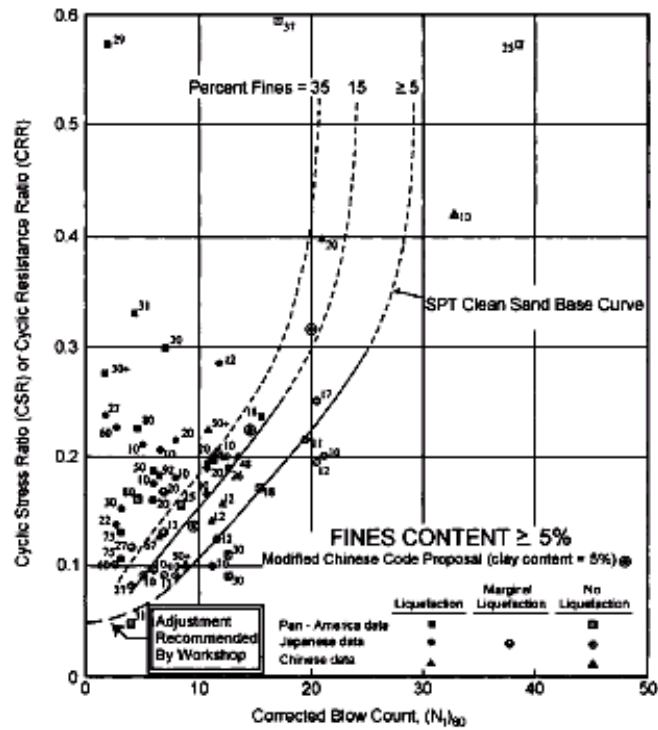


**Fig. 2.8: SPT Clean-Sand Base Curve for Magnitude 7.5 Earthquakes with Data from Liquefaction Case Histories (Modified from Seed et al. 1985)**

Figure 2.9(a) shows the probabilistic relationship proposed by Seed et al. 2001, between duration-corrected equivalent uniform cyclic stress ratio ( $CSR_{eq}$ ), and fines-corrected penetration resistances ( $N_{1,60,cs}$ ), with the correlations as well as all field data shown normalized to an effective overburden stress of  $\sigma'_v = 0.65 \text{ atm. (1,300 lb/ft}^2\text{)}$ . The contours shown (solid lines) are for probabilities of liquefaction of  $P_L=5\%$ ,  $20\%$ ,  $50\%$ ,  $80\%$ , and  $95\%$ . These are superposed (dashed lines) with the relationship proposed by Seed et al., 1984 for reference. As shown in this figure, the “clean sand” (Fines Content  $\leq 5\%$ ) line of Seed et al. (1984) appears to correspond roughly to  $P_L \approx 50\%$ . This is not the case, however, as the Seed et al., 1984 line was based on biased values of CSR (as a result of biased  $r_d$  at shallow depths, as discussed in Cetin, 2001). The new correlation uses actual event-specific seismic site response analyses for evaluation of in situ CSR in 53 of the back-analyzed case histories, and the new (and statistically unbiased) empirical

estimation of  $r_d$  (as a function of level of shaking, site stiffness, and earthquake magnitude) as presented in Equation 2.3 and Figure 2.7 for the remaining 148 case histories. The new (improved) estimates of in-situ CSR tend to be slightly lower, typically on the order of ~ 5 to 15% lower, at the shallow depths that are critical in most of the case histories. Accordingly, the CSR's of the new correlation are also, correspondingly, lower by about 5 to 15%, and a fully direct comparison between the new correlation and the earlier recommendations of Seed et al., 1984 can not be made. It was Seed's intent that the recommended (1984) boundary should represent approximately a 10 to 15% probability of liquefaction, and with allowance for the "shift" in (improved) evaluation of CSR, the 1984 deterministic relationship for clean sands (<5% fines) does correspond to approximately  $P_L \approx 10$  to 30%, except at very high CSR (CSR > 0.3), a range in which data was previously scarce (Seed et al., 2001).

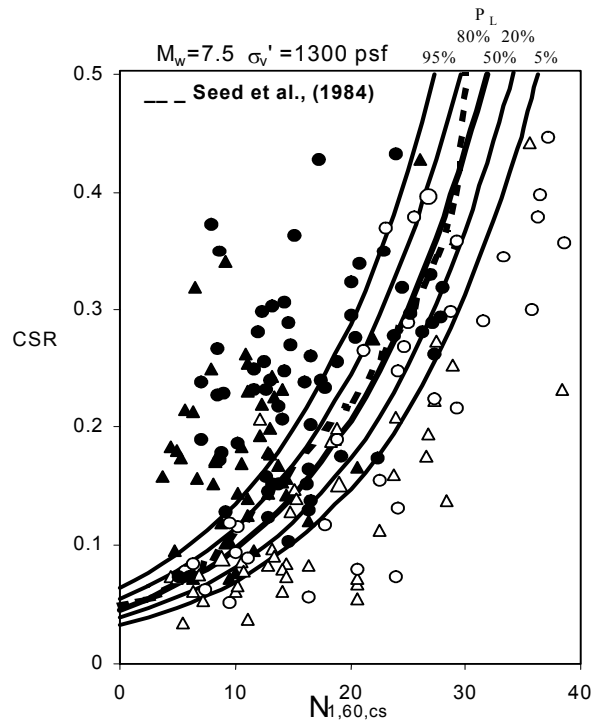


**Fig. 2.9(a): Recommended Probabilistic SPT-Based Liquefaction Triggering Correlation (for Mw=7.5) (After Seed et al., 2001)**

The new (probabilistic) boundary curve for  $P_L = 20\%$  (again normalized to an effective overburden stress of  $\sigma'_v = 0.65$  atm.) represents a suitable basis for illustration of the new correlation's regressed correction for the effects of fines content, as shown in Figure 2.9(b). In this figure, both the correlation as well as the mean values (CSR and  $N_{1,60}$ ) of the field case history data are shown not corrected for fines (this time the N-value axis is not corrected for fines content effects, so that the ( $P_L=20\%$ ) boundary curves are, instead, offset to account for varying fines content.) In this figure, the earlier correlation proposed by Seed et al., 1984 is also shown (with dashed lines) for approximate comparison (Seed et al., 2001).

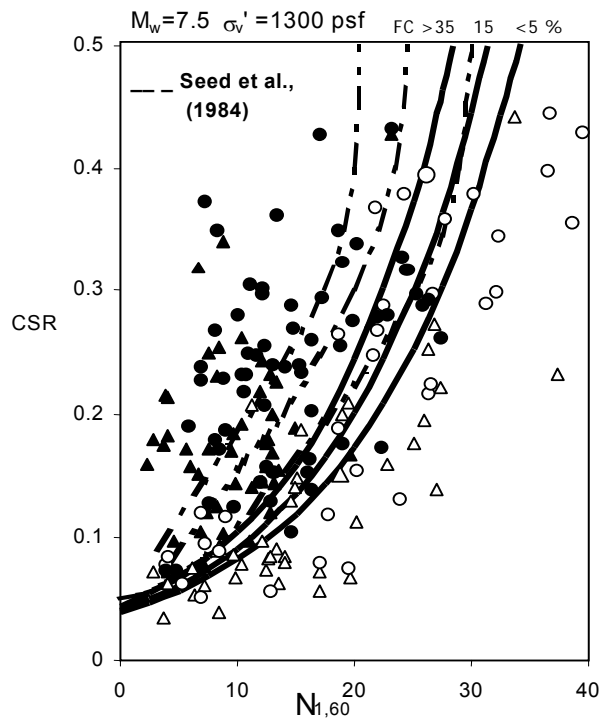


**Fig. 2.9(b): Recommended “Deterministic” SPT-Based Liquefaction Triggering Correlation (for  $M_w=7.5$ ), with Adjustments for Fines Content (After Seed et al. 2001)**

The overall correlation can be expressed concisely as a single, composite relationship as shown in Equations 2.5 and 2.6.

$$P_L(N_{1,60}, CSR, M_w, \sigma'_v, FC) = \Phi \left[ \frac{\left( N_{1,60} \cdot (1 + 0.004 \cdot FC) - 13.32 \cdot \ln(CSR) - 29.53 \cdot \ln(M_w) - 3.70 \cdot \ln(\sigma'_v) + 0.05 \cdot FC + 44.97 \right)}{2.70} \right]$$

(Eq. 2.5)

where

$P_L$  = the probability of liquefaction in decimals (i.e. 0.3, 0.4, etc.)

$\Phi$  = the standard cumulative normal distribution. Also the cyclic resistance ratio, CRR, for a given probability of liquefaction can be expressed as:

$$CRR(N_{1,60}, CSR, M_w, \sigma'_v, FC, P_L) = \exp \left[ \frac{\left( N_{1,60} \cdot (1 + 0.004 \cdot FC) - 29.53 \cdot \ln(M_w) - 3.70 \cdot \ln(\sigma'_v) + 0.05 \cdot FC + 44.97 + 2.70 \cdot \Phi^{-1}(P_L) \right)}{13.32} \right]$$

(Eq. 2.6)

where

$\Phi^{-1}(P_L)$  = the inverse of the standard cumulative normal distribution (i.e. mean=0, and standard deviation=1)

note: for spreadsheet purposes, the command in Microsoft Excel for this specific function is "NORMINV( $P_L$ ,0,1)"

All N-values used in these correlations were corrected for overburden effects (to the hypothetical value,  $N_1$ , that "would" have been measured if the effective overburden stress at the depth of the SPT had been 1 atmosphere) [1 atm.  $\approx$  2,000 lb/ft<sup>2</sup>  $\approx$  1 kg/cm<sup>2</sup>  $\approx$  14.7 lb/in<sup>2</sup>  $\approx$  101 kPa] as:

$$N_1 = N \cdot C_N \quad (\text{Eq. 2.7(a)})$$

Where  $C_N$  is taken (after Liao and Whitman, 1986) as:

$$C_N = \left( \frac{1}{\sigma'_v} \right)^{0.5} \quad (\text{Eq. 2.7(b)})$$

Where  $\sigma'_v$  is the actual effective overburden stress at the depth of the SPT in atmospheres.

The resulting  $N_1$  values should then further corrected for energy, equipment, and procedural effects to fully standardized  $N_{1,60}$  values as:

$$N_{1,60} = N_1 \cdot C_R \cdot C_S \cdot C_B \cdot C_E \quad (\text{Eq. 2.8})$$

Where  $C_R$  = correction for “short” rod length,

$C_S$  = correction for non-standardized sampler configuration,

$C_B$  = correction for borehole diameter, and

$C_E$  = correction for hammer energy efficiency.

The corrections for  $C_R$ ,  $C_S$ ,  $C_B$  and  $C_E$  employed correspond largely to those recommended by the NCEER Working Group (NCEER, 1997). Table 2.1 summarizes the correction factors used in this study. The correction for “short” rod length between the driving hammer and the penetrating sampler was taken as a nonlinear “curve” (Figure 2.10), rather than the incremental values of the NCEER Workshop recommendations, but the two agree well at all NCEER mid-increments of length.  $C_S$  was applied in cases wherein a “nonstandard” (though very common) SPT sampler was used in which the sampler had an internal space for sample liner rings, but the rings were not used. This results in an “indented” interior liner annulus of enlarged diameter, and reduces friction between the sample and the interior of the sampler, resulting in reduced overall penetration resistance (Seed et al., 1984 and 1985). The reduction in penetration resistance is on the order of ~10 % in loose soils ( $N_1 < 10$  blows/ft), and ~30 % in very dense soils ( $N_1 > 30$  blows/ft), so  $C_S$  varied from 1.1 to 1.3 over this range. Borehole diameter corrections ( $C_B$ ) were as recommended in the NCEER Workshop Proceedings. Corrections for hammer energy ( $C_E$ ), which were often significant, were largely as recommended by the NCEER Working Group, except in those cases where

better hammer/system-specific information was available. Cases where better information was available included cases where either direct energy measurements were made during driving of the SPT-sampler, or where the hammer and the raising/dropping system (and the operator, when appropriate) had been reliably calibrated by means of direct driving energy measurements.

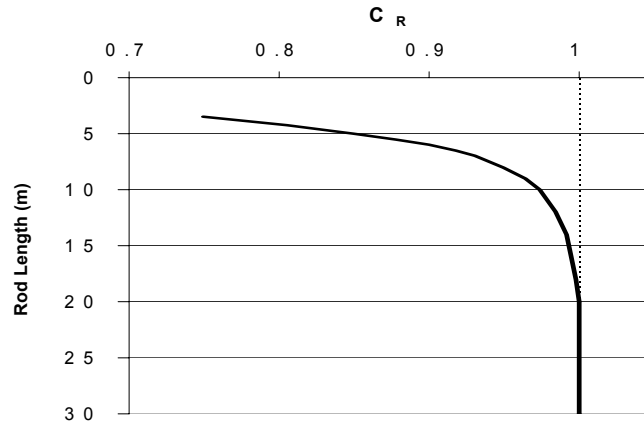


**Fig. 2.10: Recommended CR Values (rod length from point of hammer impact to tip of sampler). (After Seed et al., 2001)**

Additionally, in these current studies, based on the overall (regressed) correlation, the energy- and procedure- and overburden-corrected N-values ( $N_{1,60}$ ) are further corrected for fines content as:

$$N_{1,60,CS} = N_{1,60} \cdot C_{FINES} \quad (\text{Eq. 2.9})$$

Where the fines correction was “regressed” as a part of the Bayesian updating analyses. The fines correction is equal to one for fines contents of  $FC \leq 5\%$ , and reaches a maximum (limiting) value for  $FC \geq 35\%$ .

The regressed relationship for  $C_{FINES}$  is

$$C_{FINES} = (1 + 0.004 \cdot FC) + 0.05 \cdot \left( \frac{FC}{N_{1,60}} \right)$$

$$\text{Limits: } FC \geq 5\% \text{ and } FC \leq 35\% \quad (\text{Eq. 2.10})$$

Where  $FC$  = percent fines content, expressed as an integer (e.g. 15% as 15).

**Table 2.1: Corrections for SPT Equipment, Energy and Procedures (After Seed et al., 2001)**

$C_R$	(See Fig. 2.10 for Rod Length Correction Factors)															
$C_S$	<p>For samplers with an indented space for interior liners, but with liners omitted during sampling,</p> $C_S = 1 + (N_{1,60}/100) \quad \text{(Eq. T-1)}$ <p>With limits as <math>1.10 \leq C_S \leq 1.30</math></p>															
$C_B$	<table border="1"> <thead> <tr> <th><u>Borehole diameter</u></th> <th><u>Correction (<math>C_B</math>)</u></th> </tr> </thead> <tbody> <tr> <td>65 to 115 mm</td> <td>1.00</td> </tr> <tr> <td>150 mm</td> <td>1.05</td> </tr> <tr> <td>200 mm</td> <td>1.15</td> </tr> </tbody> </table>	<u>Borehole diameter</u>	<u>Correction (<math>C_B</math>)</u>	65 to 115 mm	1.00	150 mm	1.05	200 mm	1.15							
<u>Borehole diameter</u>	<u>Correction (<math>C_B</math>)</u>															
65 to 115 mm	1.00															
150 mm	1.05															
200 mm	1.15															
$C_E$	<p><math>C_E = ER/60 \quad \text{(Eq. T-2)}</math></p> <p>where ER (efficiency ratio) is the fraction or percentage of the theoretical SPT impact hammer energy actually transmitted to the sampler, expressed as %</p> <ul style="list-style-type: none"> <li>The best approach is to directly measure the impact energy transmitted with each blow. When available, direct energy measurements were employed.</li> <li>The next best approach is to use a hammer and mechanical hammer release system that has been previously calibrated based on direct energy measurements.</li> <li>Otherwise, ER must be estimated. For good field procedures, equipment and monitoring, the following guidelines are suggested:</li> </ul> <table border="1"> <thead> <tr> <th><u>Equipment</u></th> <th><u>Approximate ER (see Note 3)</u></th> <th><u><math>C_E</math> (see Note 3) -</u></th> </tr> </thead> <tbody> <tr> <td><u>Safety Hammer<sup>1</sup></u></td> <td>0.4 to 0.75</td> <td>0.7 to 1.2 -Donut</td> </tr> <tr> <td><u>Hammer<sup>1</sup></u></td> <td>0.3 to 0.6</td> <td>0.5 to 1.0</td> </tr> <tr> <td><u>-Donut Hammer<sup>2</sup></u></td> <td>0.7 to 0.85</td> <td>1.1 to 1.4</td> </tr> <tr> <td><u>-Automatic-Trip Hammer</u></td> <td>0.5 to 0.8</td> <td>0.8 to 1.4</td> </tr> </tbody> </table> <p>(Donut or Safety Type)</p> <ul style="list-style-type: none"> <li>For lesser quality fieldwork (e.g. irregular hammer drop distance, excessive sliding friction of hammer on rods, wet or worn rope on cathead, etc.) further judgmental adjustments are needed.</li> </ul>	<u>Equipment</u>	<u>Approximate ER (see Note 3)</u>	<u><math>C_E</math> (see Note 3) -</u>	<u>Safety Hammer<sup>1</sup></u>	0.4 to 0.75	0.7 to 1.2 -Donut	<u>Hammer<sup>1</sup></u>	0.3 to 0.6	0.5 to 1.0	<u>-Donut Hammer<sup>2</sup></u>	0.7 to 0.85	1.1 to 1.4	<u>-Automatic-Trip Hammer</u>	0.5 to 0.8	0.8 to 1.4
<u>Equipment</u>	<u>Approximate ER (see Note 3)</u>	<u><math>C_E</math> (see Note 3) -</u>														
<u>Safety Hammer<sup>1</sup></u>	0.4 to 0.75	0.7 to 1.2 -Donut														
<u>Hammer<sup>1</sup></u>	0.3 to 0.6	0.5 to 1.0														
<u>-Donut Hammer<sup>2</sup></u>	0.7 to 0.85	1.1 to 1.4														
<u>-Automatic-Trip Hammer</u>	0.5 to 0.8	0.8 to 1.4														

Notes: (1) Based on rope and cathead system, two turns of rope around cathead, "normal" release (not the Japanese "throw"), and rope not wet or excessively worn.

(2) Rope and cathead with special Japanese "throw" release.

(3) For the ranges shown, values roughly central to the mid-third of the range are more common than outlying values, but ER and  $C_E$  can be even more highly variable than the ranges shown if equipment and/or monitoring and procedures are not good.

## **CHAPTER 3**

### **SITE - SPECIFIC RESPONSE ANALYSES AND RESULTS OF THE ANALYSES**

#### **3.1 Introduction**

The influence of local soil conditions on the nature of earthquake damage has been recognized for many years. Since the early observations, the effects of local site conditions on ground motions have been illustrated in earthquakes around the world. More recently, the availability of strong ground motion instruments has allowed local site effects to be measured quantitatively in recent years. Despite considerable evidence, the existence of local site effects was a matter of some debate in past years. Indeed, provisions specifically accounting for local site effects did not appear in building codes until 1970's. On the other hand, since the 1920's seismologist and, more recently, geotechnical earthquake engineers have worked toward the development of quantitative methods for predicting the influence of local soil conditions on strong ground motion (Kramer, 1996).

In this chapter, the efforts on database compilation and the methodology used in site-specific response analyses will be summarized. Geotechnical characteristics of the local soils in Adapazarı were evaluated using the deep and shallow borehole logs and measured parameters from field and laboratory. This data is employed for developing representative one-dimensional site response models, and these models are used in site-specific response analysis. The main shock record in Sakarya strong ground motion station is situated over the site response models after proper deconvolution. The results of these analyses are digitized in order to select and determine the

parameters that should be correlated with the building damage. The spatial distribution of these parameters is provided in Section 3.4. The characteristics of the ground motion are seemed to be significantly differing due to the local soil conditions, which effects the overall distribution of building damage in the city. Relationship between distribution of building damage and selected strong ground motion parameters will be investigated in details later in Chapter 5.

### **3.2 Compilation of Necessary Parameters for Site Specific Response Analysis**

General Directorate of Disaster Affairs (GDDA) has organized a database compilation program for the purpose of officially documenting subsurface investigation studies performed in the city of Sakarya. For the purpose, over a thousand of bore logs were accessed, reviewed and screened for data quality purpose and the resulting database composed of 263 boring logs of high quality data including both laboratory and field test results as summarized in Table 3.1. The standard penetration test results are available for each borehole, where only limited number of cone penetration and shear wave tests performed through the program. Laboratory tests are also applied to one or more samples taken from each borehole in order to determine the Atterberg Limits of the cohesive soils, unit weight, water content and fines content of soil profile at various depths.

**Table 3.1: Summary of Available Data in the Database**

263 boring logs
Coordinates of borings
Borehole log descriptions
Elevation of groundwater table for each boring
2334 SPT blow-count values
Water content and USCS description of 940 soil samples retrieved from various depths
Sieve analysis and Atterberg Limits test results from 908 soil samples

Figure 3.1 shows the locations of the boring logs throughout the Sakarya city. Blue lines show the areas where most of the population of Adapazarı is settled. Red lines border the area under the interest for this study. As the figure implies, the density of the boreholes increases in the northern part due to the increase of the building stock in northern Sakarya. The distribution of the boreholes is concluded to be representative and subsurface soil data as well as strong ground motion data enabled a site specific soil response and liquefaction triggering assessments.

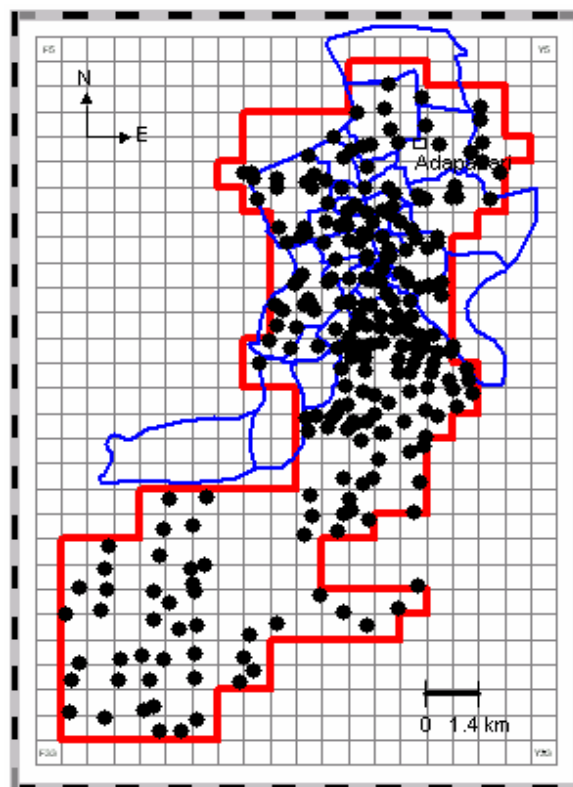


**Fig. 3.1: Location of Boreholes throughout Sakarya City and City Limits.**

Necessary parameters for site-specific response analysis are available in the database compiled by GDDA. These parameters are listed below:

- i. Shear wave velocities of soil layers through depth
- ii. Unit weight of the soil layers
- iii. Plastic limit and plasticity index values for clay layers.

### 3.2.1 Determination of Shear Wave Velocities

One of the most commonly cited  $V_s$  correlations for cohesionless soils is that with the penetration resistance obtained from the standard penetration test. Correlation studies conducted primarily in the United States and Japan have resulted in numerous relations for the variation of shear wave velocity with penetration resistance. Several of the more widely referenced N-based  $V_s$  relationships are listed in Table 3.2 and illustrated in Figure 3.2. As the figure implies, the relationship proposed by Seed and others in 1983 seems to be an upper boundary, while the relations by Sykora and Stokoe (1983) and Dickenson (1994) provide roughly similar trends. The estimated shear wave velocities using both relations are compared with the available field test results. The relationship proposed by Dickenson (1994) results in closer values to the real ones, so this correlation is used in order to determine the shear wave velocities of soil layers in this study. The most appropriate soil types of soil for the proposed relation are shown in Table 3.2, but these correlations are also valid for other types of soils.

**Table 3.2: The Correlations Used in Converting SPT-N Values to Shear Wave Velocities**

STUDY BY	APPROPRIATE FOR	PROPOSED RELATION
SEED ET AL. (1983)	Sands And Silty Sands	$V_s = 185N_{60}^{0.5}$
SYKORA AND STOKOE (1983)	Granular Soils	$V_s = 330 N_{60}^{0.29}$
DICKENSON (1994)	Sands	$V_s = 290(N_{60}+1)^{0.29}$
OHTA AND GOTO (1978)	Holocene Sands	$V_s = 194(N_{60}^{0.173})(z^{0.195})$
	Pleistocene Sands	$V_s = 254(N_{60}^{0.173})(z^{0.195})$

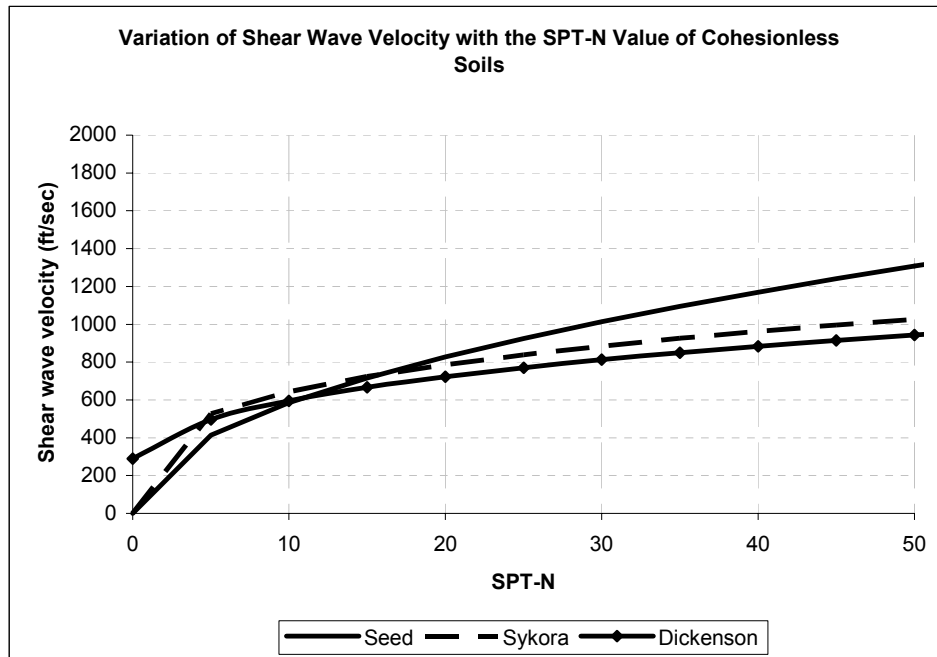


**Fig. 3.2: The Correlations Used in Converting SPT-N Values to Shear Wave Velocities**

### 3.2.2 Determination of Unit Weight of the Soil Samples

Subsurface investigation program performed in Adapazarı includes soil sampling for the laboratory testing in addition to the field tests. 208 soil samples are tested in the laboratory in order to determine the unit weight and specific gravity of soil in this study. But the results of these tests are limited and only representative for the depth that the sample is taken. The scatter of the unit weight values is used for generating a general unit weight value (Figure 3.3). Arithmetic mean of the values is found to be  $18.430 \text{ kN/m}^3$ .

Unit weight of each soil layer is necessary for site-specific response analysis. The value determined in the laboratory is used if a sample representing this layer is taken. Otherwise, the mean of laboratory results is used. Unit weight values used in this study are summarized in the Table 3.3 given below.

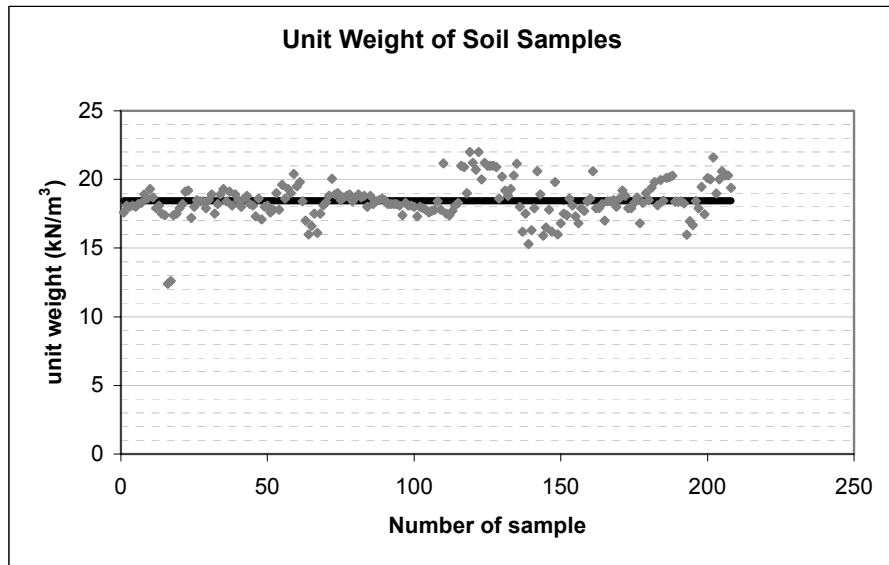


**Fig. 3.3: The Scatter of the Unit Weight of Soil Samples Tested in the Laboratory**

**Table 3.3: The Unit Weight Values Used in Response Analyses**

SOIL TYPE	UNIT WEIGHT (kN/m <sup>3</sup> )	UNIT WEIGHT (Kcf)
All soils	18.430	0.115
Soft rock	19.231	0.120
Bedrock	20.032	0.125

### 3.2.3 Effects of Plasticity of Clay Layers on Soil Response

Plasticity is an important characteristic in the case of fine-grained soils, the term plasticity describing the ability of a soil to undergo unrecoverable deformation at constant volume without cracking or crumbling. Plasticity is due

to the presence of a significant content of clay minerals or organic material. In general, depending on its water content, a soil may exist in one of the liquid, plastic, semi-solid and solid states. The water contents at which the transitions between states occur vary from soil to soil, depending on the interaction between the clay mineral particles. The upper and lower limits of the range of water content over which the soil exhibits plastic behavior are defined as *liquid limit (LL)* and the *plastic limit (PL)* respectively. The water content range itself is defined as the *plasticity index (PI)* (Craig, 1992).

Zen et al. (1978) and Kokushu et al. (1982) first noted the influence of soil plasticity on the shape of modulus reduction curve; the shear modulus of highly plastic soils was observed to degrade more slowly with shear strain than did low-plasticity soils. After reviewing experimental results from a board range of materials, Dobry and Vucetic (1987) and Sun et al. (1988) concluded that the shape of the modulus reduction curve is influenced more by plasticity index than by the void ratio and presented curves of the type is shown in Figure 3.4. These curves show that the linear cyclic threshold shear strain is greater for highly plastic soils than for soils of low plasticity. This characteristic is extremely important; it can strongly influence the manner which a soil deposit will amplify or attenuate earthquake motions.

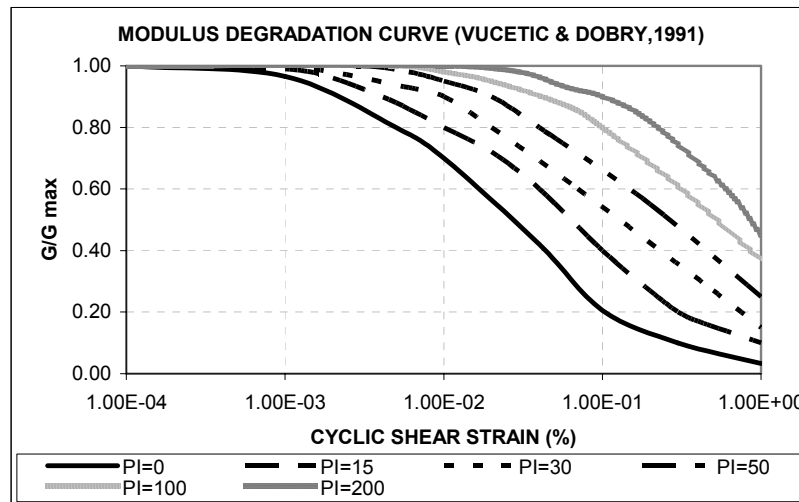


**Fig. 3.4: Modulus Reduction Curves for Fine-Grained Soils of Different Plasticity (After Vucetic And Dobry, 1991)**

The  $PI=0$  modulus reduction curve from Figure 3.4 is very similar to the average modulus reduction curve that was commonly used by sands (Seed and Idriss, 1970) when coarse and fine-grained soils were treated separately (Figure 3.5). This similarity suggests that the modulus reduction curves of Figure 3.5 may be applicable to both fine and coarse-grained soils (Kramer, 1996).

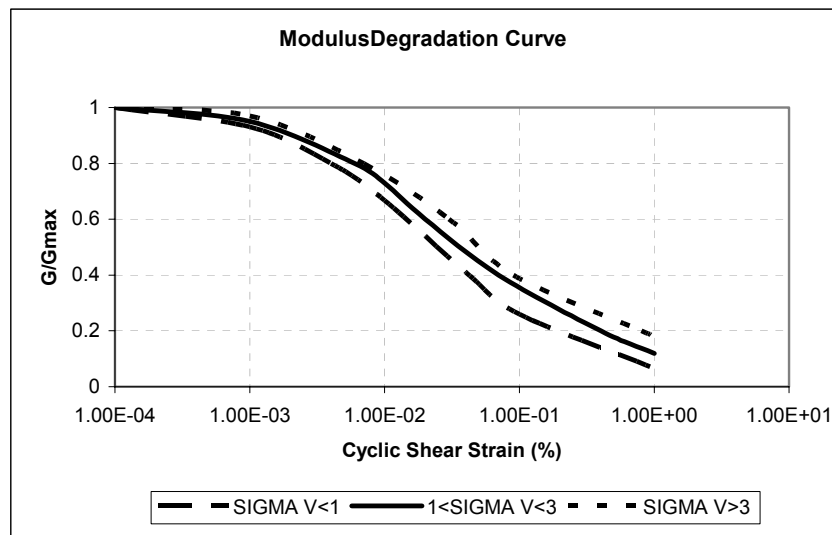


**Fig. 3.5: Modulus Reduction Curves for Sands (After Seed And Idriss, 1970)**

Just as modulus of reduction behavior is influenced by plasticity characteristics, so is damping behavior (Kokushu et al. (1982), Dobry and Vucetic (1987), Sun et al. (1988)). Damping ratios of highly plastic soils are lower than those of low plasticity soils at the same cyclic strain amplitude (see Figure 3.6).

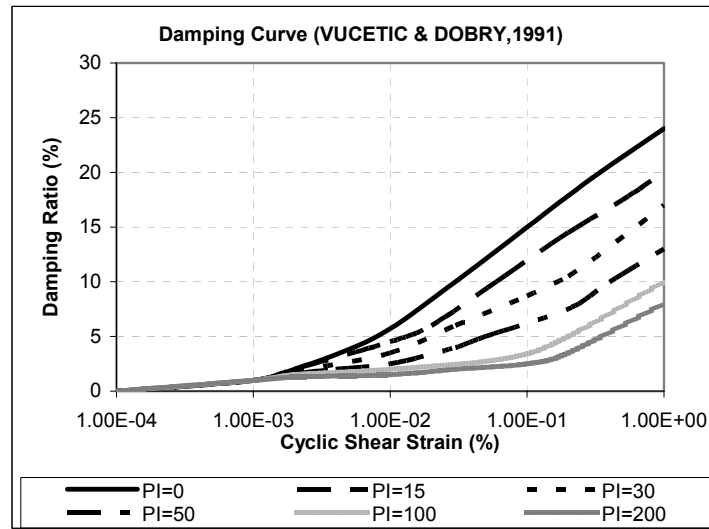


**Fig. 3.6: Damping Curves for Fine-Grained Soils of Different Plasticity (After Vucetic And Dobry, 1991)**

The PI=0 damping curve from Figure 3.6 is nearly identical to the average damping curve that was used for coarse-grained soils when they were treated separately from fine-grained soils. The damping behavior of gravel is very similar to that of sand (Seed et al., 1984).

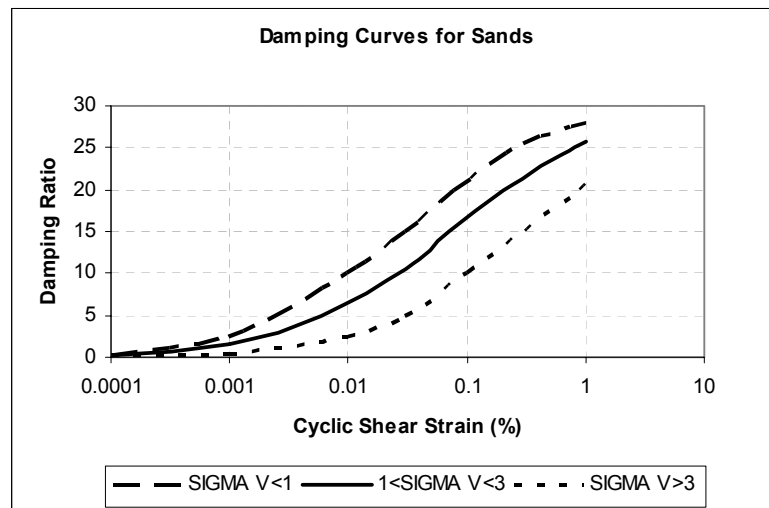


**Fig. 3.7: Damping Curves for Sands (After Seed And Idriss, 1970)**

Determination of the Atterberg limits of the cohesive soils is one of the most important tasks in the subsurface investigation program performed in Adapazarı. For this purpose, 753 soil samples taken throughout the city of Adapazarı were tested in the laboratory. Results of the tests are summarized in the Figure 3.8 below. As the figure implies the maximum value that PI takes is equal to 60 for the soils in Adapazarı. Due to the analysis results, the modulus degradation and damping curves for PI=30 and PI=50 are used for clays in the response analyses. Similarly, modulus degradation and damping curves for PI=15 are preferred for silt layers. The list of modulus degradation and damping curves used in this study is tabulated and given in Appendix A.

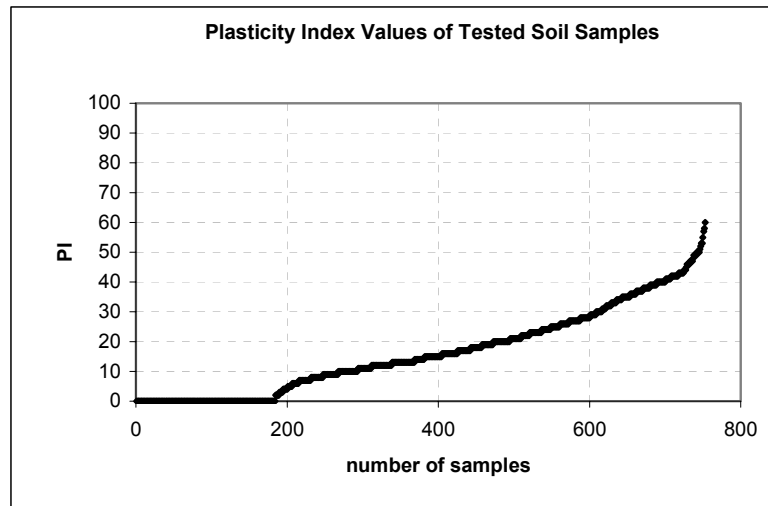


**Fig. 3.8: Plasticity Index Values of Tested Soil Samples**

### **3.3 Preparation of Input Files**

#### **3.3.1 Determination of Input Soil Profiles**

Adapazarı is located at the edge of a sedimentary basin called by the name of the city. Thick sediments of clay underlie the basin, which is a former lakebed. Quaternary alluvium, primarily consisting of silt and fine sand, deposited by Sakarya River and its tributaries overlay the lake sediments. A

deep boring recently performed in Yenigün District by the State Hydraulic Works did not reach bedrock at a depth of 200 m (Bakır et al., 2002). The shallow soils (10 m) are recent deposits laid down by the Sakarya and Çark rivers, which frequently flooded the area until flood control dams were built recently. Sands accumulated along bends of the meandering rivers, and the rivers flooded periodically leaving behind predominantly non-plastic silts, silty sands, and clays throughout the city. Clay-rich sediments were deposited in lowland areas where floodwaters pounded (Sancio et al., 2002)

Depth to the bedrock exceeds 300 m at several locations over the basin. Variation of the bedrock depth underneath the city is depicted in Figure 3.9 (Sakarya University, 1998). Accordingly, thickness of the alluvium is highly variable, increasing from a few meters on the south to north, reaches 200 m under the densely urbanized central section, parts of which constitute earlier marshland dried-up with the continued development.

In the course of this study, the database compiled by General Directorate of Disaster Affairs (GDDA) for the purpose of officially documenting subsurface investigation studies performed in the city of Adapazarı was used. Over a thousand of bore logs were accessed from all possible sources, reviewed and screened for data quality purpose and the resulting database is composed of 263 boring logs of high quality data including both laboratory and field test.

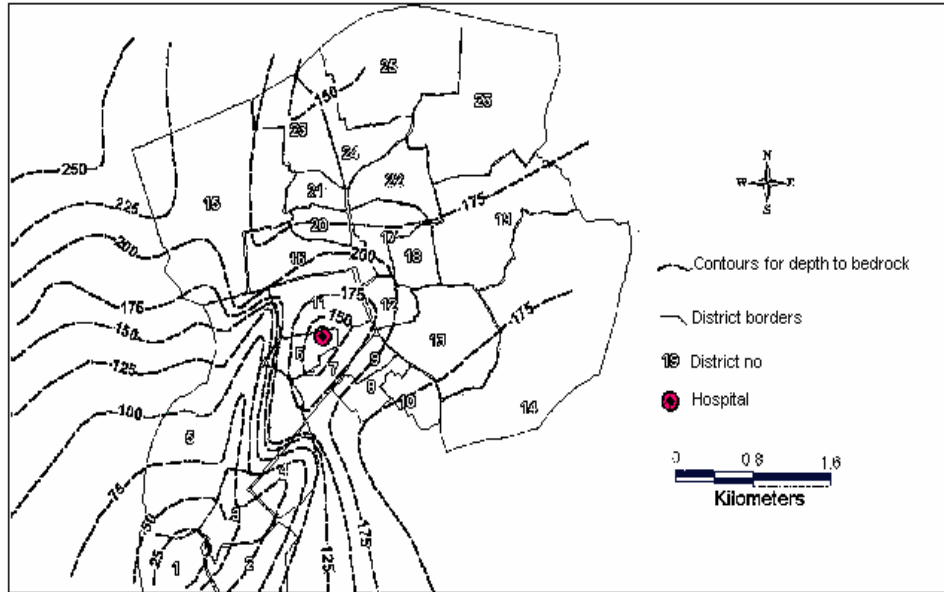


**Fig. 3.9: Variation of Bedrock Depth throughout Adapazarı (Sakarya University, 1998)**

In order to consolidate the data points and determine the topsoil profile of Adapazarı, following steps were made:

- i. For the sake of simplicity, city of Adapazarı was divided into 150 grids (each of which has 500 x 500 m dimensions).
- ii. Boring logs from various sources (Sakarya University, GDDA and others) were collected and classified due to their locations. Figure 3.10 shows an example of borehole data corresponding to Grid No: Q10. List of grids and corresponding boreholes are given in Appendix B-1.

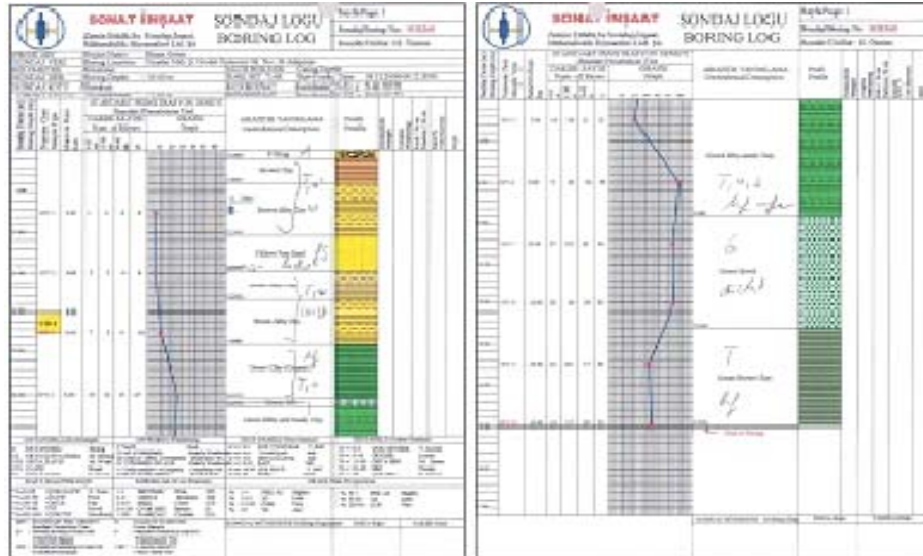


**Fig. 3.10: Borehole Data Corresponding To Grid No: Q10**

- iii. The database was consolidated based on the reliability and consistency of the borehole data corresponding to a grid, and representative soil profile for each grid was determined. Figure 3.11 shows the representative soil profile for Grid No: Q10.

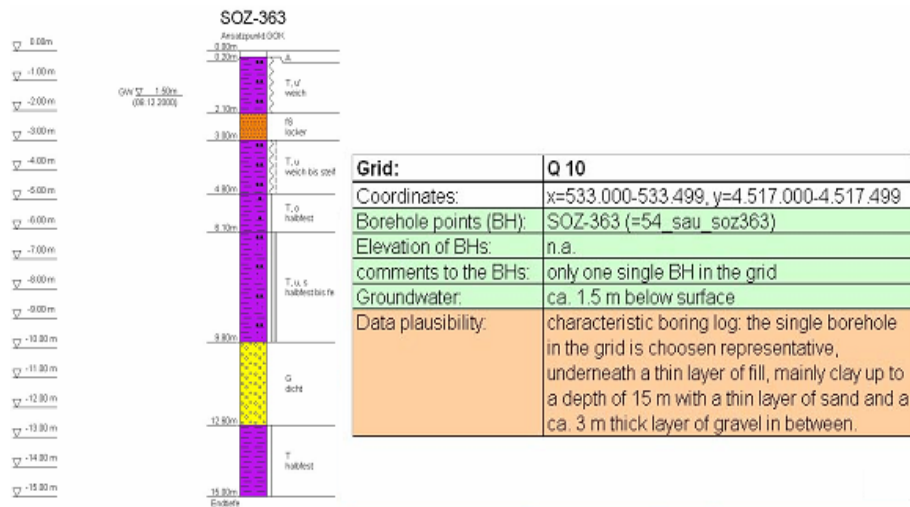


**Figure 3.11: Representative Soil Profile For Grid No: Q10**

- iv. Using the representative soil profiles for each grid and necessary parameters calculated due to test results (defined in part 3.2) input topsoil profile for each borehole was determined.

These profiles were used for the first 10 m of the soil profile since the majority of the borehole data is limited to this depth. For the rest of the soil profile, a different set of borehole data was used. This second set of boreholes reaching up to 150 m depth, drilled by the State Hydraulic Works to assess the ground water reserve in the area. While results of field and laboratory tests on extracted disturbed and undisturbed samples were available for the first set of boreholes, no such tests are conducted for the second set. Logs of deep boreholes, however, reveal useful qualitative information regarding types of soils and stratification of profile. Thick layers of occasionally silty and sandy clay are observed to underlie the surface soils consistently in the logs of all four deep boreholes, none of which attaining the bedrock. Available data within limited depths up to 50 m indicate a consistency range generally between stiff to hard and a highly variable plasticity index range (17-58%). Clays persist until the end of boreholes, except being intersected by strata of gravel of valuable thickness below a depth of 80 m [4]. Logs of all four available deep boreholes are presented in Figure 3.12. Using this information, the soil profile between the bedrock and topsoil is modeled. Figure 3.13 shows the model and parameters used for site-specific response analysis in this study. The soil profiles used in this study and list of boreholes and corresponding grid numbers are given in Appendix B.

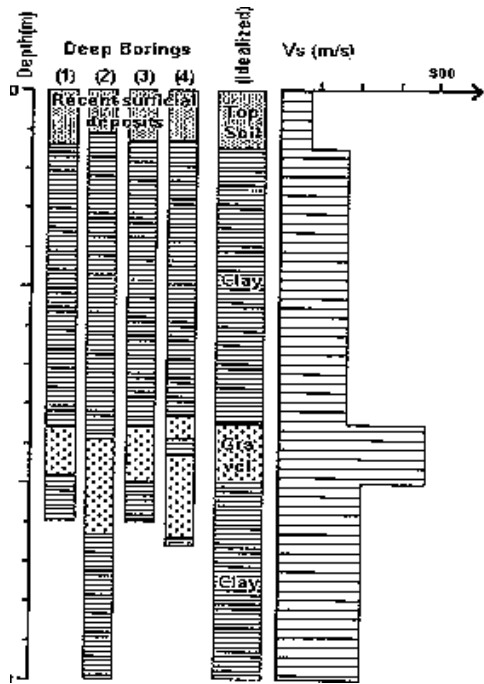


Figure 3.12: Second Set Of Borehole Logs (Deep)

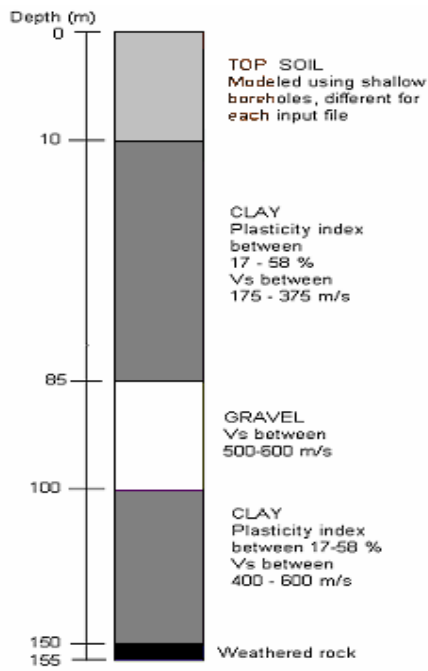
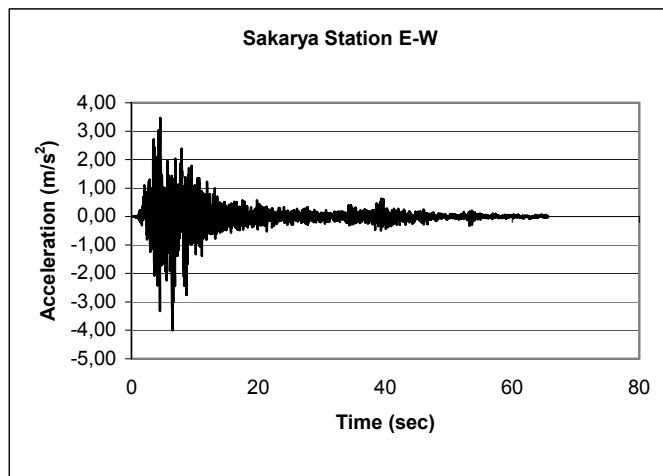


Figure 3.13: Modeled Deep Borehole Logs

### 3.3.2 Input Strong Ground Motion

The strong motion stations operated by the General Directorate of Disaster Affairs, the Kandilli Observatory and Earthquake Research Institute of Bogazici University and Istanbul Technical University have produced at least 27 strong motion records for the Kocaeli earthquake within 200 km of the fault. Kocaeli earthquake has generated six motions within 20 km of the fault (Sakarya, Yarimca, Izmit, Düzce, Arcelik, and Gebze), adding significantly to the near-field database of ground motions for  $M_w \geq 7.0$  strike-slip earthquakes (Erdik, 2003). The two stations closest to the fault rupture are Sakarya (located in southwestern Adapazarı at a distance of 3.3 km) and Yarimca (4.4 km). Sakarya is founded on stiff soil, while Yarimca is founded on soft soil. The acceleration vs. time (east – west) plot recorded at Sakarya strong ground motion station is provided in Figure 3.14. The Sakarya station recorded a peak horizontal (east–west) ground acceleration (PGA), velocity, and displacement of 0.41g, 81 cm/s, and 220 cm, respectively. Downtown Adapazarı is located at a distance of about 7 km from the fault rupture, and due to softer ground conditions, amplification of long period components of the ground motion would be expected.



**Fig. 3.14: The Acceleration vs. Time (East – West) Plot Recorded At Sakarya Strong Ground Motion Station**

### **3.5 Site Specific Response Analysis**

The computer program SHAKE was written in 1970-1971 by Dr. Per Schnabel and Professor John Lysmer and was published in December 1972 by Dr. Per Schnabel and Professor John Lysmer and H. Bolton Seed in report No. UCB/EERC 72/12, issued by the Earthquake Engineering Research Center at the University of California, Berkeley. This has been by far the most widely used program for computing the seismic response of the horizontally layered soil deposits.

The program computes the response of a semi-infinite horizontally layered soil deposit overlying a uniform half space subjected to vertically propagating shear waves. The analysis is done in frequency domain, and, therefore, for any set of properties it is a linear analysis. The object motion can be specified in at the top of any sub-layer within the soil profile or at the corresponding outcrop. The soil profile is idealized as a system of homogeneous, visco-elastic sub-layers of infinite horizontal extent. The response of the system is calculated considering vertically propagating shear waves. The algorithm in the original program SHAKE is based on the continuous solution to the wave equation, which was adapted for transient motions using the Fast Fourier Transform techniques. An equivalent linear procedure (Idriss and Seed, 1968; Seed and Idriss, 1970) is used to account for the non-linearity of the soil using an iterative procedure to obtain values for modulus and damping that are compatible with the equivalent, uniform strain induced in each sub-layer. Thus, at the outset, a set of properties (shear modulus, damping and total unit weight) is assigned to each layer of the soil deposit (Schnabel et al., 1972).

The analysis is conducted using these properties and the shear strains induced in each sub-layer is calculated. The shear modulus and the damping ratio for each sub-layer are then modified based on the applicable relationship relating these two properties to shear strain. The analysis is repeated until strain-compatible modulus and damping values are arrived at. Starting with the maximum shear modulus for each sub-layer and a low value of damping, essentially (i.e., difference less than one percent) strain compatible properties

are obtained in 5 to 8 iterations. To be on the safe side, 15 iterations are done before the program terminated.

Following assumptions are incorporated in the analysis (Schnabel et al., 1972):

- i. Each sub-layer,  $m$ , is completely defined by its shear modulus,  $G_m$ , damping ratio,  $\lambda_m$ , total unit weight,  $\gamma_{tm}$  (or corresponding mass density,  $\rho_m$ ) and thickness,  $h_m$ ; these properties are independent of frequency.
- ii. The responses in the soil profile are caused by upward propagation of shear waves from the underlying rock half-space.
- iii. The shear waves are specified as acceleration ordinates at equally spaced time intervals. (Cyclic repetition of the acceleration time history is implied in the solution.)
- iv. The strain dependence of the shear modulus and damping in each sub-layer is accounted for by an equivalent linear procedure based on an equivalent uniform strain computed by in that sub-layer. The ratio of this equivalent uniform shear strain divided by the calculated maximum strain is specified by the user and is assumed to be the same for all sub-layers.

The computer program SHAKE has been widely used throughout the United States and in many parts of the world for conducting ground response studies. Its use in recent studies involving recordings obtained in several sites from 1989 Loma Prieta earthquake have indicated that the calculated surface motions are in reasonably good agreement with the recorded values when the appropriate soil properties and input rock motions are used. Therefore this program remains a convenient tool for conducting such analyses at many sites for a variety of applications.

### 3.5 Results

One of the most important targets of this study is to verify a relation between building damage and local soil conditions. For this purpose one-dimensional soil profile models are prepared using the data gathered from boreholes throughout Adapazarı. The record from the nearest strong ground motion station (Sakarya) is used for shaking in order to simulate the real case conditions of 1999 Kocaeli Earthquake. The computer program SHAKE is used to determine the effects of local soils on rock outcrop motion.

Processed output files include following information:

- Acceleration – time histories of ground motion at each sub-layer
- Response spectrum for 5% damping
- Maximum stress and strain values at each layer
- Amplification and Fourier Spectrum...etc.

Second step is to select soil response parameters that should affect the building response. Peak ground acceleration is one of them since it directly affects the force applied to structure during the earthquake. Maximum values of acceleration – time histories are determined and digitized using GIS implementation tools for the area of study. Figure 3.15a shows the distribution of peak ground acceleration throughout Adapazarı. Moderately and heavily damaged buildings are overlaid on PGA map and shown in Figure 3.15b. Relation between building damage and peak ground acceleration can be clearly seen from this figure but it will be formulated later in Chapter 5.

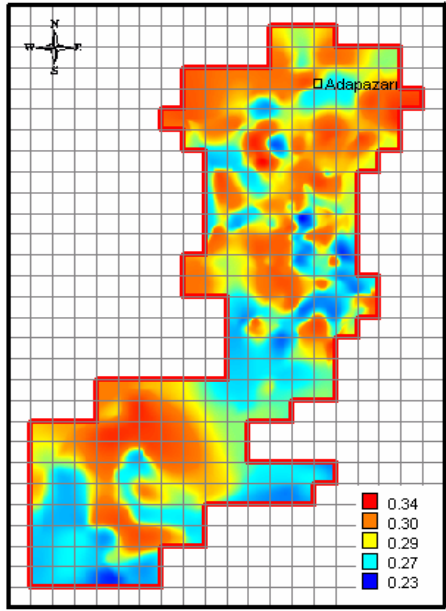


**Fig. 3.15a: Distribution of Peak Ground Acceleration throughout Adapazari.**

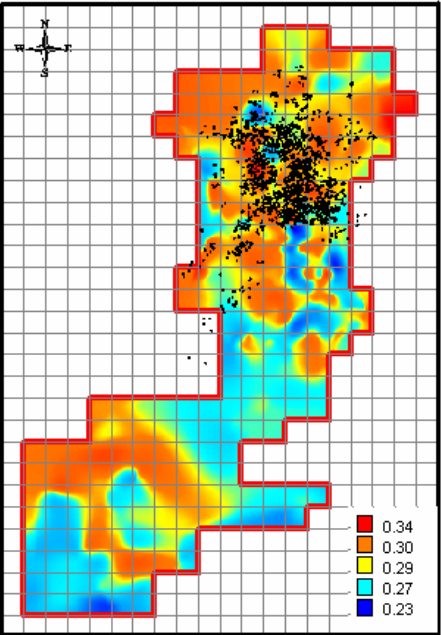


**Fig. 3.15b: Peak Ground Acceleration Map Overlaid on Damaged Buildings throughout Adapazari.**

Spectral acceleration is another important parameter that should be correlated with the building damage. Spectral accelerations corresponding to various periods are determined from the response spectrum for 5% damping. Spatial distributions of spectral accelerations values corresponding to  $T=0.1$ ,  $T=0.2$ ,  $T=0.3$ ,  $T=0.4$ ,  $T=0.5$  and  $T=0.6$  sec. periods are given in Figures 3.16 to 3.21. Relation between building damage and spectral acceleration is not independent from building period. Since the building period is correlated with the height of the building, it should be a better idea to classify the buildings with respect to number of storeys and find a correlation between damage percent and spectral acceleration in different period bins. Limit state functions corresponding to these relations will be given in Chapter 5.

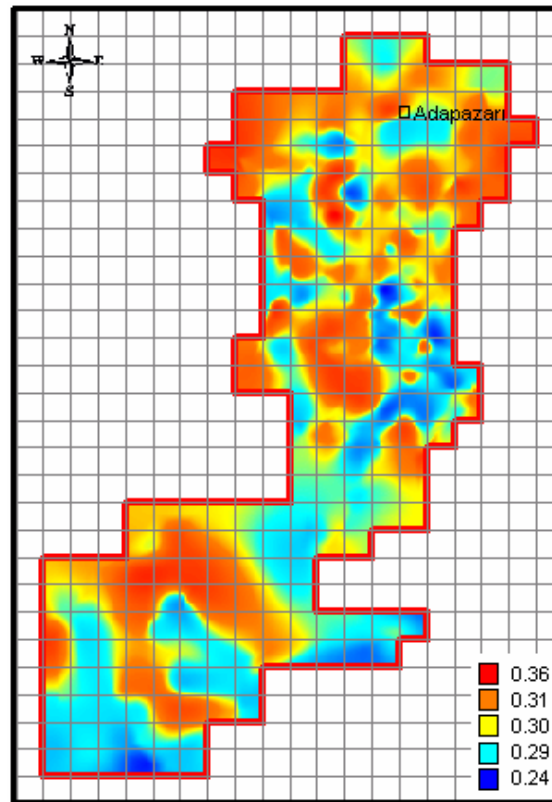


**Fig. 3.16: Distribution of Spectral Acceleration for  $T=0.1$  second throughout Adapazari.**

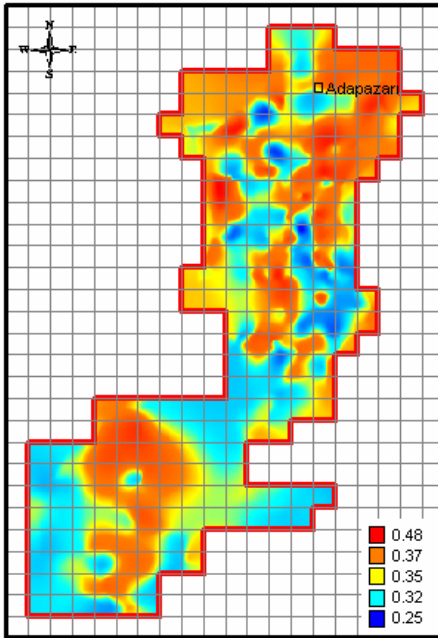


**Fig. 3.17: Distribution of Spectral Acceleration for T=0.2 second throughout Adapazari.**

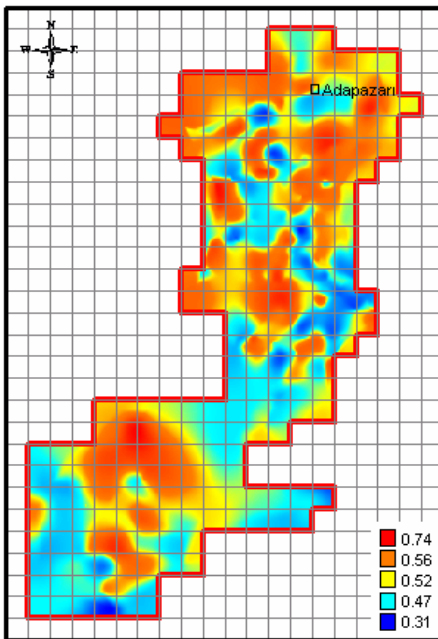


**Fig. 3.18: Distribution of Spectral Acceleration for T=0.3 second throughout Adapazari.**

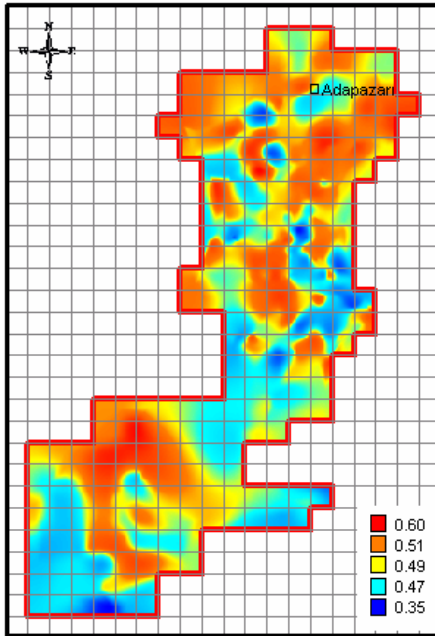


**Fig. 3.19: Distribution of Spectral Acceleration for T=0.4 second throughout Adapazari.**

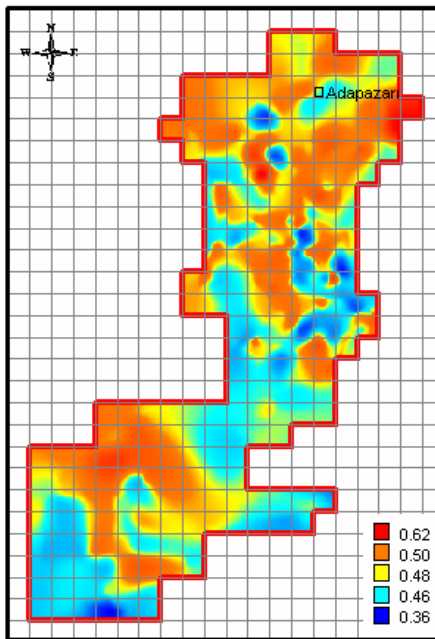


**Fig. 3.20: Distribution of Spectral Acceleration for T=0.5 second throughout Adapazari.**

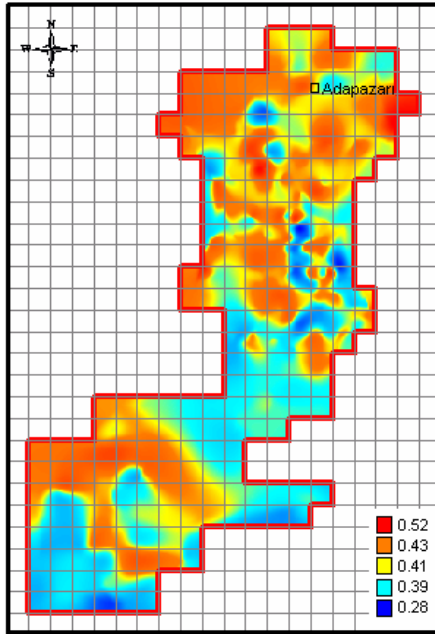


**Fig. 3.21: Distribution of Spectral Acceleration for T=0.6 second throughout Adapazari.**

## CHAPTER 4

### SEISMIC SOIL LIQUEFACTION ASSESSMENT AND RESULTS OF THE ANALYSES

#### 4.1 Introduction

The August 17, 1999 Kocaeli Earthquake ( $M_w=7.4$ ) caused severe damage to the structures and lifelines in the Marmara region. Soil liquefaction was identified as one of the major causes of damage during this earthquake. The majority of building collapses were observed in the towns located on southern shorelines of Marmara Sea and in the city of Sakarya. In Sakarya, located over young riverbed sediments with soft and liquefiable silts and sands, hundreds of buildings sank, as much as 1.5 m, or tilted due to shear failure of the foundation media and liquefaction.

One of the most important parts of this study is the evaluation of potentially liquefiable sites in Adapazarı. Both laboratory and field test results summarized in Chapter 3 are combined in order to analyze the soil layers through the boreholes. The parameters necessary for seismic soil liquefaction assessment like soil classification, depth of groundwater table, fines content, plastic and liquid limits of the soil layers...etc. for each borehole are determined after this careful analyzing and screening process. The methodology described in Chapter 2 is used for the assessment of liquefaction triggering of local soils in Adapazarı. First part of this chapter briefly summarizes the application of the methodology on the collected database. Several parameters related to liquefaction are selected in order to correlate structural performance with soil liquefaction initiation potential. These parameters are introduced in Section 4.3. Relationship between distribution of

building damage and selected soil liquefaction parameters will be investigated later in details in Chapter 5.

#### **4.2 Liquefaction Assessment of Local Soils in Adapazari**

Seismic soil liquefaction assessment methodology described in Chapter 2 was applied to the local Adapazari soils within the limitations of the available database. These efforts are briefly summarized step by step below:

1. General Directorate of Disaster Affairs (GDDA) has organized a database compilation program for the purpose of officially documenting subsurface investigation studies performed in the city of Sakarya. For the purpose, over a thousand of bore logs were accessed, reviewed and screened for data quality purposed and the resulting database composed of 263 boring logs of high quality data including both laboratory and field test results.
2. Necessary soil related parameters for seismic soil liquefaction analysis are selected as; fines content, Atterberg limits for cohesive soil layers, groundwater depth, soil density and SPT N-value. These parameters are gathered from each borehole and a final database for liquefaction analysis was prepared.
3. For the sake of simplicity, city of Adapazari was divided into 150 grids (each of which has 500 x 500 m dimensions). The database was consolidated based on the reliability and consistency of the borehole data corresponding to a grid, and representative soil profile for each grid was determined.
4. Soils vulnerable to liquefaction are evaluated using the methodology described in Section 2.2 with the help of representative soil profiles and borehole log descriptions.
5. The necessary earthquake related parameters are in-situ  $CSR_{eq}$  and moment magnitude of 1999 Kocaeli Earthquake (which was taken as 7.4). In-situ  $CSR_{eq}$  was evaluated directly, based

on performance of full seismic site response analyses (using SHAKE 91; Idriss and Sun, 1992), since sufficient sub-surface information was available in the database, and suitable “input” motions could be developed from nearby strong ground motion records. Details of these analyses are given in Chapter 3.

6. After compiling necessary parameters (in-situ  $CSR_{eq}$ , moment magnitude, vertical total and effective stress, fines content, groundwater depth, and  $N_{1,60}$  value) for each data point,  $r_d$  and probability of liquefaction values were estimated as defined in Equation 2.3 and 2.5.

### 4.3 Selection of Liquefaction Related Parameters and Correlations with Building Damage

#### 4.3.1 Liquefaction Severity Index

Currently, there are various methods, including the one implemented in Chapter 2 recommended by Seed et al. 2001, for the estimation of the probability of liquefaction initiation of a soil layer. However, it is of more importance to estimate the potential of ground failure at a given site rather than potential failure of a particular soil layer. It must be noticed that the damage to structures due to liquefaction is considerably affected by the severity of the liquefaction degree. Iwasaki et al., 1982 proposed the Liquefaction Potential Index term, IL, for the evaluation of the ground failure risk as recommended in the Japanese Highway Bridge Design Code. The index, IL, is defined as follows:

$$IL = \int_0^{20} (F_1 \cdot W(z)) \cdot dz \quad (\text{Eq. 4.1})$$

Where  $F_1$  is an index defined as:

$$F_1 = 1 - F_s, \quad \text{if } F_s < 1.0$$

$$F_1 = 0 \quad \text{if } F_s > 1.0$$

$F_s$  is the factor of safety against liquefaction initiation and  $W(z)$  is the weight function term expressed as a function of depth  $z$ , representing the relative contributions of liquefaction initiations at different depths to the ground failure. As given in Equation 4.2, the weight function is assumed to be a linear function of depth from ground surface, where  $z$  is in meters.

$$W(z) = 10 - 0.5 \cdot z \quad (\text{Eq. 4.2})$$

Based on his analysis of a database of 64 liquefied and 23 non-liquefied sites from 6 earthquakes, Iwasaki et al. 1982 provided the following liquefaction risk criteria for different ground failure levels as given below:

- $IL = 0$ , the liquefaction failure potential is extremely low;
- $0 > IL > 5$ , the liquefaction failure potential is low;
- $5 > IL > 15$ , the liquefaction failure potential is high;
- $IL > 15$ , the liquefaction failure potential is extremely high

Iwasaki et al., 1982 methodology is widely adopted for the evaluation of liquefaction failure risk in Japan and Taiwan. However, a question arises on the factor of safety in Equation 4.1. Is the method still applicable if a different method for calculation of factor of safety is used? Various authors apply Iwasaki's methodology to the CPT- based liquefaction assessments. Two different studies from last year are taken here as examples of the efforts on this subject. Juang et al. (2003) method is a CPT-based method, which is used to analyze the sites that experienced liquefaction damages and those that did not. A total of 72 sites with CPT measurements are analyzed in this study. Similarly Toprak et al.'s study is based on 243 CPT soundings that were performed at 27 sites, where the term site indicates a location of concentrated field investigation (may include areas both with and without liquefaction.) In both of these studies, the exact distinctions of liquefaction risk criteria could not be found.

Inspired by Iwasaki's Liquefaction Potential Index, a new Liquefaction Severity Index, LSI, definition is introduced here as a function of;

- i) probability of liquefaction,  $PL$ ,
- ii) thickness of the potentially liquefiable layer,  $TH$ ,

iii) depth to the potentially liquefiable layer,  $z$ , in meters, as given in Eq. 4.3.

$$LSI = \int_0^{20} PL \cdot TH \cdot WF \quad (\text{Eq. 4.3})$$

Where  $PL$  is estimated as recommended by Seed et al. 2001 and  $WF(z)$  is the weighting factor as defined in Equation 4.4.

$$WF(z) = 1 - 0.05 \cdot z \quad (\text{Eq. 4.4})$$

LSI for 263 soil profiles in the database is calculated and the results are presented in the GIS framework. Limits of the index are selected due to the frequency of the data points as follows:

- $0 > LSI > 0.35$ , the liquefaction failure potential is extremely low;
- $0.35 > LSI > 1.30$ , the liquefaction failure potential is low;
- $1.30 > LSI > 2.5$ , the liquefaction failure potential is high;
- $2.5 > LSI = 10.0$ , the liquefaction failure potential is extremely high

Figure 4.1(a) shows the distribution of LSI throughout Sakarya city. In Figure 4.1 (b), moderately and heavily damaged buildings were overlaid on the LSI base map. Fig. 4.1 suggests a correlation between LSI and structural performance, as LSI increases structural performance gets poorer. To present this correlation better, statistics of the LSI, number of storeys of the buildings for various structural performances is also presented in Chapter 5.

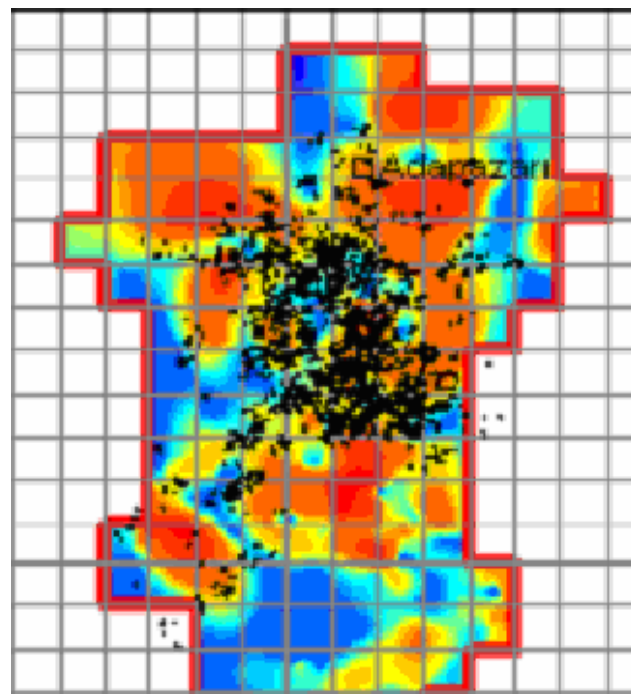
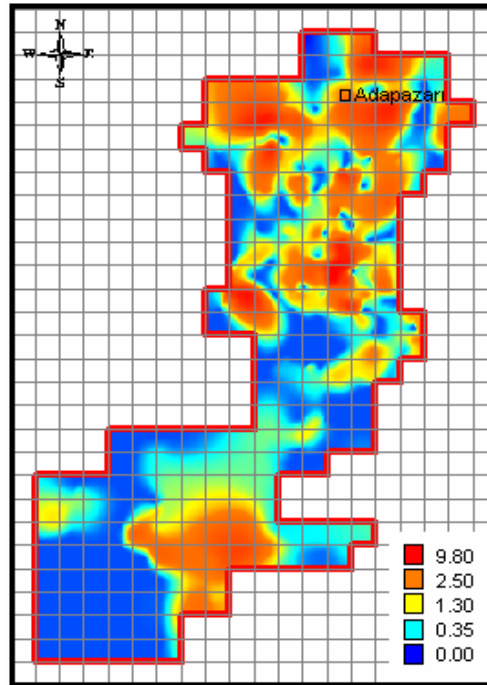


**Fig. 4.1 (a): Liquefaction Severity Index Map (b): Damaged Buildings (Black Dots) Overlaid on the Map of Liquefaction Severity Index.**

### 4.3.2 Thickness of the Potentially Liquefiable Layer

Both Japanese and U.S researchers (e.g., Hamada and O'Rourke 1992, Bartlett and Youd 1995) have identified thickness of the liquefiable layer as a significant parameter affecting the magnitude of lateral spread. The magnitude of settlement caused by post-liquefaction consolidation is directly related to the liquefiable layer thickness. Recent studies have shown that loss of shear stiffness in a liquefied soil will increase its predominant period and thereby amplify transient accelerations and displacements conveyed to an overlaying, non-liquefiable layer (Zeghal and Elgamal 1994, Pease and O'Rourke 1995). Under these conditions transient displacements may be directly proportional to liquefiable layer thickness.

The distribution of soils vulnerable to liquefaction can be complex, and hence it is desirable to define the characteristic dimensions related to liquefaction at a given location. O'Rourke and Pease, 1997 has described submerged thickness" as the gross thickness of a layer that contains soils susceptible to liquefaction, and "maximum liquefiable thickness" as the maximum thickness of soil that would experience liquefaction under extreme conditions of shaking.

Ishihara (1985) investigated the effects that the thickness of liquefiable soil and non-liquefied surface layer has on liquefaction damage. Ishihara suggests, based on empirical observations from a number of Japanese earthquakes, that surface manifestations of liquefaction will not be significant if (1) the site is relatively level, (2) the edges are constrained so that lateral spreading towards a free face is prevented, and (3) the ratio of the thickness of the non-liquefied surface "crust" ( $H_1$ ) to the thickness of the liquefied underlying soils ( $H_2$ ) is greater than the values indicated in Figure 4.2 (as a function of peak ground surface acceleration, as shown.)

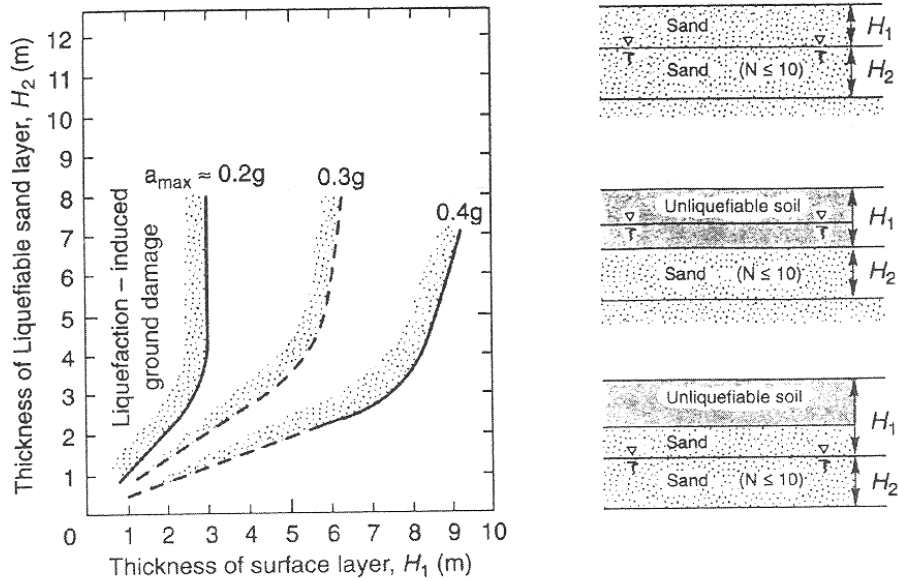


**Fig. 4.2: Proposed Boundary Curves for Site Identification of Liquefaction-Induced (Surface) Damage (After Ishihara, 1985)**

Because of the influence of liquefaction layer thickness on permanent and transient ground displacements, as well as the potential ease with which this parameter can be mapped and incorporated into geographic information systems, it is of considerable importance to investigate the areas that have experienced liquefaction and assess this parameter's relationship with building damage. Within the scope of this study thickness of the potentially liquefiable layer is defined as the total thickness of the soil layers where probability of liquefaction is greater than 20%. A possible correlation between the structural damage and the thickness of the potentially liquefiable layer is questioned as shown in Figure 4.3(a) and 4.3(b). Great portion of the collapsed buildings were located on the districts where thickness of potentially liquefiable layer is estimated to be greater than 5 m. Figure 4.3 shows that as the thickness of the potentially liquefiable layer increases, structural performance get poorer. To present this correlation better, statistics of the liquefiable layer thickness, number of storeys of the buildings for various structural performances is also presented in Chapter 5.

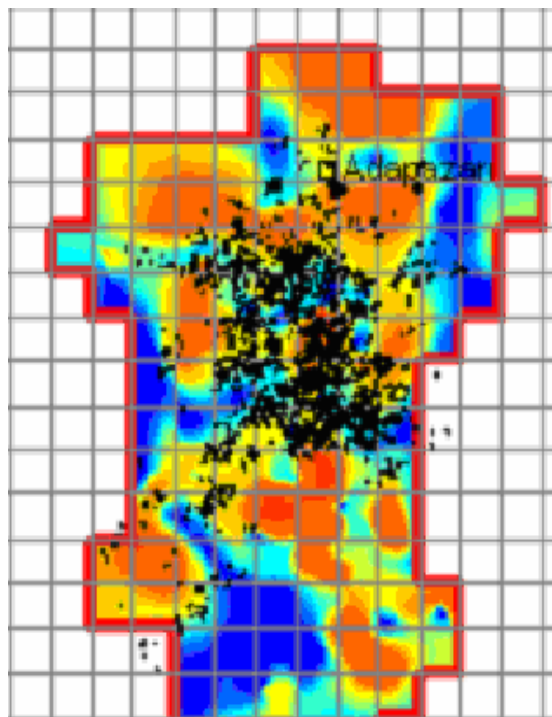
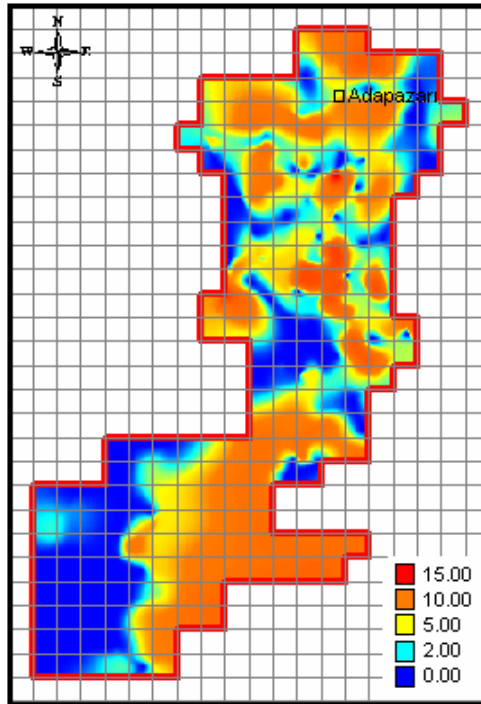


**Fig. 4.3(a): Thickness of the Potentially Liquefiable Layer Map (b): Damaged Buildings (Black Dots) Overlaid on the Map of Thickness of the Potentially Liquefiable Layer**

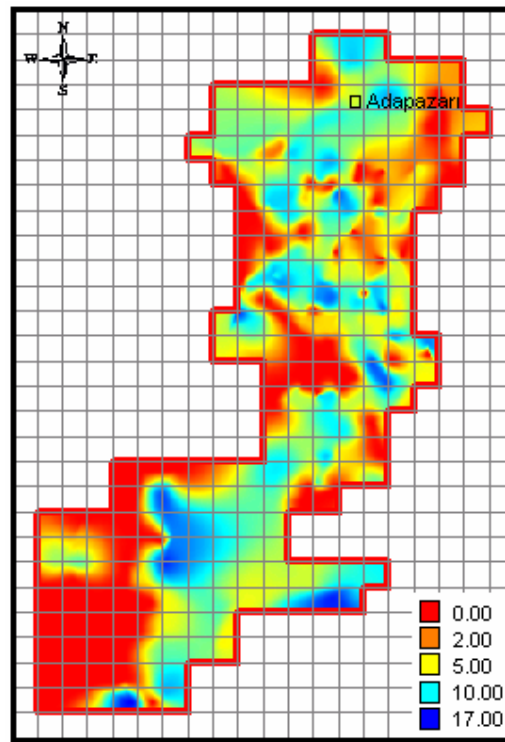
### 4.3.3 Representative Depth to Potentially Liquefiable Layer (DPLL)

In addition to the thickness of the liquefiable soil layer, depth to it is also acknowledged as a significant parameter for the assessment of ground failures. For the purpose of addressing this potential issue, representative depth to potentially liquefiable soil layer defined as the weighted average depth to potentially liquefiable layers.

$$DPLL = \frac{\sum LSI \cdot z}{\sum LSI} \quad (\text{Eq. 4.5})$$

Where  $z$  is the mid-depth to the soil layer of interest.

Figure 4.4(a) shows the areal distribution of representative depth to liquefiable layers throughout Sakarya city. In Figure 4.4(b), moderately and heavily damaged buildings were overlaid on DPLL base map. However, since for the majority of Sakarya city the DPLL parameter does not vary significantly, this parameter is concluded to be of a less sensitive parameter for potentially explaining the variability in structural performance.



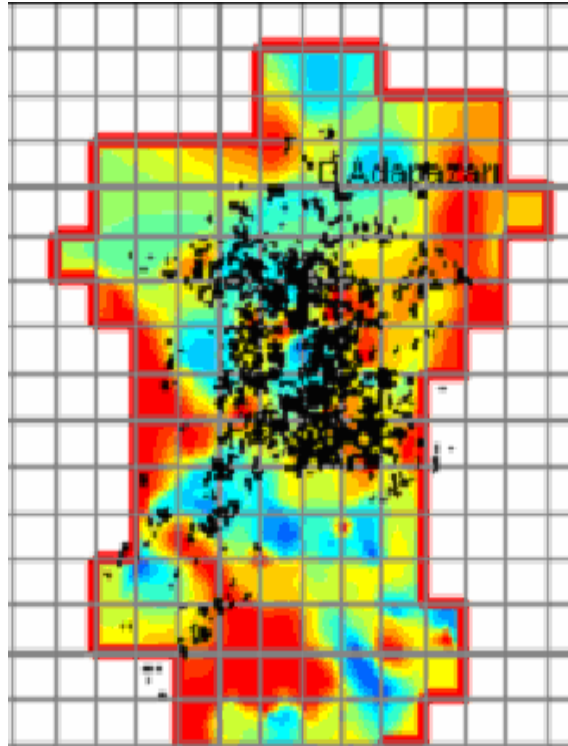


**Fig. 4.4(a): Representative Depth to the Potentially Liquefiable Layer Map  
(b): Heavily Damaged Buildings (Black Dots) Overlaid on the Map of  
Representative Depth to the Potentially Liquefiable Layer.**

#### **4.3.4 Post Liquefaction Volumetric Settlements**

Another consequence of liquefaction resulting from an earthquake is the volumetric strain caused by the excess pore pressures generated in saturated granular soils by the cyclic ground motions. The volumetric strain, in the absence of lateral flow or spreading, results in settlement. Permanent ground deformations resulting from liquefaction induced deviatoric and volumetric straining were identified as the major causes of foundation deformations and thus a major contributor to structural performance.

Lee and Albaisa (1974) and Yoshimi (1975) studied the volumetric strains (or settlements) in saturated sands due to dissipation of excess pore pressures developed during laboratory cyclic loading. They observed that, for a given relative density, the volumetric strains increased with the mean grain

size of sand. However, later studies (Martin et al., 1978) have shown that the effects of grain size can be attributed to membrane penetration. Effects of shear strains were not considered in those studies. Tatsuoka et al. (1984) observed that, for a given relative density, volumetric strain after initial liquefaction can be significantly influenced by the maximum shear strain developed, but is relatively unaffected by the overburden. Tokimatsu and Seed (1987) used the findings by Tatsuoka et al. and developed a practical method that correlates the SPT N-value, earthquake magnitude, and induced cyclic stress ratio to volumetric strains of saturated sands subjected to earthquake shaking (Figure 4.5).

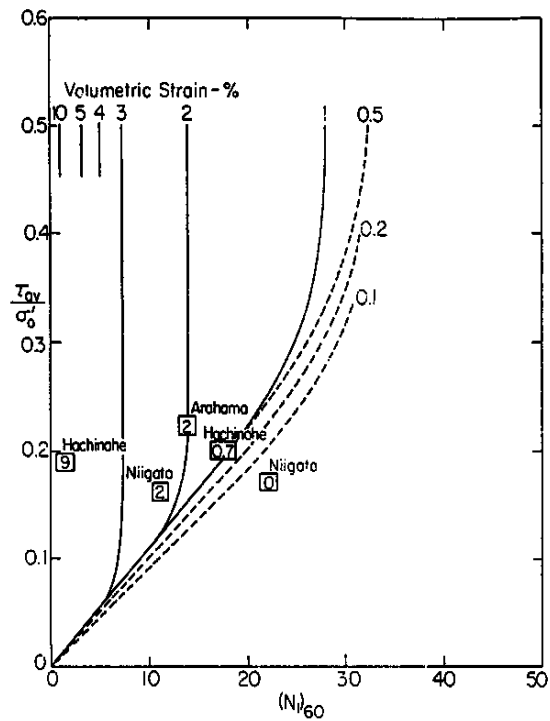


**Fig. 4.5: Chart for Determination of Post-Liquefaction Volumetric Strain of Clean Sands (After Tokimatsu and Seed, 1984)**

Ishihara and Yoshimine (1992) developed a similar practical method by correlating the volumetric strain to the relative density and the factor of safety of the sand against liquefaction state, which was found to generally agree with

the Tokimatsu and Seed method. It should be noted that the relationships developed in the Ishihara and Yoshimine (1992) method are based on laboratory tests of clean sands deposited at various relative densities. Consequently, their associated penetration resistances (SPT-N value and CPT tip resistance) are based on correlations which vary according to the effective stress of the soil. Therefore, direct use of the suggested penetration resistance values should be used carefully. Furthermore, it should be noted that indicated N-values correspond to the standard Japanese SPT, which typically delivers an effective energy of about 80% (Figure 4.6).

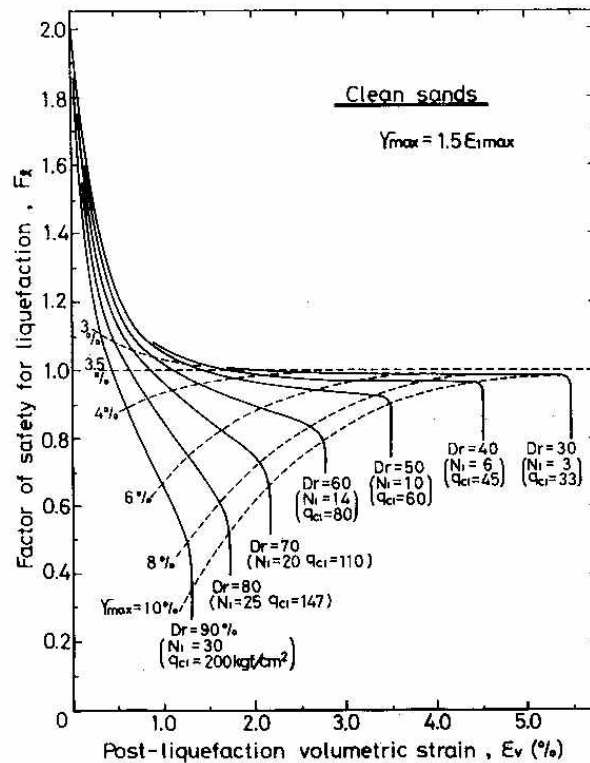


**Fig. 4.6: Chart for Determination of Post-Liquefaction Volumetric Strain of Clean Sands as a Function of Factor of Safety (After Ishihara, 1996).**

Assessment of the post liquefaction volumetric strain potential of Sakarya city soil profiles were performed by following the methodology proposed by Unutmaz and Cetin, 2004. After studying the well-known relations

of SPT-N values with the cyclic stress ratios for shear strains 3%, 10% and 20% (Seed, 1976, Tokimatsu, 1987, and Ishihara 1979), Unutmaz proposed a closed form estimation of post liquefaction settlement and lateral displacements. The main advantage of this method, in addition to closed form expression, is that it gives an unbiased average estimate of Seed's (1983), Tokimatsu's (1987) and Ishihara's (1980) predictions.

Proposed formulations of deviatoric and volumetric strain are given in Equations 4.6 and 4.7 respectively.

$$\gamma = \frac{-N_{1,60} \cdot (1 + 0.001 \cdot FC) + 29.2231 \ln M_w + 3.6604 \ln \sigma'_v - 0.05 \cdot FC + 13.3247 \ln CSR - 40.1031}{0.0508 N_{1,60} + 0.1853}$$

$$\varepsilon_v = \frac{-N_{1,60} \cdot (1 + FC) + 152.0203 \cdot \ln M_w + 467.0402 \cdot \ln \sigma'_v - 0.05 \cdot FC + 847.4096 \cdot \ln CSR - -16.3942}{104.2823 \cdot N_{1,60} + 464.1991}$$

(Eq. 4.6 and 4.7)

Where;  $N_{1,60}$  = SPT-N value corrected for energy and overburden,  
 FC = fines content,  
 Mw = moment magnitude of the earthquake  
 $\sigma'_v$  = effective vertical stress, and  
 CSR = cyclic stress ratio

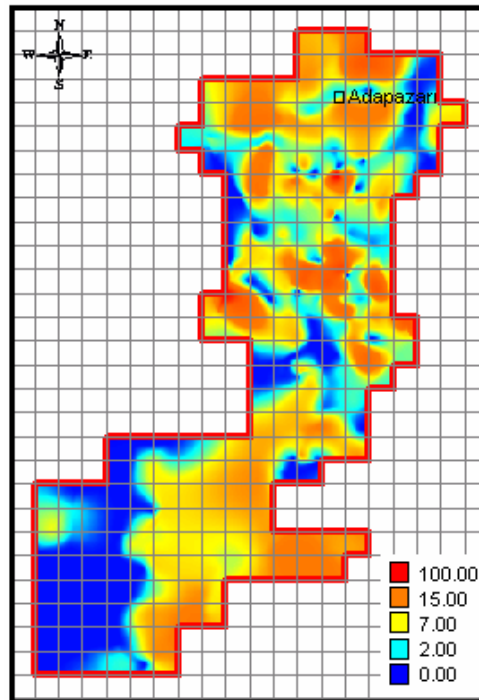
Total strain at a point is determined as:

$$\text{Total strain} = 0.9 \times \varepsilon_v \text{ (volumetric strain)} + 0.1 \times \gamma \text{ (deviatoric strain)}$$

Finally, post-liquefaction settlement of a soil layer is calculated by multiplying the sum of total strain values throughout the soil layer with the layer thickness.

Figure 4.7(a) shows the areal distribution of post liquefaction settlements throughout Sakarya city. In Figure 4.7(b), moderately and heavily damaged buildings were overlaid on settlement base map. Note that in Figure

4.7(b) most of the failures are on the contours where high settlements are expected. Moreover, most of the poor structural performance cases are located at the edges of settlement contours, which clearly address differential settlement problem and out of phase foundation shaking. To present this correlation better, statistics of the post liquefaction volumetric settlement, numbers of storeys of the buildings for various structural performances are presented in Chapter 5.



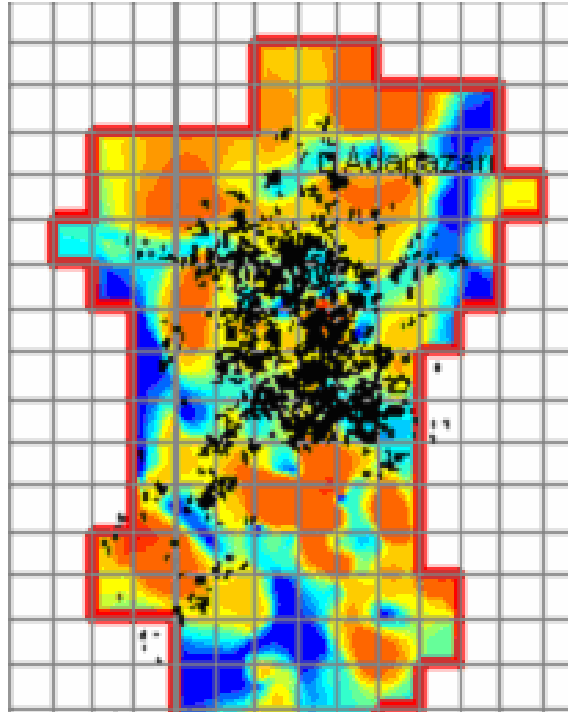


**Fig. 4.7(a): Post Liquefaction Volumetric Settlement Map (b): Heavily Damaged Buildings (Black Dots) Overlaid on the Map of Post Liquefaction Volumetric Settlement.**

#### **4.4 Summary and Conclusions**

The aim of these studies is to determine geotechnical engineering factors that contribute to the structural damage observed after 1999 Kocaeli Earthquake. After series of sensitivity analyses, important geotechnical engineering parameters of the problem were selected as i) liquefaction severity index, ii) thickness of the possibly liquefied layer, iii) representative depth to possibly liquefied layer and iv) post liquefaction volumetric settlement. In addition to these geotechnical engineering parameters, structural performance defined as a) no damage, b) moderate damage, c) heavy damage and collapse, as well as the number of storeys of each structure were used as to correlate structural damage with geotechnical factors. These correlations are given in details in Chapter 5.

## CHAPTER 5

### DEVELOPMENT OF PROBABILISTIC MODELS FOR THE ESTIMATION OF DAMAGE INDEX

#### 5.1 Introduction

The most important part of this study is to determine geotechnical engineering factors that contribute to the structural damage observed after 1999 Kocaeli Earthquake. The effects of local site conditions on strong ground motion and building response were investigated by series of seismic soil response analyses, which were summarized in Chapter 3. Details of soil liquefaction analyses and liquefaction related parameters affecting the damage distribution are also presented in Chapter 2 and Chapter 4.

After these efforts, a database including the number of storeys and damage level of buildings in Adapazarı was compiled by using the records of GDDA. These buildings are classified by their number of storeys and damage level, which are shown in Table 5.1.

**Table 5.1: Statistics of Buildings in Adapazarı**

Damage Level	Number of Storeys						Total
	1	2	3	4	5	> 5	
No Damage: 1	8395	5012	2355	989	349	42	17142
Moderate Damage:2	289	301	131	163	139	22	1045
Heavy Damage: 3	972	557	209	167	112	12	2029

In order to develop a model for the assessment of seismic performance of buildings, first a series of sensitivity analysis are performed, which are summarized in Section 5.2. Then, series of limit state functions are defined according to the results of the sensitivity analyses and maximum likelihood framework for the probabilistic assessment of seismically induced building performance is described. Results of this study are summarized in Section 5.4

## **5.2 Sensitivity Studies**

For the purpose of defining important parameters relevant to the problem addressed as well as the possible mathematical form of the relationship among damage index and selected descriptive parameters, a series of sensitivity studies were performed. The parameters defined in Chapter 3 and Chapter 4 are consolidated in order to minimize the correlations. The descriptive variables are selected as; number of storeys of the building (N), peak ground acceleration (PGA) in g, spectral acceleration values corresponding to the period range of conventional buildings in g (SA), liquefaction severity index (LSI) as described in Chapter 4 and liquefaction induced ground settlements (S) in meters. For each variable a cumulative number of damaged buildings versus descriptive variable plots are prepared and the tendency of the change in the percentage of damaged buildings with respect to the variable is investigated.

In these sensitivity studies, the database summarized in Table 5.1 excluding 1- or 2-storeys are used. The reason for screening these buildings could be partially explained by the simple reason that most of these structures are not engineered and thus the effects of geotechnical factors could be washed out in great randomness of other structural engineering parameters. Also geotechnical factors representing Adapazarı city soil conditions could be of lesser importance for structures with two storeys or less where bearing capacity is an more important factor.

Fig. 5.1 shows the change in percentage of damaged buildings with respect to change in number of storeys. As it can be seen from this figure, the

increase in percent damaged buildings with respect to the number of storeys shows an exponential trend. The contribution of number of storeys to the damage index should then be explained by an exponential function as given in Figure 5.1.

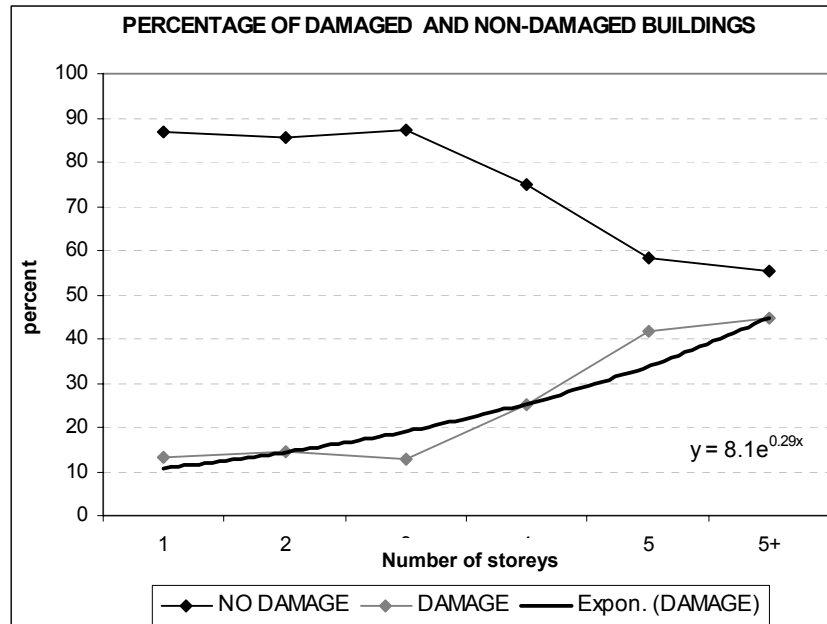


**Fig. 5.1: Distribution of the Percent Number of Damaged Buildings with Number of Storeys.**

Similarly, Figure 5.2(a) and 5.2(b) shows the effect of PGA on damage distribution for 4 and 5 storey buildings respectively. As the PGA increases the percentage of damaged buildings is increasing. In both figures, linear and exponential trend lines are added to the PGA vs. percent number of damaged buildings plots. Even though theoretically an exponential trend is commonly preferred, due to its simplicity and very close  $r^2$  values, a linear relationship is also used between PGA and damage level.

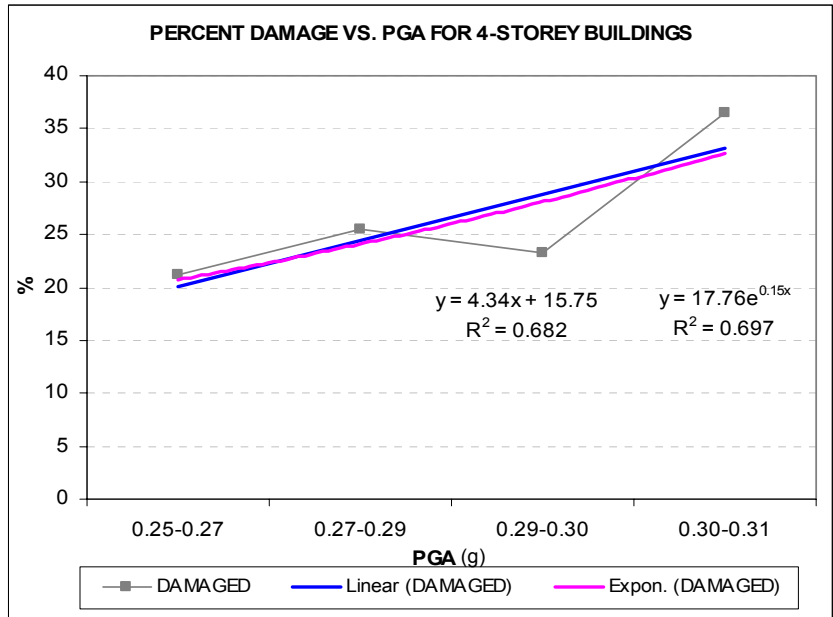


**Fig. 5.2(a): Distribution of the Percentage of Damaged Buildings with PGA for 4-Storey Buildings**

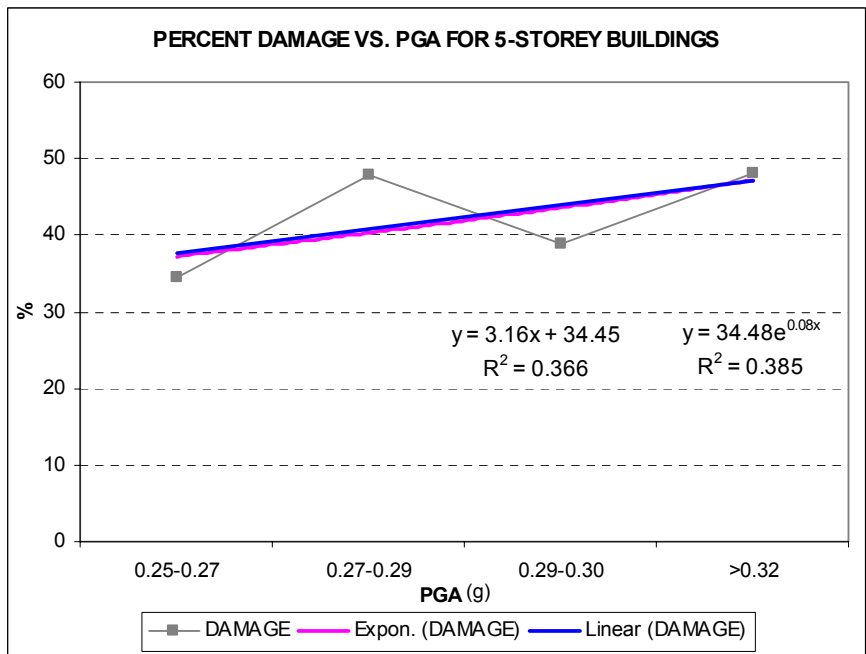


**Fig. 5.2(b): Distribution of the Percentage of Damaged Buildings with PGA for 5-Storey Buildings**

In order to find a correlation between the distribution of building damage and spectral acceleration, the percentage of damaged 4-storey buildings are plotted with respect to spectral acceleration for T=0.4 sec period. Similarly, the percent number of damaged 5-storey buildings is plotted with respect to spectral acceleration values corresponding to T=0.5 sec period. These plots are given in Figure 5.3(a) and 5.3(b), respectively. The observed trend between spectral acceleration and cumulative number of damaged buildings can be both represented by linear and exponential type relationships in these figures.

Figure 5.4 and 5.5 shows the effects of liquefaction susceptibility on damage distribution. In Figure 5.4, liquefaction susceptibility is expressed as the liquefaction severity index of the soil profile whereas in Figure 5.5, as the liquefaction induced ground settlements along soil profile (which are explained in details in Chapter 4). In Figure 5.4, linear increase in cumulative damage with respect to increase in liquefaction severity index is clear. Change in the percent number of damaged buildings with respect to liquefaction induced ground settlements also shows a linear trend as expected.

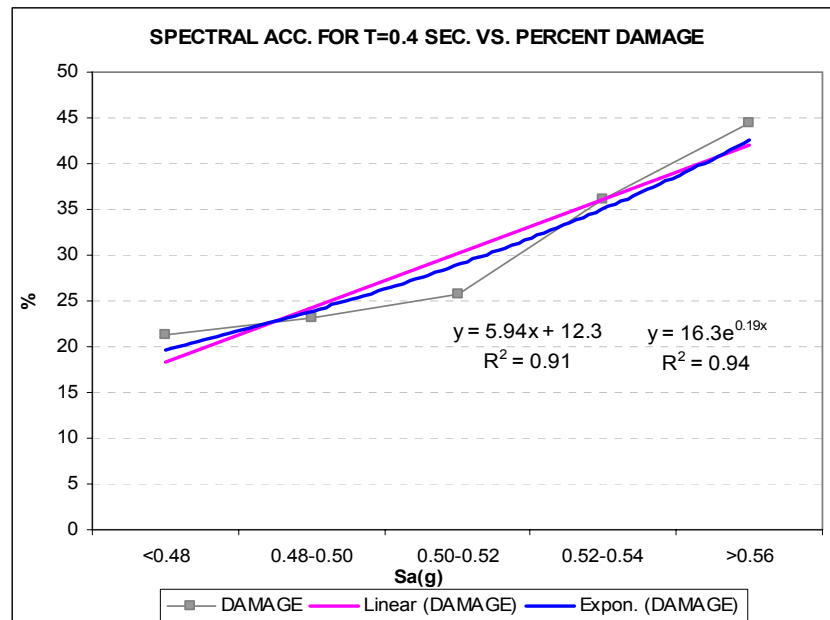


**Fig. 5.3(a): Distribution of the Percentage of Damaged Buildings with Spectral Acceleration Corresponds to T = 0.4 Sec for 4-Storey Buildings.**

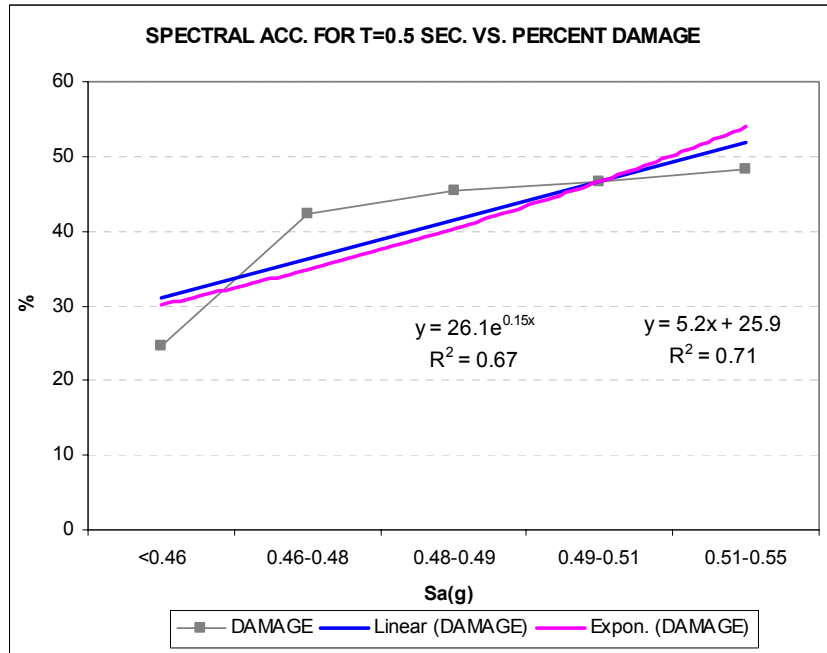


**Fig. 5.3(b): Distribution of the Percentage of Damaged Buildings with Spectral Acceleration Corresponds to T= 0.5 Sec for 5-Storey Buildings.**

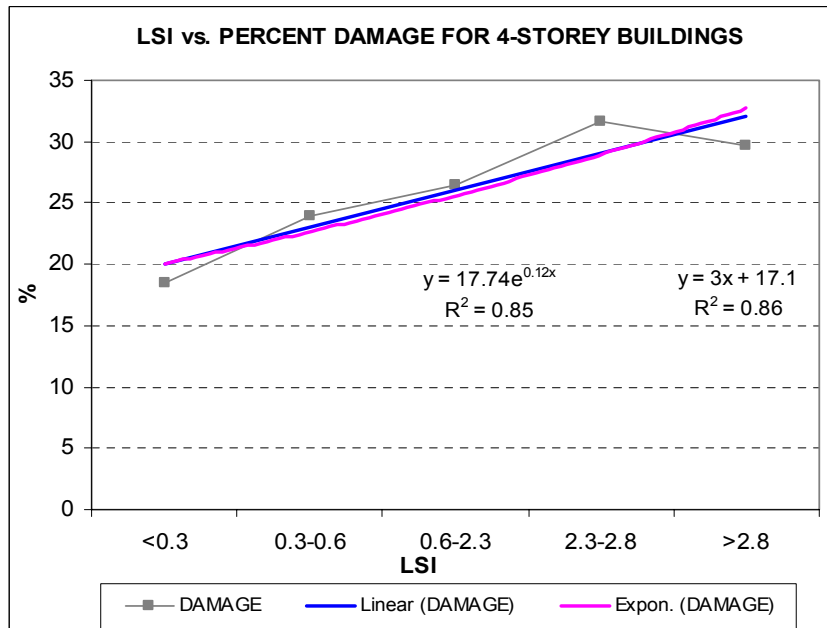


**Fig. 5.4: Distribution of the Cumulative Number of Damaged Buildings with Liquefaction Severity Index.**

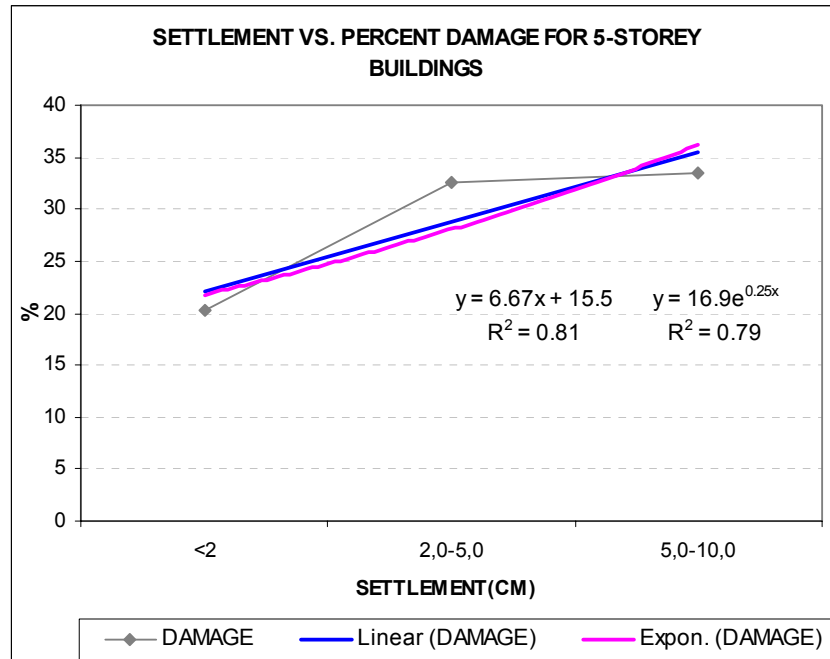


**Fig. 5.5: Distribution of the percent number of damaged buildings with liquefaction induced ground settlements.**

### 5.3 Construction of the Limit State Function

Maximum likelihood approach for developing a model for the assessment of seismic performance of structures requires the selection of a mathematical model. The model for the correlation has the general form  $\hat{g} = g(\mathbf{x}, \Theta)$ , where  $\mathbf{x}$  is a set of descriptive variables and  $\Theta$  is the set of unknown model parameters. The limit-state surface  $g(\mathbf{x}, \Theta) = 0$  denotes the damage level which is represented as the “Damage Index”.

Motivated by prior research studies, number of storeys of the building is selected as the dominating variable for defining the damage level. In addition to number of storeys, descriptive variables included to the model to better characterize the local soil conditions. After a rigorous sensitivity study, the form of function given below is found to be representative. Following improved models for the limit state function were adopted:

$$\hat{g}(N,PGA,\Theta) = \exp(N \cdot \theta_1) + \theta_2 \cdot PGA - \theta_8 \quad (5.1)$$

$$\hat{g}(N,PGA,\Theta) = \exp(N \cdot \theta_1) + \theta_2 \exp(PGA \cdot \theta_3) - \theta_8 \quad (5.2)$$

$$\hat{g}(N,PGA,SA,LSI,\Theta) = \exp(N \cdot \theta_1) + \theta_2 \cdot PGA + \theta_3 \cdot SA + \theta_4 \cdot LSI - \theta_8 \quad (5.3)$$

$$\hat{g}(N,PGA,SA,LSI,\Theta) = \exp(N \cdot \theta_1) + \theta_2 \exp(PGA \cdot \theta_3) + \theta_4 \exp(SA \cdot \theta_5) + \theta_6 \cdot LSI - \theta_8 \quad (5.4)$$

$$\hat{g}(N,PGA,SA,LSI,S,\Theta) = \exp(N \cdot \theta_1) + \theta_2 \cdot PGA + \theta_3 \cdot SA + \theta_4 \cdot LSI + \theta_5 \cdot S - \theta_8 \quad (5.5)$$

$$\hat{g}(N,PGA,SA,LSI,S,\Theta) = \exp(N \cdot \theta_1) + \theta_2 \exp(PGA \cdot \theta_3) + \theta_4 \exp(SA \cdot \theta_5) + \theta_6 \cdot LSI + \theta_7 \cdot S - \theta_8 \quad (5.6)$$

Where;

N : Number of storeys of the building

PGA : Peak ground acceleration in meter per square second

SA : Spectral acceleration for the period range of conventional buildings

LSI : Liquefaction severity index as defined in Section 4.3.1

S : The estimated liquefaction-induced ground settlements (S) in meters

$\Theta = (\theta_1, \dots, \theta_5)$  is the set of model parameters

The limit state functions in Equations 5.1- 5.6 assume that damage level can be completely estimated by the descriptive variables N, PGA, SA, LSI, and S. Obviously other variables exist which may influence structural damage. Even if the selected descriptive variables were to fully explain this

phenomenon, the adopted mathematical expression may not have the ideal form. Hence, Equations 5.1-5.6 are imperfect models of the limit-state function. This is signified by use of a superposed hat on  $\mathbf{g}$ . To account for the influences of the missing variables and the possible incorrect model form, a random model correction term,  $\mathcal{E}$ , is introduced and the corrected limit state functions are written as:

$$\hat{\mathbf{g}}(N,PGA,\Theta) = \exp(N \cdot \theta_1) + \theta_2 \cdot PGA - \theta_8 + \mathcal{E} \quad (5.7)$$

$$\hat{\mathbf{g}}(N,PGA,\Theta) = \exp(N \cdot \theta_1) + \theta_2 \exp(PGA \cdot \theta_3) - \theta_8 + \mathcal{E} \quad (5.8)$$

$$\begin{aligned} \hat{\mathbf{g}}(N,PGA,SA,LSI,\Theta) &= \exp(N \cdot \theta_1) + \theta_2 \cdot PGA \\ &+ \theta_3 \cdot SA + \theta_4 \cdot LSI - \theta_8 + \mathcal{E} \end{aligned} \quad (5.9)$$

$$\begin{aligned} \hat{\mathbf{g}}(N,PGA,SA,LSI,\Theta) &= \exp(N \cdot \theta_1) + \theta_2 \exp(PGA \cdot \theta_3) \\ &+ \theta_4 \exp(SA \cdot \theta_5) + \theta_6 \cdot LSI - \theta_8 + \mathcal{E} \end{aligned} \quad (5.10)$$

$$\begin{aligned} \hat{\mathbf{g}}(N,PGA,SA,LSI,S,\Theta) &= \exp(N \cdot \theta_1) + \theta_2 \cdot PGA \\ &+ \theta_3 \cdot SA + \theta_4 \cdot LSI + \theta_5 \cdot S - \theta_8 + \mathcal{E} \end{aligned} \quad (5.11)$$

$$\begin{aligned} \hat{\mathbf{g}}(N,PGA,SA,LSI,S,\Theta) &= \exp(N \cdot \theta_1) + \theta_2 \exp(PGA \cdot \theta_3) \\ &+ \theta_4 \exp(SA \cdot \theta_5) + \theta_6 \cdot LSI + \theta_7 \cdot S - \theta_8 + \mathcal{E} \end{aligned} \quad (5.12)$$

It is reasonable and also convenient to assume that  $\mathcal{E}$  has a normal distribution. With the aim of producing an unbiased model (i.e., one that, in the average, makes the correct prediction), we set the mean of  $\mathcal{E}$  to zero. The standard deviation of  $\mathcal{E}$ , denoted by  $\sigma_{\mathcal{E}}$ , however is unknown and must be estimated. The set of unknown parameters of the model, therefore, is  $\Theta = (\theta, \sigma_{\mathcal{E}})$ .

#### 5.4 Formulation of the Likelihood Function:

For assessing the damage index model, field case histories at sites where structural damage has or has not occurred after Kocaeli Earthquake were used. Let  $N_i, PGA_i, SA_i, LSI_i$  and  $S_i$  be the values of damage index, number of storeys, peak ground acceleration, spectral acceleration, liquefaction severity index and post liquefaction settlement at the  $i^{\text{th}}$  observation, respectively, and let  $\varepsilon_i$  be the corresponding realization of the model correction term. If the  $i^{\text{th}}$  observation is a non-damaged case, then  $g(N_i, PGA_i, SA_i, LSI_i, S_i, \boldsymbol{\theta}) \leq 0$ . On the other hand, if the  $i^{\text{th}}$  observation is a damaged case, then  $g(N_i, PGA_i, SA_i, LSI_i, S_i, \boldsymbol{\theta}) > 0$ . Assuming the observations to be statistically independent, we can write the likelihood function as the product of the probabilities of the observations, i.e.:

$$L(\boldsymbol{\theta}, \sigma_\varepsilon) = \prod_{non-damaged} P[g(N_i, PGA_i, SA_i, LSI_i, S_i, \boldsymbol{\theta}) \leq 0] \times \prod_{damaged} P[g(N_i, PGA_i, SA_i, LSI_i, S_i, \boldsymbol{\theta}) > 0] \quad (5.13)$$

Suppose the measured or estimated values  $N_i, PGA_i, SA_i, LSI_i$  and  $S_i$  at each observation are exact, i.e., no measurement or estimation error is present. Then, noting that;

$$g(N_i, PGA_i, SA_i, LSI_i, S_i, \boldsymbol{\theta}) = \hat{g}(N_i, PGA_i, SA_i, LSI_i, S_i, \boldsymbol{\theta}) + \varepsilon_i \quad (5.14)$$

has the normal distribution with mean  $\hat{g}(N_i, PGA_i, SA_i, LSI_i, S_i, \boldsymbol{\theta})$  and standard deviation  $\sigma_\varepsilon$ , the likelihood function (Eq. 5.13) can be written as:

$$L(\boldsymbol{\theta}, \sigma_{\varepsilon}) = \prod_{non-damaged} \varphi \left[ \frac{g(N_i, PGA_i, SA_i, LSI_i, S_i, \varepsilon_i, \boldsymbol{\theta})}{\sigma_{\varepsilon}} \right] \times \prod_{damaged} \varphi \left[ \frac{g(N_i, PGA_i, SA_i, LSI_i, S_i, \varepsilon_i, \boldsymbol{\theta})}{\sigma_{\varepsilon}} \right] \quad (5.15)$$

Where  $\varphi[\cdot]$  is the normal probability function. Note that the above is a function of the unknown parameters  $\boldsymbol{\theta}$  and  $\sigma_{\varepsilon}$ .

A difficult issue in the development of the probabilistic limit-state model for damage index is the fact that the observed data over-represent the number of non-damaged buildings relative to the number of damaged buildings. The final data set of 4186 buildings contained 3244 non-damaged and 942 damaged buildings. This kind of data represents a sampling disparity problem and does not provide an unbiased reflection of actual field occurrences. Simply put, post-earthquake field investigators of GDDA have to classify each and every building throughout Adapazarı due to their damage level for statistical purposes. Huge difference between the number of non-damaged and damaged buildings addresses the uneven sampling problem as a result of choice-based sampling process. In order to correct for the resulting bias, Cetin et al. (2002) recommended weighting the observations to better reflect the actual population. For the present application, the approach essentially amounts to re-writing the likelihood function of Equation 5.15 in the form:

$$L(\boldsymbol{\theta}, \sigma_{\varepsilon}) = \prod_{non-damaged} P[g(N_i, PGA_i, SA_i, LSI_i, S_i, \varepsilon_i, \boldsymbol{\theta}) \leq 0]^{W_{non-damaged}} \times \prod_{damaged} P[g(N_i, PGA_i, SA_i, LSI_i, S_i, \varepsilon_i, \boldsymbol{\theta}) > 0]^{W_{damaged}} \quad (5.16)$$

Where the weight factors  $W_{non-damaged}$  and  $W_{damaged}$  are defined as:

$W_{non-damaged} = \frac{Q_{ND}}{Q_T} \quad (5.17)$
---

$W_{\text{damaged}} = \frac{Q_D}{Q_T}$	
--	--

Where  $Q_{ND}$  = number of non-damaged buildings

$Q_D$  = number of damaged buildings

$Q_T$  = total number of buildings

This approach led to approximately  $w_{\text{non-damaged}} = 0.45$  and  $w_{\text{damaged}} = 1.55$  with the ratio  $w_{\text{non-damaged}} / w_{\text{damaged}} = 3$ .

Model parameters,  $\theta$ 's and  $\sigma_\epsilon$  were estimated as the values that will maximize the likelihood functions as shown in Table 5.2.

**Table 5.2 Maximum Likelihood Estimates of Model Parameters**

	<b>Model 1</b>	<b>Model 2</b>	<b>Model 3</b>	<b>Model 4</b>	<b>Model 5</b>	<b>Model 6</b>
$\theta_1$	0.007	0.009	0.008	0.005	0.015	0.006
$\theta_2$	0.111	0.173	0.167	2.367	-0.027	-0.078
$\theta_3$		0.701	-0.009	0.048	0.297	0.128
$\theta_4$			-0.001	-0.002	0.001	1.86
$\theta_5$				1.577	-0.081	0.061
$\theta_6$				-0.001		0.001
$\theta_7$						-0.032
$\theta_8$	1.058	1.245	1.072	3.415	1.125	2.831
$\sigma_{\epsilon_k}$						
<b>(maximum likelihood value)</b>	-826.26	-826.283	-824.169	-824.167	-817.51	-817.468

As it can be seen from Table 5.2, maximum likelihood value of the limit state models given in Equations 5.1-5.6 are slightly different from each other. In order to determine the model giving the better solution, percent number of true predictions for each model are calculated and shown in Figures 5.6-5.8.

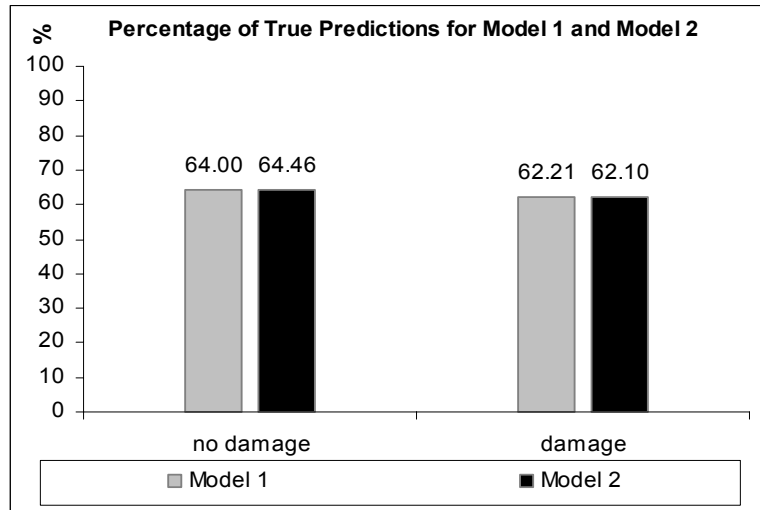


**Fig. 5.6: Percentage on True Predictions for Damaged and Non-damaged Cases in Model 1 and Model 2.**

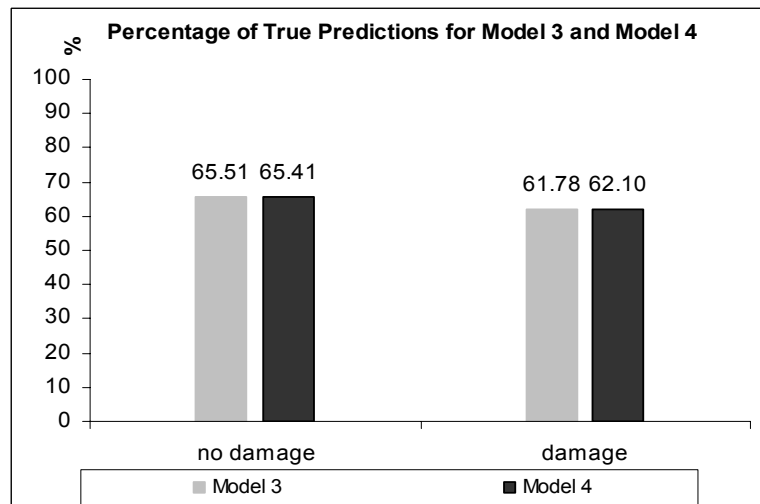


**Fig. 5.7: Percentage on True Predictions for Damaged and Non-damaged Cases in Model 3 and Model 4.**

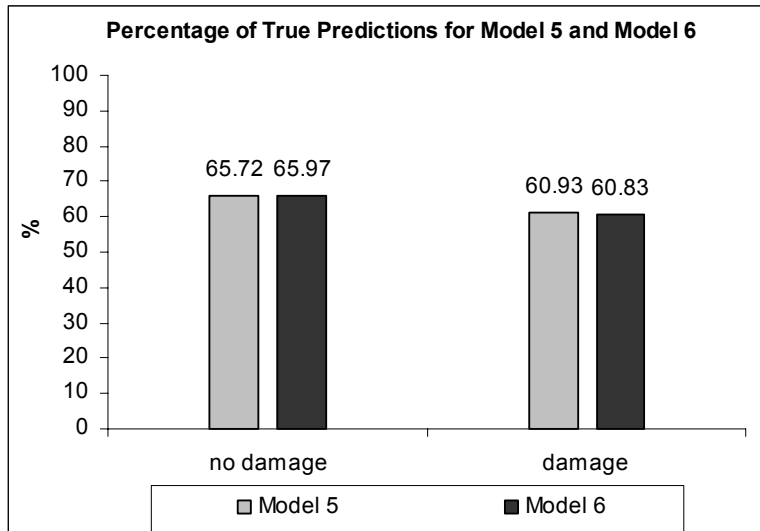


**Fig. 5.8: Percentage on True Predictions for Damaged and Non-damaged Cases in Model 5 and Model 6.**

## CHAPTER 6

### SUMMARY AND CONCLUSIONS

In August 17, 1999 a magnitude  $M_w=7.4$  earthquake struck Kocaeli and Sakarya provinces which are densely populated regions in the industrial heartland of Turkey. The aim of this study is to determine geotechnical engineering factors that contribute to the structural damage observed in Sakarya city after 1999 Kocaeli Earthquake. For this purpose an extensive field investigation program was implemented including subsurface soil characterization, and documenting structural performance data. The database was carefully screened for poor quality data and was transferred to geographic information system (GIS) framework.

Within the scope of this study, a maximum likelihood framework for the probabilistic assessment of seismically induced structural performance is described. A database, consisting of post-earthquake field observations of structural performance after Kocaeli earthquake in conjunction with in-situ "index" test results, is used for the development of probabilistically based structural performance correlations.

For the purpose of defining important parameters of the problem as well as the possible mathematical form of the relationship among damage index and selected descriptive parameters, series of sensitivity studies were performed. In these sensitivity studies, buildings having three or more storeys are used. The reason for screening lower buildings could be partially explained by the simple reason that most of these structures are not engineered and thus the effects of geotechnical factors could be washed out

in great randomness of other structural engineering parameters. Also geotechnical factors representing Adapazarı city soil conditions could be of lesser importance for structures with two stories or less where bearing capacity can be listed as an example of this reasoning.

After series of sensitivity analyses, important geotechnical engineering parameters of the problem were selected as i) liquefaction severity index, ii) thickness of the possibly liquefied layer, iii) representative depth to possibly liquefied layer and iv) post liquefaction volumetric settlement. In addition to these geotechnical engineering parameters, structural performance defined as a) no damage, b) moderate damage, c) heavy damage and collapse as well as the number of stories of each structure were used as to correlate structural damage with geotechnical factors.

Motivated by the results of sensitivity studies, following improved model for damage index estimations are adopted:

$$g = 10.65 \cdot \exp(N)^{0.01} + 1.09 \cdot \text{PGA} - 11.23 \quad (6.1)$$

$$g = 10.65 \cdot \exp(N)^{0.01} + 1.09 \cdot \text{PGA} - 11.23$$

$$g = 8.05 \cdot \exp(N)^{0.01} + 1.06 \cdot \text{PGA} - 0.05 \cdot \text{SA} - 0.01 \cdot \text{LSI} - 8.88 \quad (6.2)$$

$$g = 8.05 \cdot \exp(N)^{0.01} + 1.06 \cdot \text{PGA} - 0.05 \cdot \text{SA} - 0.01 \cdot \text{LSI} - 8.88$$

$$g = 8.47 \cdot \exp(N)^{0.01} - 0.09 \cdot \text{PGA} + 1.11 \cdot \text{SA} + 0.01 \cdot \text{LSI} - 0.3 \cdot S + 2.56 - 11.51 \quad (6.3)$$

$$g = 8.47 \cdot \exp(N)^{0.01} - 0.09 \cdot \text{PGA} + 1.11 \cdot \text{SA} + 0.01 \cdot \text{LSI} - 0.3 \cdot S + 2.56 - 11.51$$

Where;

N : Number of stories of the building

- PGA : Peak ground acceleration in meter per square second
- SA : Spectral acceleration for the period range of conventional buildings
- LSI : Liquefaction severity index as defined in Section 4.3.1
- S : The estimated liquefaction-induced ground settlements (S) in meters

Third model includes more descriptive variables and has a slightly higher likelihood value and thus usage of this model will give more precise results. According to this model, damage index (DI) exponentially increases with the increase of number of stories of the building, and linearly increases with peak ground acceleration (PGA), spectral acceleration (SA), liquefaction severity index (LSI), and settlement (S).

For future studies, updating the database with the new data from future earthquakes is suggested.

## REFERENCES

- Andrews, D. C. A. and Martin, G. R. (2000), "Criteria for Liquefaction of Silty Soils", Proceedings, 12<sup>th</sup> World Conference on Earthquake Engineering, 2000, Auckland, New Zealand.
- Bakır, B. S., Sucuoglu, H., and Yılmaz, T. (2002), "An Overview of Local Site Effects and the Associated Building Damage in Adapazarı During the 17 August 1999 Kocaeli Earthquake", Bulletin of Seismological Society Am 2002, 92(1), 509-26.
- Bartlett, S.F. and Youd, T.L. (1995) "Empirical Prediction of Liquefaction-Induced Lateral Spreads", Journal of Geotechnical Engineering, ASCE, 121 (4), pp. 316-329.
- Bray, J. D, Sancio, R. B., Reimer, M. Durgunoglu, H. T. (2003), "Liquefaction Susceptibility of Fine-Grained Soils", Proceedings, 11<sup>th</sup> International Conference on Soil Dynamics and Earthquake Engineering – 3<sup>rd</sup> International Conference on Earthquake Geotechnical Earthquake Engineering (11th ICSDEE), University of California Berkeley, 7-9 January, 2003, Vol. 1, pp. 655-662.
- Cetin, K. O. (2000), "Reliability-based Assessment of Seismic Soil Liquefaction Initiation Hazard", Dissertation Submitted in Partial Satisfaction of the Requirements for the Degree of Doctor of Philosophy, University of California at Berkeley.
- Cetin, K. O., Der Kiureghian, A., and Seed, R. B. (2002), "Probabilistic Models for the Initiation of Seismic Soil Liquefaction", Structural Safety, 24(2002), pp.67-82.

- Craig, R. F. (1992), "Soil Mechanics", London, UK, Chapman & Hall, 1992
- Dickenson, S. E. (1994), "Dynamic Response of Soft and Deep Cohesive Soils During the Loma Prieta Earthquake of October 17, 1989", Dissertation Submitted in Partial Satisfaction of the Requirements for the Degree of Doctor of Philosophy, University of California at Berkeley.
- Dobry, R. and Vucetic, M. (1987), "Dynamic Properties and Seismic Response of Soft Clay Deposits", Proceedings, International Symposium on Geotechnical Engineering of Soft Soils, Mexico City, Vol.2, pp.51-87.
- Erdik, M. (2003), "Report on 1999 Kocaeli and Düzce (Turkey) Earthquakes," [online], Chapter 7, pp.13–14, available at [http:// www.koeri.boun.edu.tr/depremmuh/Kocaelireport.pdf](http://www.koeri.boun.edu.tr/depremmuh/Kocaelireport.pdf)
- Finn, W. D. L. (1981), "Liquefaction Potential: Developments Since 1976", Proceedings, 1<sup>st</sup> International Conference on Recent Advances in Geotechnical Earthquake Engineering and Soil Dynamics, St. Louis, Vol. 2, pp. 655-681.
- Finn, W. D. L., Ledbetter, R. H., and Wu, G. (1994), "Liquefaction in Silty Soils: Design and Analysis", Ground Failures under Seismic Conditions, Geotechnical Special Publication 44, ASCE, New York, pp. 51-76.
- Hamada, M. and O'Rourke, T. D. (1992), "Case Studies of Liquefaction and Lifeline Performance during Past Earthquakes", NCEER-92-0001, Vol.1, Nat. Ctr. for Earthquake Engineering Research, Buffalo, N.Y.
- Idriss, I. M., Sun, J. I., (1992), "Users Manual for SHAKE91, A Computer Program for Conducting Equivalent Linear Seismic Response Analyses of Horizontally Layered Soil Deposits, Program Modified Based on the Original SHAKE Program Published in December 1972, by Schnabel, Lysmer and Seed", August 1992.

- Ishihara, K. (1985), "Stability of Natural Deposits During Earthquakes", 11<sup>th</sup> International Conference on Soil Mechanics and Foundation Engineering, Proceedings, San Francisco, Vol.1, pp. 321-376.
- Ishihara, K. (1993), "Liquefaction and Flow Failure during Earthquakes", the 33<sup>rd</sup> Rankine Lecture, *Geotechnique*, 43(3): 351-415
- Ishihara, K., "Soil Behavior in Earthquake Geotechnics", Oxford, Clarendon Press, 1996.
- Ishihara, K. and Yoshimine, M. (1992), "Evaluation of Settlements in Sand Deposits Following Liquefaction During Earthquakes", *Soils and Foundations*, Vol. 32, No. 1, March, pp. 173-188.
- Iwasaki T., Arakawa, T. and Tokida, K. (1982), "Standard Penetration Test and Liquefaction Potential Evaluation", Proceedings, International Conference on Soil Dynamics and Earthquake Engineering, Southampton, Vol.2, pp. 925-941.
- Koester, J.P. (1992), "The Influence of Test Procedure on Correlation of Atterberg Limits With Liquefaction in Fine-Grained Soils", *Geotechnical Testing Journal*, Vol. 15(4): 352-361, 1992.
- Kokusho, T., Yoshida, Y. and Esashi, Y. (1982), "Dynamic Properties of Soft Clay for Wide Strain Range", *Soils and Foundations*, Vol.22, No.4, pp.1-18.
- Kramer, S. L. (1996), "Geotechnical Earthquake Engineering", Upper Saddle River, N.J., Prentice Hall, 1996.
- Lee, K. L. and Albaisa, A. (1974), "Earthquake Induced Settlements in Saturated Sands", *Journal of Soil Mechanics and Foundations Division*, ASCE, Vol.100, No.GT4.

- Liao, S. S. C., Whitman, R. V. (1986), "A Catalog of Liquefaction and Non-liquefaction Occurrences during Earthquakes", Research Report, Department of Civil Engineering, MIT, Cambridge, MA
- Liao, S. S. C., Whitman, R. V. (1986), "Overburden Correction Factor for SPT in Sand", *Journal of Geotechnical Engineering*, ASCE, Vol. 112, No. 3, March 1986, pp. 373-377.
- Mogami and Kubo (1953), "The Behavior of Soil during Vibration", *Proceedings, 3<sup>rd</sup> International Conference on Soil Mechanics and Foundation Engineering*, Vol. 1, pp. 152-153.
- NCEER (1997), "Proceedings of the NCEER Workshop on Evaluation of Liquefaction Resistance of Soils", Edited by Youd, T. L., Idriss, I. M., Technical Report No. NCEER-97-0022, December 31, 1997.
- Ohta, Y. and Goto, N. (1978), "Empirical Shear Wave Velocity Equations in Terms of Characteristic Soil Indexes", *Earthquake Engineering and Structural Dynamics*, Vol. 6, pp. 167-187.
- O'Rourke, T. D. and Pease, J. W. (1997), "Mapping Liquefiable Layer Thickness for Seismic Hazard Assessment", *Journal of Geotechnical and Geoenvironmental Engineering*, pp. 46–56, January 1997.
- Pease, J. W. and O'Rourke, T. D. (1995), "Liquefaction Hazards in the San Francisco Bay Region: Site Investigation, Modeling, and Hazard Assessment at Areas Most Seriously Affected by 1989 Loma Prieta Earthquake", Final Report to U.S. Geological Survey, Grant No.1439-93-G-2332, Cornell University, Ithaca, N.Y.
- Robertson P. K. and Fear, C. E. (1995), "Liquefaction of Sands and Its Evaluation" *Proceedings, IS Tokyo 95, 1<sup>st</sup> International Conference on Earthquake Geotechnical Earthquake Engineering*, Keynote Lecture.

- Robertson, P. K. and Wride, C. E. (1998), "Evaluating Cyclic Liquefaction Potential Using The Cone Penetration Test", Canadian Geotechnical Journal, 35(3), 442-459.
- Sakarya University (1998), "Geology and Geomorphology of Adapazarı" Report No.1 (in Turkish).
- Sancio, R. B., Bray, J. D., Stewart, J.P., Youd, T.L., Durgunoglu, H. T., Onalp, A., Seed, R.B., Christensen, C., Baturay, M.B, and Karadayılar, T. (2002), "Correlation Between Ground Failure and Soil Conditions in Adapazarı, Turkey", Soil Dynamics and Earthquake Engineering, 22, pp. 1093-1102.
- Schnabel, P.B., Lysmer, J. and Seed, H. B. (1972), "SHAKE: A Computer Program for Earthquake Response Analysis of Horizontally Layered Sites", Earthquake Engineering Research Center, University of California, Berkeley, Berkeley, CA. Report No. EERC 72-12.
- Seed, H. B. (1979), "Soil Liquefaction and Cyclic Mobility Evaluation for Level Ground During Earthquakes", Journal of Geotechnical Engineering Division, ASCE, 105 (GT2): 201-255.
- Seed, H. B., Idriss, I. M. (1970), "Soil Moduli and Damping Factors for Dynamic Response Analyses", Report No. EERC 70-10, Earthquake Engineering Research Center, University of California, Berkeley, Berkeley, CA.
- Seed, H. B., Idriss, I. M. (1971), "Simplified Procedure for Evaluating Soil Liquefaction Potential", Journal of the Soil Mechanics and Foundations Division, ASCE, Vol. 97, No SM9, Proc. Paper 8371, September 1971, pp. 1249-1273.
- Seed, H.B. and Idriss, I.M. (1982), "Ground Motions and Soil Liquefaction during Earthquakes", EERI Monograph, Berkeley, CA, 1982.

- Seed, H. B., Idriss, I.M and Arango, I. (1983), "Evaluation of Liquefaction Potential Using Field Performance Data and Cyclic Mobility Evaluation for Level Ground During Earthquakes ", Journal of Geotechnical Engineering, ASCE, Vol.109, No.3, pp. 458-482.
- Seed, H. B., Tokimatsu, K., Harder, L. F., Chung, R. M. (1984), "The Influence of SPT Procedures in Soil Liquefaction Resistance Evaluations", Earthquake Engineering Research Center Report No. UCB/EERC-84/15, University of California at Berkeley, 1984.
- Seed, H. B., Tokimatsu, K., Harder, L. F., and Chung, R. M. (1985). "Influence of SPT Procedures in Soil Liquefaction Resistance Evaluations", Journal of Geotechnical Engineering, ASCE, 111(12), 1425-1445.
- Seed, R. B., Cetin, K. O., Der Kiureghian, A., Tokimatsu, K., Harder, L. F. Jr., and Kayen, R. E. (2001), "SPT-Based Probabilistic and Deterministic Assessment of Seismic Soil Liquefaction Potential", Submitted to the ASCE Journal of Geotechnical and Geoenvironmental Engineering.
- Seed, R. B., Cetin, K. O., Moss, R. E. S., Kammerer, A. M., Wu, J., Pestana, J. M. and Reimer, M. F. (2001), "Recent Advances in Soil Liquefaction Engineering and Seismic Site Response Evaluation," Proceedings, 4<sup>th</sup> International Conference on Recent Advances in Geotechnical Earthquake Engineering and Soil Dynamics, San Diego, March 28-31, 2001.
- Sun, J.I., Golezorkhi, R. and Seed, H. B. (1988), "Dynamic Moduli and Damping Ratios for Cohesive Soils", Report No. EERC 88/15, Earthquake Engineering Research Center, University of California, Berkeley, Berkeley, CA.
- Tatsuoka, F., Sasaki, T., and Yamada, S. (1984), "Settlement in Saturated Sand Induced by Cyclic Undrained Simple Shear", Proceedings of the 8<sup>th</sup>

World Conference on Earthquake Engineering, San Francisco, California, July 21-28.

Terzaghi, K. and Peck, R. B. (1948), "Soil Mechanics in Engineering Practice", John Wiley and Sons, Inc., 2<sup>nd</sup> Edition.

Tokimatsu, K. and Seed, H.B., (1987), "Evaluation of Settlements in Sands Due to Earthquake Shaking", Journal of Geotechnical Engineering, ASCE, August, Vol. 113, No. 8, pp. 861-878.

Toprak, S., Holzer, L. (2003), "Liquefaction Potential Index: Field Assessment", Journal of Geotechnical and Geoenvironmental Engineering, ASCE, April, pp.315-322.

Unutmaz, B., "Assessment of Seismic Soil-Structure Interaction Induced Post Liquefaction Soil Deformations," Ph.D. Thesis, Civil Eng. Program, Middle East Technical University, Ankara, Turkey, expected to be completed in June 2005.

Youd, T.L. and Idriss, I. M. (1997), "NCEER Workshop on Evaluation of Liquefaction Resistance of Soils", Technical Report NCEER-98-XXXX, November 19, 1997.

Youd, T.L. and Idriss, I. M., (2001), "Liquefaction Resistance of Soils: Summary Report from the 1996 NCEER and 1998 NCEER/NSF Workshops on Evaluation of Liquefaction Resistance of Soils", Journal of Geotechnical and Geoenvironmental Engineering, ASCE, April, pp.297-313.

Yoshimi, Y., Kuwabara, F., and Tokimatsu, K. (1975), "One -Dimensional Volume Change Characteristics of Sands under Very Low Confining Stresses", Soils and Foundations, JSSMFE, Vol. 15, No .3, September.

- Yoshimi, Y., Richart, F. E., Prakash, S., Balkan, D. D. and Ilyichev (1977), "Soil Dynamics and Its Application to Foundation Engineering ", Proceedings, 9<sup>th</sup> International Conference on Soil Mechanics and Foundation Engineering, Tokyo, Vol. 2, pp. 605-650.
- Yoshimi, Y., Tokimatsu, K., Ohara, J. (1994), "In-situ Liquefaction Resistance of Clean Sands Over a Wide Density Range", *Geotechnique*, Vol. 44, No. 3, pp. 479-494
- Yuan, H., Juang, C.H., Yang, S.H. (2003), "Predicting Liquefaction Severity at Foundation—An Empirical Approach", Proceedings, The 11<sup>th</sup> International Conference on Soil Dynamics and Earthquake Engineering – 3<sup>rd</sup> International Conference on Earthquake Geotechnical Earthquake Engineering (11<sup>th</sup> ICSDEE), University of California Berkeley, 7-9 January, 2003, Vol. 1, p. 478-483.
- Zeghal, M. and Elgemal, A. W. (1994), "Analysis of Site Liquefaction Using Earthquake Records", *Journal of Geotechnical Engineering, ASCE*, 120(6), 996-1017.
- Zen, K., Umehara, Y. and Hamada, K. (1978), "Laboratory Tests and In-situ Seismic Survey on Vibratory Shear Modulus of Clayey Soils with Different Plasticities", Proceedings, 5<sup>th</sup> Japan Earthquake Engineering Symposium, Tokyo, pp. 721-728.

## **APPENDIX A**

List of modulus degradation and damping curves used in site-specific response analyses and corresponding soil types are given in Table 1. Name of boreholes with their locations and corresponding grid numbers are listed in Table 2.

**Table 1: List of Modulus Degradation and Damping Curves Used in Site-specific Response Analyses and Corresponding Soil Types.**

SOIL TYPE	MODULUS DEGRADATION CURVE	DAMPING CURVE
SAND	Damping for SAND, Average (Seed & Idriss 1970)	S2 (SAND $\sigma_v=1-3$ KSC) 3/11, 1988
CLAY	Soil with PI=30, OCR=1-8 (Vucetic and Dobry, 1991)	Soil with PI=30, OCR=1-15 (Vucetic and Dobry, 1991)
	Soil with PI=50, OCR=1-8 (Vucetic and Dobry, 1991)	Soil with PI=50, OCR=1-15 (Vucetic and Dobry, 1991)
SILT	Soil with PI=15, OCR=1-8 (Vucetic and Dobry, 1991)	Soil with PI=15, OCR=1-15 (Vucetic and Dobry, 1991)
GRAVEL	Gravel, Average (Seed et al. 1986)	Damping for Gravel, Average (Seed et al. 1986)
ROCK	Rock, Schnabel (1973)	Damping for Rock, Schnabel (1973)

**Table 2: Name of Boreholes with Their Locations and Corresponding Grid Numbers**

NORTH (x)	EAST (y)	GRID NO	BOREHOLE NAME
4509050	528349	G26	54_229_sk24
4508528	528092	G27	54_229_sk32
4507534	528354	G29	54_229_sk25
4507188	528172	G30	54_229_sk26
4506550	528158	G31	54_229_sk27
4509880	528896	H25	54_229_sk19
4509426	528836	H26	54_229_sk30
4508998	528847	H27	54_229_sk20
4508605	528761	H27	54_229_sk31
4506454	528838	H32	54_229_sk33
4507602	529129	I29	54_229_sk21
4507200	529083	I30	54_229_sk22
4510221	529937	J24	54_229_sk29
4509672	529883	J25	54_229_sk12
4508972	529783	J27	54_229_sk13
4508396	529774	J28	54_229_sk14
4507679	529543	J29	54_229_sk15
4507617	529963	J29	54_229_sk34
4507192	529685	J30	54_229_sk16
4506692	529776	J31	54_229_sk17
4506606	529571	J31	54_229_sk23
4506205	529882	J32	54_229_sk18
4510816	530058	K23	54_229_sk28
4508726	530068	K27	54_229_sk38
4508215	530236	K28	54_229_sk35
4506209	530302	K32	54_229_sk11
4510847	530771	L23	54_229_sk3
4510295	530515	L24	54_229_sk4
4509134	530507	L26	54_229_sk36
4509494	530734	L26	54_229_sk5
4508982	530549	L27	54_229_sk6
4508300	530584	L28	54_229_sk7
4507747	530569	L29	54_229_sk8
4507235	530548	L30	54_229_sk9
4506414	530583	L32	54_229_sk10
4507660	531489	M29	54_244_sk8
4507170	531430	M30	54_244_sk9
4517290	531640	N10	54_230_sk40
4517300	531500	N10	54_230_sk78
4517198	531661	N10	54_sau_ssk584
4516760	531770	N11	54_230_sk77
4513970	531980	N17	54_230_sk67
4513490	531780	N18	54_230_sk71

**Table 2 (Continued): Name of Boreholes with Their Locations and Corresponding Grid Numbers**

NORTH (x)	EAST (y)	GRID NO	BOREHOLE NAME
4508106	531594	N28	54_244_sk7
4517180	532110	O10	54_230_sk30
4517011	532109	O10	54_sau_ssk341
4516220	532150	O12	54_230_sk41
4515890	532330	O13	54_sau_smp566
4515083	532465	O14	54_sau_scm210
4515103	532498	O14	54_sau_smp416
4514545	532248	O15	54_230_sk3
4514657	532077	O15	54_sau_smp438
4514250	532110	O16	54_230_sk72
4513820	532380	O17	54_230_sk65
4508339	532129	O28	54_244_sk6
4517114	532675	P10	54_sau_ssk342
4517258	532841	P10	54_sau_ssk349
4516980	532820	P11	54_230_sk25
4516310	533050	P12	54_230_sk27
4516000	532590	P12	54_230_sk76
4516190	532640	P12	54_230_sk88
4516081	532671	P12	54_sau_ssk360
4515260	532610	P14	54_230_sk73
4514714	532749	P15	54_230_sk4
4514790	532710	P15	54_230_sk94
4514572	532838	P15	54_sau_smp428
4514682	532635	P15	54_sau_smp461
4513852	532902	P17	54_230_sk2
4512450	532860	P20	54_232_sk18
4512420	532680	P20	54_232_sk66
4512170	532710	P20	54_232_sk67
4510890	532760	P23	54_sau_shn10
4510460	532816	P24	54_222_sk1
4510076	532647	P24	54_sau_shn09
4508892	532955	P26	54_244_sk5
4517620	532720	P9	54_230_sk24
4517155	533067	Q10	54_sau_soz363
4516990	533350	Q11	54_230_sk26
4516705	533107	Q11	54_sau_sis572
4516330	533440	Q12	54_230_sk29
4516230	533480	Q12	54_230_sk93
4516260	533319	Q12	54_sau_scm242
4515574	533262	Q13	54_230_sk6
4515582	533257	Q13	54_sau_ssm177
4515909	533039	Q13	54_sau_ssm186
4515180	533164	Q14	54_230_sk5

**Table 2 (Continued): Name of Boreholes with Their Locations and  
Corresponding Grid Numbers**

NORTH (x)	EAST (y)	GRID NO	BOREHOLE NAME
4515117	533114	Q14	54_sau_syd160
4514690	533360	Q15	54_230_sk92
4514730	533496	Q15	54_sau_sdl464
4514164	533247	Q16	54_230_sk1
4513840	533440	Q17	54_232_sk57
4513800	533280	Q17	54_232_sk59
4513400	533370	Q18	54_232_sk53
4513060	533450	Q18	54_232_sk54
4512510	533260	Q19	54_232_sk4
4512640	533320	Q19	54_232_sk6
4512230	533090	Q20	54_232_sk2
4512430	533160	Q20	54_232_sk3
4512210	533480	Q20	54_232_sk5
4511230	533420	Q22	54_sau_shn08
4510501	533419	Q23	54_sau_shn13
4510172	533281	Q24	54_222_sk6
4508543	533388	Q27	54_244_sk4
4517990	533200	Q8	54_230_sk43
4517590	533420	Q9	54_230_sk23
4517410	533840	R10	54_230_sk36
4516652	533622	R11	54_sau_sis326
4516986	533823	R11	54_sau_ssa392
4516040	533870	R12	54_230_sk62
4516105	533764	R12	54_sau_scm224
4516332	533982	R12	54_sau_sor265
4515631	533840	R13	54_230_sk11
4515959	533500	R13	54_230_sk31
4515920	533700	R13	54_230_sk64
4515587	533840	R13	54_sau_ssm189
4515180	533802	R14	54_230_sk7
4515169	533935	R14	54_sau_syc123
4515191	533503	R14	54_sau_syd158
4514660	533940	R15	54_232_sk49
4514676	533800	R15	54_sau_sho485
4514240	533610	R16	54_232_sk61
4514250	533840	R16	54_232_sk62
4514470	533710	R16	54_232_sk63
4513880	533910	R17	54_232_sk48
4513620	533830	R17	54_232_sk55
4513620	533570	R17	54_232_sk56
4513850	533690	R17	54_232_sk58
4513360	533810	R18	54_232_sk52
4512870	533990	R19	54_232_sk13

**Table 2 (Continued): Name of Boreholes with Their Locations and  
Corresponding Grid Numbers**

NORTH (x)	EAST (y)	GRID NO	BOREHOLE NAME
4512960	533784	R19	54_sau_ser593
4512330	533840	R20	54_232_sk12
4512320	533630	R20	54_232_sk7
4512360	533590	R20	54_232_sk8
4511110	533760	R22	54_222_sk3
4511210	533980	R22	54_sau_shn12
4510586	533557	R23	54_222_sk2
4510810	533510	R23	54_222_sk7
4508277	533858	R28	54_244_sk3
4518510	533650	R7	54_230_sk45
4517870	533910	R9	54_230_sk20
4517740	533570	R9	54_230_sk91
4517830	533760	R9	54_sau_ste403
4516540	534160	S11	54_230_sk14
4516980	534260	S11	54_230_sk15
4516898	534387	S11	54_sau_sko409
4516010	534163	S12	54_230_sk13
4516331	534493	S12	54_230_sk34
4516460	534320	S12	54_230_sk89
4515648	534227	S13	54_230_sk12
4515661	534286	S13	54_sau_so3383
4515784	534254	S13	54_sau_sti028
4515383	534108	S14	54_230_sk10
4515111	534130	S14	54_230_sk8
4515365	534148	S14	54_sau_syc122
4514730	534350	S15	54_232_sk45
4514890	534230	S15	54_232_sk68
4514170	534360	S16	54_232_sk41
4514480	534400	S16	54_232_sk42
4514220	534120	S16	54_232_sk44
4514440	534120	S16	54_232_sk46
4513590	534470	S17	54_232_sk28
4513900	534140	S17	54_232_sk47
4513324	534448	S18	54_sau_ser540
4512700	534280	S19	54_232_sk14
4512100	534100	S20	54_232_sk10
4512113	534173	S20	54_sau_ser536
4511590	534067	S21	54_sau_ser543
4508640	534449	S28	54_244_sk2
4519040	534253	S6	54_230_sk37
4518577	534205	S7	54_sau_ste406
4518170	534310	S8	54_230_sk54
4517910	534440	S9	54_230_sk19

**Table 2 (Continued): Name of Boreholes with Their Locations and Corresponding Grid Numbers**

NORTH (x)	EAST (y)	GRID NO	BOREHOLE NAME
4516860	534830	T11	54_230_sk16
4516760	534980	T11	54_230_sk46
4516179	534731	T12	54_sau_sdl483
4515965	534786	T13	54_sau_sya308
4515127	534636	T14	54_230_sk32
4515020	534860	T14	54_230_sk51
4515320	534503	T14	54_230_sk9
4515222	534601	T14	54_sau_syg62
4514740	534680	T15	54_232_sk43
4514160	534690	T16	54_232_sk32
4514460	534700	T16	54_232_sk39
4514060	534870	T16	54_232_sk40
4514230	534610	T16	54_232_sk64
4513510	534760	T17	54_232_sk22
4513830	534510	T17	54_232_sk30
4513840	534790	T17	54_232_sk34
4513860	534940	T17	54_232_sk36
4513694	534836	T17	54_sau_ser548
4513310	534670	T18	54_232_sk17
4512940	534670	T19	54_232_sk16
4512580	534960	T19	54_232_sk26
4512340	534570	T20	54_232_sk15
4512060	534980	T20	54_232_sk65
4511748	534666	T21	54_sau_ser531
4511872	534928	T21	54_sau_ser533
4511130	534850	T22	54_222_sk5
4510560	534750	T23	54_222_sk4
4509071	534840	T27	54_244_sk1
4518800	534910	T7	54_230_sk22
4518243	534987	T8	54_sau_stz620
4516822	535448	U11	54_sau_sya307
4516008	535203	U12	54_sau_sya311
4515900	535220	U13	54_230_sk17
4515800	535014	U13	54_sau_syg87
4515120	535280	U14	54_232_sk35
4515060	535040	U14	54_232_sk37
4515034	535010	U14	54_sau_syg079
4514854	535263	U15	54_230_sk35
4514060	535140	U16	54_232_sk33
4513850	535490	U17	54_232_sk25
4513720	535190	U17	54_232_sk29
4513742	535458	U17	54_sau_skp506
4513490	535110	U18	54_232_sk27

**Table 2 (Continued): Name of Boreholes with Their Locations and  
Corresponding Grid Numbers**

NORTH (x)	EAST (y)	GRID NO	BOREHOLE NAME
4513304	535081	U18	54_sau_sym513
4513151	535445	U18	54_sau_sym611
4512450	535212	U20	54_sau_sym507
4517860	535250	U9	54_230_sk21
4517015	535543	V10	54_sau_sya304
4513150	535790	V18	54_232_sk21
4513390	535760	V18	54_232_sk23
4512970	535520	V19	54_232_sk19
4512890	535890	V19	54_232_sk20
4512641	535583	V19	54_sau_sym607
4517700	535828	V9	54_226_sk6
4517298	536405	W10	54_226_sk8
4516769	536228	W11	54_226_sk9
4518615	536041	W7	54_226_sk2
4518347	536011	W8	54_226_sk4
4517897	536071	W9	54_226_sk5
4517525	536048	W9	54_226_sk7